UNIVERSIDADE DE LISBOA
FACULDADE DE CIÊNCIAS
DEPARTAMENTO DE BIOLOGIA ANIMAL

Backing up under pressure: Role of sensory afferents in walking direction

Manuel Tanqueiro

Mestrado em Biologia Evolutiva e do Desenvolvimento

Dissertação orientada por:
César Mendes
Margarida Matos

2022

Acknowledgments

The last year and a half has been definitely one of the hardest I have had. Thankfully, I have had the support of so many people that I am afraid this section might be larger than the rest of the thesis.

For a start, I want to thank my supervisors César and Margarida, for all the hours spent reading my thesis and giving me the so important feedback that I needed to make sure it was ready. Writing was never my cup of tea, and writing something so large and with so many small details was definitely one of the hardest parts of my life as a student. César, I am truly grateful for your patience with all my moments of weird randomness in the lab where suddenly there were more 3D printed objects in my desk than flies. I know I get distracted a lot and I need a small dose of micromanaging to keep me under control, and I hope that you feel it was worth the time we spent in zoom meetings throughout all this time trying to understand why the flies were messing with us. I truly learned a lot. Margarida, I thank you for all the patience you had with my crisis of "this should be done", and I hope that my hour-long presentations on what I have been doing for the past months followed by radio silences were not too boring. Your input as someone outside the area was one of the most important parts, and made me understand how to write and present something to someone that, unlike me, has not been working on this dataset for the last year.

For the members of this lab, I would like to start by thanking Alexandra. I hope you feel like I treated your project the best I could, because I really tried to. The work you have done before I got into this was incredible, and I tried my best to keep up with the pace and deliver the best I could. You were there not only as an unofficial supervisor, but as a lab partner that was always available to help even when I stubbornly wouldn't ask for it. I would also like to thank Ricardo and Inês, the other duo of the lab. Ricardo, we were the two guys of the lab and you always made me feel supported when surrounded by all the girls. I will not forget all the moments where a simple phrase would send us to uncontrollable laughter and weird looks from the rest of the lab. And for Inês, you were my master's companion, and it was truly incredible to see you work. I wish someday I will have 10% of the organisation you have, because I am pretty sure your Excel tables had Excel tables of their own, and I couldn't even keep a notebook in order. I also want to thank Anna, you were an incredible source of knowledge and ideas for both experiments and data analysis, and my thesis would not have half the results it does if it weren't for you. It was a pleasure being a blue blur behind you in the COLife video. I would like to finish this part of the acknowledgments by thanking the Rita Teodoro lab, that was always there to listen to our group talking for two hours about our work when it had nothing to do with them, and gave hugely important feedback as outsiders, and to thank the histology facility members Ana Farinho and Maria Domingues, my company in the lab and unofficial DJ's, keeping the room always filled with music.

Jumping out of the lab and into college, I would like to thank the members of the Fecundados group. Pati and Manel, you were my brothers in arms in the MBED, always so supportive and ready to call me out when I was doing something stupid. I will never forget the amount of help you gave me when writing, with me explaining to you things you could not care less about. We are one hell of a trio and I wish we could do thesis like we did works, with Pati on the writing and Manel on the discussion, and I'll keep doing my pretty graphs and weird analysis. Susana, Maria, and Miguel, even though you three were not a part of our masters, you were always ready to help, to give feedback and to react to all the tea, and I truly appreciate you. I would also like to thank Fresa, the weirdo that kept listening to my existential crisis as if she still cared about them. We might not see each other for a whole year but when we do, it's as if we talked every single day.

From college to the Twitch/Discord, I want to thank some special members of the Bentesticles. Starting with the one and only Ben, you were there to listen to the fly weirdo and show enthusiasm about work that I had done and that I really did not understand how it could be interesting because I was talking about it for the past year, and I really appreciate you. I would also like to thank the support of so many others, such as Mr.R and Tex, Jolienn and LeinLein, Alex and Coop, Dani and Darknight, Sathwik and Sasaki, Tech and Rhodano. You were my refuge outside my country and all of you have been an incredible support, even if it isn't for making me laugh. Aqua will always be thankful.

From Twitch/Discord to the sea, I would like to give a special thanks to some of my friends from 7ª Essência. First, the one and only Jota, my "adoptive dad" as some say, that has seen me grow up since I was 13, and more than 10 years later still has the patience to listen to me ramble about some weird flies that walk backwards. I would also like to thank some of my fellow "researfers" Jess, João, Dora, Sofia, and Leonor, with whom I was able to talk about all of my work, my struggles, my stresses about research and how to cope with it. Listening to your work was truly inspiring and even if I end up leaving this work branch, I want to guarantee you know how much you helped me with coping with all that this life entails. I would also like to thank Manel, Duarte, Edu, Bruno, and Pedro, you all make my surfing mornings worth it by keeping my spirits up and pushing me to try harder and do better.

Keeping the sea theme, and jumping from Lisbon to Costa Nova, I would like to end the friend section by thanking my fellow colleague Sofia Duque. You have been helping me ever since I was trying to get into college, you helped me when I needed during my Bachelors, and you helped me now when I am in my masters. I cannot put into words how much our talks have helped me with going through all of this, and I cannot thank you enough for it.

Now, my family. You do not have any clue on how important you were to keep me sane during this last year. For Paulinha and José, that kept pushing me to go forward when I needed the help, that were able to support me when I told them that it was going to have to be a month more, and another, and another, and that in the end showed me that sometimes I need to hear the hard stuff to understand that I need help and I need others, and cannot do all by myself. For Ba and Becas, you were my companions too. You listened to me talking about all the random things I did to flies, you saw all the plots and graphs like you cared, you laughed when I told you that for the 18th time I had changed my room because I needed to change the setting I was working in, and you never complained once. Okay, maybe you complained a bit when I was tired and became extremely annoying, but you were all used to it by now. I am truly thankful for your support, and I know I could not have done it without you.

Lastly, I want to thank my best friend and partner Madarrena. You have really been my biggest support when I needed. You made me laugh when I needed, feel sad when I refused to deal with things, and you make me a better person because of it. You will always be my rubber-duck and I thank you for it.

This has really been a journey filled with ups and downs. Waking up at 5h30 every day, working 10-12h in some days, with little to no breaks was absolutely brutal. But I learned a lot. I learned how to think even more outside the box to solve issues, I learned to code, I learned to solder, and so many more things that will truly be crucial for my future. It was really tough, but it's done now.

Thank you.

Resumo

A capacidade de produzir movimento é importante para uma grande variedade de organismos, dos mais simples aos mais complexos. De facto, é graças a movimentos como a locomoção que a maioria dos organismos são capazes de procurar alimento ou fugir de predadores. A base por detrás deste controlo de movimento é descrita como sendo bastante conservada entre organismos de complexidades bastante distintas, como por exemplo entre vertebrados (como os mamíferos) e invertebrados (como os insetos). Ambos os grupos apresentam um sistema nervoso central dividido em duas secções, o cérebro e a espinal medula (ou cordão nervoso).

A *Drosophila melanogaster*, mais conhecida como mosca da fruta, é um modelo de invertebrado extremamente utilizado graças à facilidade com que se obtêm grandes amostras em curto espaço de tempo, possuindo ainda um conjunto de ferramentas genéticas bastante variado. Este é um modelo bastante comum no estudo do movimento e da locomoção, por ser relativamente bem conhecida a rede que está por detrás do controlo motor. A informação começa por partir de centros de ordem superior, que a partir de neurónios descendentes chegam do cérebro ao cordão nervoso central (equivalente em inseto à espinal medula). Aqui, a informação é transmitida através de interneurónios, que em conjunto com os geradores de padrão centrais (responsáveis pela criação de sinais nervosos cíclicos e periódicos), vão fazer chegar aos músculos, via neurónios motores, ordens para contrair ou distender. Contudo, o sistema necessita de receber informação de volta, de modo a saber se o movimento está a ser produzido de forma controlada, para providenciar a capacidade de obter controlo motor fino, assim como para informar sobre estímulos que venham de fora do organismo. Para que esta informação volte para o sistema, são necessárias estruturas de proprioceção associadas a neurónios sensoriais.

Na mosca da fruta, existem quatro estruturas sensoriais na pata que fazem parte do sistema propriocetivo, sendo elas as Mechanosensory bristles (MB), as Hair plates (HP), o Chordotonal organ (CO) e as Campaniform sensilla (CS). Cada uma destas estruturas está dedicada a informar o sistema neuronal sobre um tipo específico de estímulos: as MB são a fonte de informação sobre estímulos táteis na cutícula, dada a ausência de outros recetores neste exosqueleto rígido; as HP são responsáveis por informar sobre a posição de segmentos adjacentes da pata; o CO providencia informação sobre o ângulo da pata em cada momento; e por fim, as CS são sensores de carga, responsáveis por informar o corpo sobre deformações no exoesqueleto causadas por pressão aplicada sobre o corpo da mosca, ou quando a pata é pousada no solo. Todas estas estruturas já foram descritas e sua função estudada durante a locomoção, com especial ênfase para o CO. Contudo, a informação sobre o papel destas estruturas como iniciadores de movimento continuava por descrever.

Este foi o início de um projeto no laboratório Neurogenética da locomoção (CEDOC), do Dr. César Mendes e aluna de doutoramento Alexandra Medeiros. Neste projeto, utilizando optogenética (técnica que tem por base o uso de luz em certos comprimentos de onda para despolarizar neurónios específicos, graças a canais iónicos sensíveis à luz) para estimular estas estruturas sensoriais, foi possível observar que cada uma das estruturas produzia um padrão motor específico. Três das estruturas (MB, HP e CO) produziam uma locomoção para a frente, com padrões de resposta distintos entre as três, contudo as CS produziam um comportamento motor completamente diferente. Quando ativadas, estas estruturas faziam com que a mosca andasse para trás, virasse para uma outra direção, e depois prosseguisse com marcha à frente nessa outra direção. Foi também descrito que três das quatro estruturas (HP, CO e CS) necessitavam de circuitos no cérebro para produzir o seu padrão motor, dado que quando decapitadas, as moscas não reagiam ao estímulo luminoso. De modo a compreender melhor o que poderia produzir este comportamento originário da ativação das campaniform sensilla, foi estudado o seu padrão de expressão, que parecia demonstrar que as células marcadas nas patas projetavam cada uma para o

respetivo neurópilo do cordão nervoso central. Contudo, mostrou também um conjunto de projeções vindas das antenas, e que inervavam os lóbulos antenais. Com receio de que o comportamento fosse originário destas projeções, foram testadas moscas que tinham as antenas amputadas, e que continuavam a produzir o mesmo padrão motor.

O presente projeto tem assim como objetivos: I) descrever o comportamento motor produzido aquando da ativação das *campaniform sensilla*, assim como investigar a função das antenas no mesmo; II) testar o comportamento das moscas quando as CS são inativadas; III) criar um paradigma que possibilite o teste destas estruturas sensoriais em moscas em movimento; IV) investigar os intermediários entre o estímulo das campaniform sensilla e o padrão motor originado; V) e por fim, fazer um pequeno rastreio de linhas que possam servir como novas ferramentas para o estudo das campaniform sensilla, utilizando o sistema Split-Gal4.

Na primeira secção do estudo das *campaniform sensilla*, observámos que a estimulação das mesmas de facto produz um padrão motor trifásico, composto por um momento de velocidade de valor negativo (marcha à ré), seguido de um momento de elevada velocidade angular (consistente com a viragem), e um momento de velocidade de valor positivo (marcha à frente, após a viragem). De seguida, tirando partido dos dados obtidos anteriormente no laboratório para moscas com as antenas amputadas, e utilizando um segundo grupo de moscas com o sistema de expressão alterado para restringir a expressão à cabeça, mostramos como as moscas sem antenas produzem um comportamento similar ao comportamento das moscas originais, e que a estimulação das projeções das antenas produz um padrão motor distinto daquele previamente observado.

Na segunda secção do estudo, tentamos criar um novo paradigma que permite estimular as moscas optogeneticamente, durante a sua locomoção, fazendo-as atravessar uma linha laser. Contudo, este paradigma mostrou-se não eficaz para as linhas em estudo no projeto, e, portanto, foi abandonado.
Na terceira secção utilizámos um conjunto de túneis em que a altura diminui à medida que a mosca avança, tentando criar novas pressões que ativem as *campaniform sensilla*. Utilizando moscas onde estas estruturas foram geneticamente inativadas, observamos que apresentam uma tendência para avançar mais do que moscas com as estruturas intactas, e eventualmente ficam presas no túnel. Mostramos também, em túneis com altura constante ao longo do comprimento, que estas moscas não apresentam problemas em recuar, pelo que o motivo pelo qual acabam presas aparenta de facto ser a sua incapacidade em sentir o aumento da pressão sobre o corpo.

Na quarta secção do projeto produzimos uma linha recombinante que nos permite utilizar um segundo sistema de expressão (LexA-LexAop) para inativar diferentes conjuntos de neurónios que foram previamente descritos como importantes para comportamentos de recuo e de viragem, enquanto ao mesmo tempo ativamos as campaniform sensilla com o sistema original (Gal4-UAS). Contudo, devido a constrições temporais, apenas fomos capazes de testar um controlo negativo para o sistema LexA-LexAop, que demonstrou que o recombinante tem um comportamento semelhante à linha original.
Por fim, na última secção do estudo tirámos partido do sistema Split-Gal4, que transforma o clássico sistema binário Gal4-UAS em um sistema de três partes, dividindo a proteína GAL4 em duas subunidades (AD – Activation domain – e DBD – DNA binding domain). Ao cruzar cinco linhas AD com quatro linhas DBD, para um total de 20 combinações possíveis, conseguimos identificar 13 linhas que marcam as CS nas patas da mosca, e uma linha que marca CS e CO. As restantes seis linhas não apresentavam expressão, ou apresentavam um padrão de expressão aberrante.

Com este trabalho procuramos providenciar mais informação sobre o funcionamento das estruturas sensoriais que são as campaniform sensilla, assim como dar novas técnicas para o seu estudo. Tendo em

conta o quão conservado o controlo motor é entre organismos de diferentes complexidades, acreditamos que uma melhor compreensão do funcionamento das CS pode vir a dar novo conhecimento em organismos como os mamíferos, podendo até originar novos métodos de análise e tratamento de patologias que originem deficiências nos sistemas de proprioceção e controlo motor.

Palavras-chave: *Drosophila*, Proprioceção, Sensila campaniforme, Optogenética.

Abstract

Movement is an important part of the life of most organisms. Whether it is to find sustenance or flee from danger, animals need to produce movement. The system behind motor control is conserved amongst a large variety of animals. In the current study, we utilise *Drosophila melanogaster* as a model for locomotor behaviour, a particular form of movement. The fruit fly can control its movement thanks to a set of neural circuits distributed along the central nervous system, composed by the brain and the ventral nerve cord. To produce a motion, information coming from higher order centres in the brain through descending neurons gets to the ventral nerve cord, where interneurons will interact with the output from central pattern generators (source of rhythmic signals), to induce muscle contractions via the motor neurons. To adjust this movement and provide a fine motor control, there is the need for proprioceptors, structures attached to sensory neurons that inform the circuit on how a movement is being produced. In the legs of the fly, there are four mechanosensory proprioceptors, each with a specific function: the Mechanosensory bristles, the Hair plates, the Chordotonal organ and the Campaniform sensilla. Previous work has shown that optogenetic activation of each proprioceptor in immobile flies induces a specific motor output. Leg campaniform sensilla (load-sensors that inform of cuticle deformation, such as during the stance phase of locomotion), upon activation, produce a movement composed by three phases: backward walking, followed by turning and forward walking. Contrasting, the chordotonal organ (structure that encodes the angle of the joints) induces forward walking. It has also been described that decapitated flies do not present these behaviours, meaning that the central brain is necessary to produce them. So, the objectives of this project were to further characterize the behaviour produced upon optogenetic activation of leg campaniform sensilla in immobile and in motion flies, in comparison with the chordotonal organ induced behaviour. We also intended to describe the behaviour of flies with inactive leg campaniform sensilla. And lastly, we wanted to produce new tools to study this mechanosensory structure, starting with a system to identify intermediates between sensory input and motor output, as well as searching combinations of Split-Gal4 lines that drive the expression in leg campaniform sensilla. We started by confirming that the activation of the leg campaniform sensilla induced a three phased behaviour, starting with a peak of negative velocity (backward walking). This is followed by a change in velocity sign, and accompanied by a peak in angular velocity, correspondent to the turning behaviour that precedes the forward motion phase. We also found that inactivation of the leg campaniform sensilla inside a narrowing tunnel caused flies to get stuck, not sensing the load increase from the decreasing height. Lastly, we created two new tools to study the leg campaniform sensilla, by creating a recombinant that allows to use two expression systems for activation of campaniform sensilla and inactivation of other structures that might be a part of the neural circuit responsible for this behaviour. We also performed a small screen of Split-Gal4 lines that drive expression in the leg campaniform sensilla ending with 13 possible combinations. With this work, we hope to provide new insight into the working of these mechanosensory structures, hoping this information can someday be useful for the comprehension of similar systems in other organisms such as humans.

Keywords: *Drosophila*, Proprioception, Campaniform sensilla, Optogenetics.

Index

Figures index

Tables index

Abbreviations

ATR – All trans-retinal
AD – Activation domain unit
CNS – Central nervous system
CO – Chordotonal organ
CPG – Central pattern generators
CS – Campaniform sensilla
CSV – Comma-separated values
CX – Central complex
Dac – *Dachshung*
DacRE – Dac's regulatory enhancer
DBD – DNA binding domain unit
DNA – Desoxyribonucleic acid
EB – Ellipsoid body
F – Field (of campaniform sensilla)
Fe – Femur
FeFF – Femoral field of the front leg
FFF – Fused filament fabrication
FRT – Flippase recognition target
Flp or FLP – Flippase (gene and protein, respectively)
HP – Hair plates
G – Group (of campaniform sensilla)
GFP – Green fluorescent protein
LED – Light-emitting diodes
MB – Mechanosensory bristles
MDN – Moonwalker descending neurons
MOSFET – Metal–oxide–semiconductor field-effect transistor
PAb – Primary antibody
PBS – Phosphate-buffered saline
PBST – Triton solution diluted in PBS
PFA – Paraformaldehyde
PFV4 – Photron fastcam viewer 4
PLA – Polylactic acid
S – Single campaniform sensilla
SAb – Secondary antibody
SG[1-9] – Split-Gal4 [1-9]
Ta[1-5] – Tarsus [1-5]
Ti - Tibia
Tr - Trochanter
UAS – Upstream activation sequence
UV - Ultraviolet
VNC – Ventral nerve cord
WT – Wild-type

1 Introduction

1.1 Movement and motor control

The Cambridge Dictionary defines movement as a change of position or place (Cambridge University Press, n.d.). However, in a biological setting, movement means much more than a simple action. Movement allows organisms to change place and interact with their surroundings, to find new resources and flea from dangerous situations, to stimulate and to be stimulated. Organisms rely on movement on such an intrinsic level, that even within the organism there is movement, such as during the contraction of the heart or the peristaltic movements in the digestive system. Movement is mainly the outcome of a complex interaction between different systems of the body, usually resulting on the contraction of a single (or a set of) muscle(s). This can be voluntary, like the case of willingly bending a joint (Tresch et al., 1999), or involuntary, like a beating heart (Sperelakis, N., 1979).

Drosophila melanogaster, more commonly known as "fruit-fly", is an excellent model to study movement, not only due to its classical benefits of being a simple organism, with a fully sequenced genome, and a fast lifecycle, but also due to its rather conserved Central Nervous System (CNS) composed of a central brain and a Ventral Nerve Cord – VNC (the functional analogue of the mammalian spinal cord – Court et al., 2020), that allows researchers to make assumptions about other organisms, such as mammals (Tsubouchi et al., 2017).

A lot of work has been put into invertebrates regarding movement and motor control (more specifically, locomotion), notably in stick insect and locust (Orlovsky et al., 1999) and many of the observed features are transposable to flies (Strausfeld, N. J., 2009) – where the main components behind motor control can be found in Figure 1.1. From here on the details presented will involve studies in *Drosophila melanogaster* though, as will be shown, many are very general across taxa.

As previously mentioned, for movement to occur, there is usually the need for muscles to contract. This is done via signalling coming from the motor neurons, that innervate muscles leading to movement. These sets of neurons, however, need signals coming from specific motor circuits. In locomotion, it is thought that these signals come from the Central Pattern Generators (CPG), sets of neurons responsible for regular, reoccurring signalling that are going to produce a consistent motor pattern (Marder, E., Burcher, D., 2001). For motor signals to be coordinated and maintained in synchrony with each other, the interneurons come to play. These are responsible for making the connections between sets of neurons inside a circuit, and between different circuits (for example, keeping the coordination of the movement between sections of one leg, or the coordination between this specific leg and the remaining ones). This ensures that the motor output is consistent. There is also the need for feedback to be brought back into the circuit where the undergoing movement is being executed (proprioception), and that is the work of the sensory neurons. These sets of neurons, connected to sensory structures called proprioceptors, are responsible for informing the body on internal and external stimuli, resulting in the capability of producing fine motor control during the present task. Above all these systems, there is a higher-order centre in the central brain, with sets of ascending and descending neurons to transport information to and from it (Namiki et al., 2018). Besides all the other tasks the central brain is responsible, it also commands and controls more complex motor behaviours, as well as process some information coming from the sensory neurons (Dickinson et al., 2000).

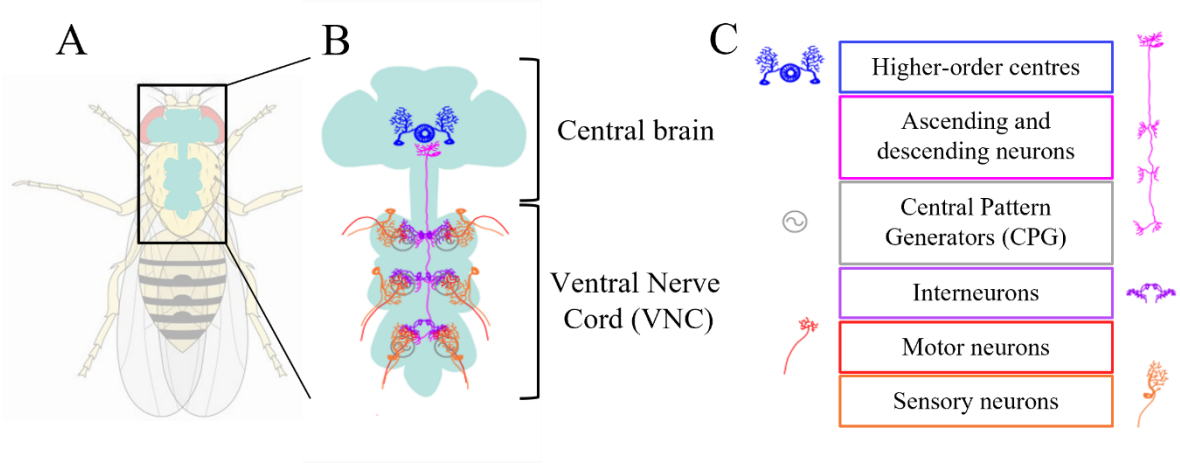

Figure 1.1– Central Nervous System and Motor Control in *Drosophila melanogaster*
Visual representation of the Central Nervous System (CNS) of the fruit fly. The CNS is composed of the Central brain, located in the head, and the Ventral Nerve Cord, located in the thorax of the fly (panels A and B). In panel C) are represented the different components necessary for motor control, that can be observed in location in panel B). These are: the higher order centres, located in the head; the ascending and descending neurons, that make the connection between the head central brain and the VNC; the CPG, thought to be in each leg neuropil, as well as the motor and sensory neurons; and last, the interneurons, responsible for making the links between different regions of the neural circuit, such as inter and intra-neuropil connections.

1.2 Proprioception

Proprioception is a highly important part for movement as the body relies on cues from the inside and the outside, in order to adapt to the always changing conditions of the environment (Kernan, M. J., 2007). Just like the nervous system, the proprioceptors are also very similar between insects and mammals, which allows for direct comparisons amongst these two quite distinct groups of organisms, even if they present contrasting levels of complexity (Tuthill, J. C., Azim, E., 2018). In the fly's leg, there are four main mechanosensory structures that inform the body of several different parameters of the movement (Figure 1.2). These are the Chordotonal Organ (CO), the Campaniform Sensilla (CS), the Mechanosensory Bristles (MB) and the Hair Plates (HP) (Tuthill, J. C., Wilson, R. I., 2016).

The femoral Chordotonal Organ is a widely studied structure that has been associated with encoding joint angle of the fly's leg (Agrawal et al., 2020). The campaniform sensilla are dome-like structures that inform the body on cuticle deformations, caused by pressure being applied to the body of the fly (whether by weight - Dean, J., 1991) - or additional stimuli such as during the stance phase of locomotion -Zill et al., 2010) (Spinola, S. M., Chapman, K. M., 1975). Mechanosensory Bristles are, as the name suggests, single tactile hairs that cover the leg of the fly, to inform about external stimuli (Tuthill, J. C., Wilson, R. I., 2016). At last, the Hair Plates are sets of tactile hairs that inform the body of joint proximity. All these structures project almost exclusively to the neuropil of the respective leg (Tsubouchi et al., 2017).

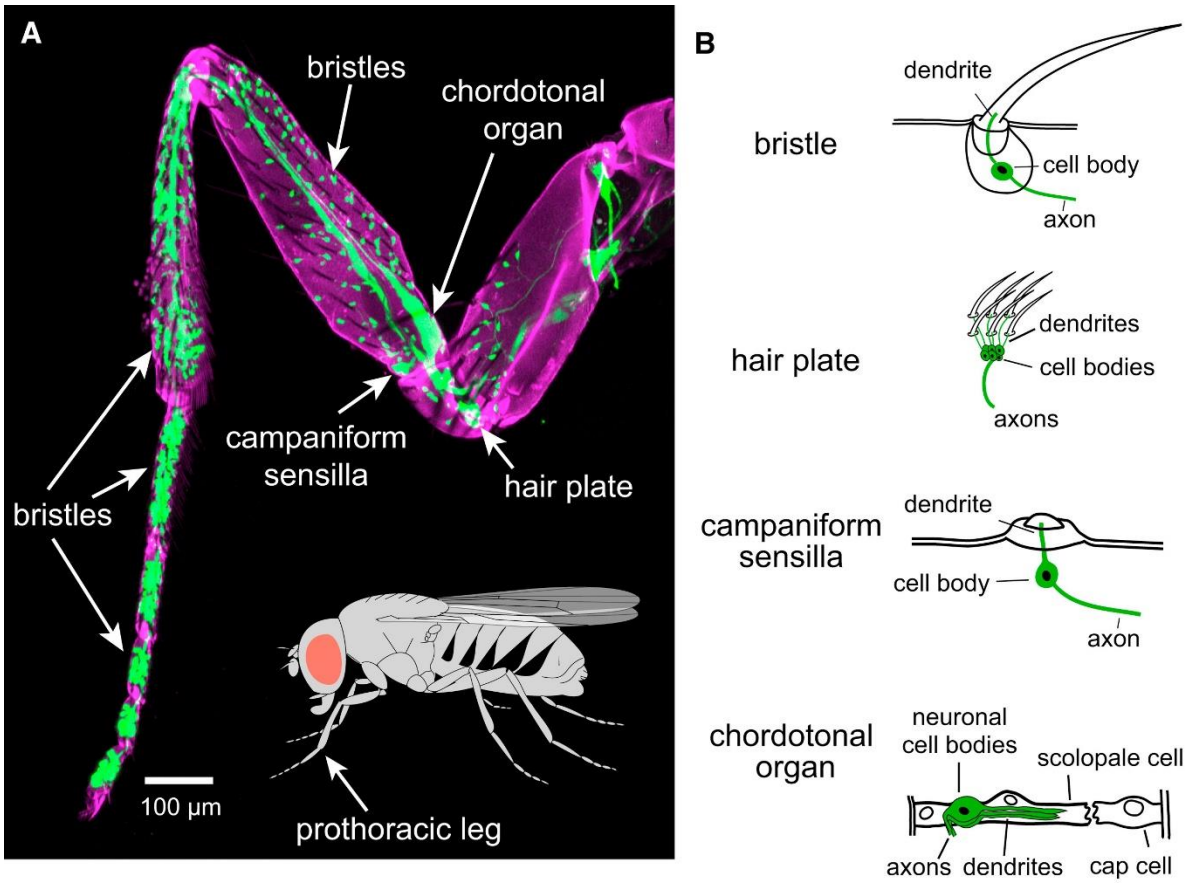

Figure 1.2– Mechanosensory structures present in the leg of *Drosophila melanogaster*
Localization and morphology of proprioceptive structures in the leg of D. melanogaster. A) GFP expression under the control of ChAT-Gal4, marking all mechanosensory neurons of the prothoracic leg. B) Visual representation of each proprioceptive structure, with the corresponding sensory neuron in green.
Adapted from Tuthill, J. C., Wilson, R. I., 2016.

1.3 Leg campaniform sensilla

The CS are domed structures attached to a singular sensory neuron (Keil, T. A., 1998), and that can be found in several places along the legs of the flies (Dinges et al., 2020, Merritt, D. J., Murphey, R. K., 1992, Figure 1.3). These structures are very well characterized in other insects such as cockroaches as load-sensors, that detect when the cuticle of the leg is deformed (Pringle, J. W. S., 1938, Schnorbus, H., 1971). This happens when, for example, in stance phase during motion (Zill et al., 1999, Noah et al., 2004), or when the organism is placed under some sort of downward pressure over the body (Ridgel et al., 2000, Noah et al., 2001), increasing the forces applied.

In Figure 1.3 we can see the distribution of the leg campaniform sensilla along the front legs. These are organized in three categories: single, groups and fields of CS (1, 2 - 4 and ≥ 5 CS, respectively), and can be found in the Trochanter, the Femur, the Tibia and the Tarsus (Dinges et al., 2020).

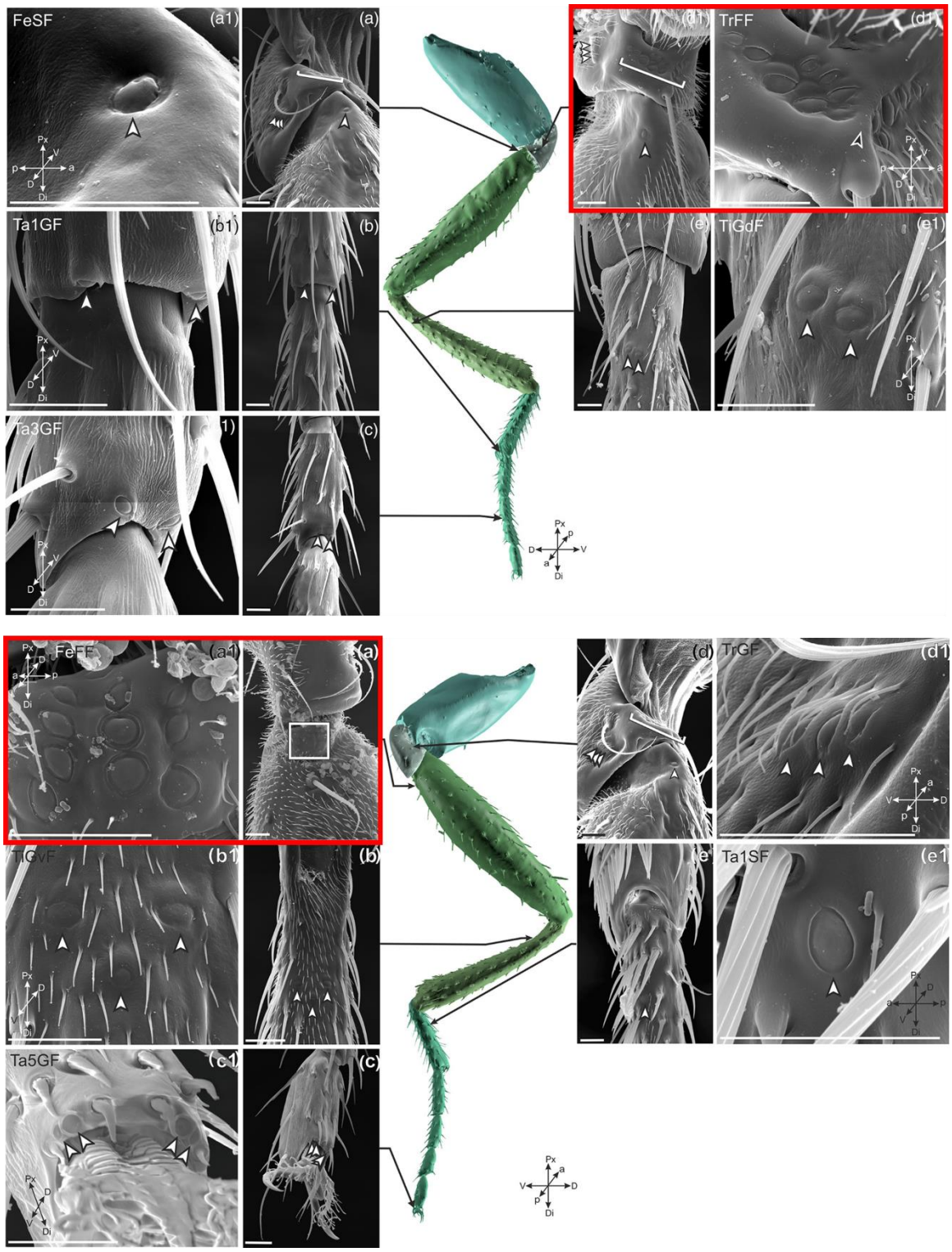

Figure 1.3 – Leg campaniform sensilla localisation
Scanning electron microscope imaging of campaniform sensilla along the prothoracic leg of *Drosophila melanogaster*. CS can be in the Femur (Fe), Trochanter (Tr), Tibia (Ti) and Tarsus (Ta [1-5]), and arranged in Fields (F), Groups (G) or as Single CS (S). Scale bar corresponds to 15 µm. Adapted from Dinges et al., 2020. Red rectangles indicate sets of CS marked in Figure 1.4.

1.4 Previous work from the laboratory

Although there are descriptions of the roles of the mechanosensory structures mentioned above during locomotion (Mendes et al., 2013; Dean, J., Wendler, G., 1983; Buschges, A., Manira, A., 1998; Ridgel et al., 2000: Zill et al., 2004), it is not clear on what is their function regarding movement initiation. The Neurogenetics of Locomotion lab of Dr. César Mendes (CEDOC), where the project of this thesis was developed, has previously done a small, unpublished screen for Gal4-drivers that mark the sensory neurons associated with these structures in the *Drosophila* leg (more information in section 2.2 - Materials and Methods). From this screen, the lab focused on four lines, each for one of the mechanosensory structures present in the fly's leg (Medeiros and Mendes, unpublished). All lines were tested on an open arena, using optogenetics (Fiala et al., 2010) to activate the mechanosensory structures with a 100 ms stimulus, triggered when, and only when, the fly stood immobile. This is important to understand what is the motor output that the sensory structures produce when no other walking behaviour is going underway (more information can be found in Materials and Methods, under section 2.3).

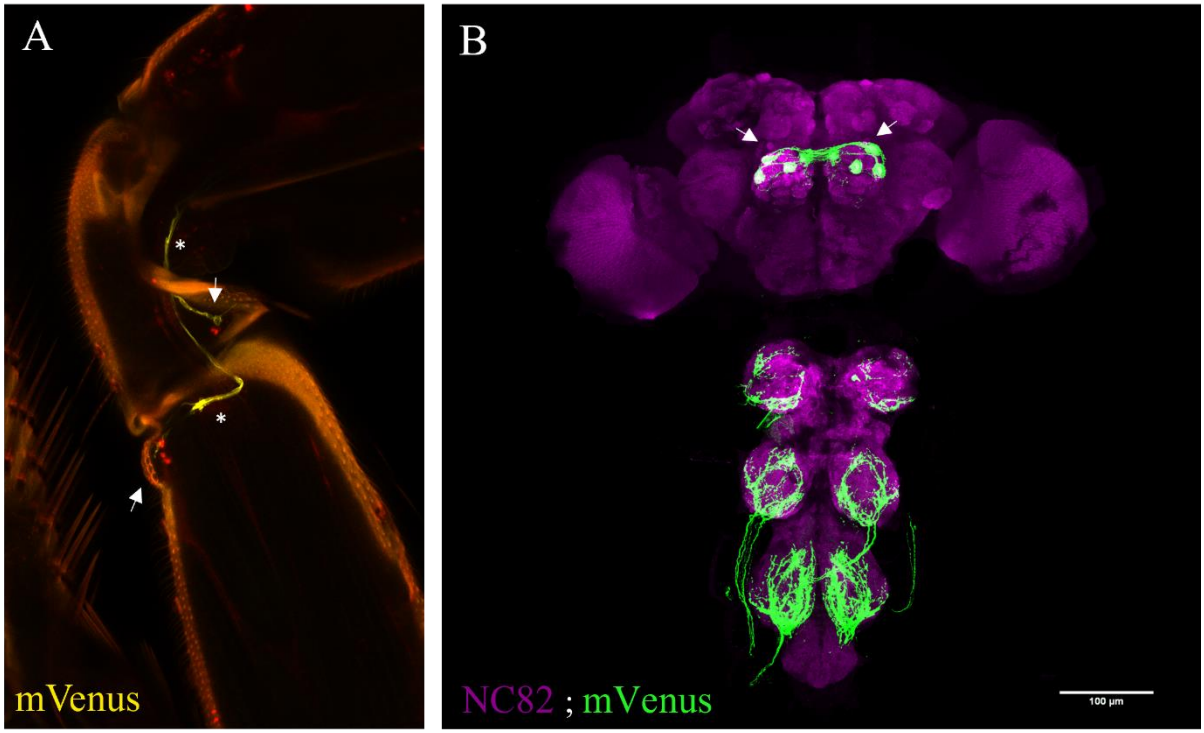

Figure 1.4 – Expression pattern of the CS (DacRE-FLP) line
Imaging of all cells marked by the campaniform sensilla line. A) In yellow are the sensory neurons associated with the campaniform sensilla, marked with mVenus (a fluorescent protein that emits fluorescence at 530 nm (Kremers et al., 2006)); in red is the autofluorescence of the cuticle. There is a clear set of cells (asterisk) which are the sensory neurons attached to the campaniform sensilla (white arrow). This set of three to four campaniform sensilla corresponds to a subset of the Femoral field of the front leg (FeFF, using the terminology from Dinges et al., 2020. B) In green are the projections of the neurons marked by the CS line, shown with mVenus. In magenta is NC82, an antibody for presynaptic active zones that shows the overall structure of the CNS. There are clear sets of projections coming from the legs and into each leg neuropil, as well as some projections coming from the antennae to the antennal lobes (white arrows). Scale bar represents 100 µm. Source: Medeiros and Mendes, unpublished.

Once all four structures were tested, it was observed that the Chordotonal Organ (CO) and Hair Plates (HP) lines induced frontward walking, the Mechanosensory Bristles (MB) line induced an uncoordinated forward walking motion, and the campaniform sensilla line presented a distinct motor output that no other line had. When stimulated, flies of this line would start by moving backwards for a

small period, followed by a quick change in direction, and then they would initiate forward motion in another direction.

Upon inspection of the expression pattern of this line, it was observed: the leg CS marked with this driver (Figure 1.4.A) are subsets of the Trochanter and Femur fields of CS (TrFF and FeFF, in Figure 1.3); there were some projections in the antennal lobes coming from the antennae (Figure 1.3.B). To exclude the possibility of this behaviour being a response to the activation of those same neurons (as it has been described that antennal activation can lead to motor responses (Hampel et al., 2020)), another experiment was performed. This consisted in the amputation of the antennae, followed by a period of one week to ensure that the projections had been degraded. These flies showed a similar behaviour to the non-amputated ones when stimulated with the 100 ms pulse of red-light.

It is also worth mentioning that, when decapitated, only the MB flies did present some induced behaviour (Medeiros and Mendes, unpublished). Taking previous work into consideration, where it has been shown that decapitated flies can maintain posture and walk (Booker, R., Quinn, W. G., 1981), this provided more insight into the mechanism behind the motor response upon activation of the CS. In fact, this result suggested that the neural circuit relies on the processing power of some structure in the Central brain, as well as ascending and descending neurons that would carry information to and from it, as is represented in Figure1.4.

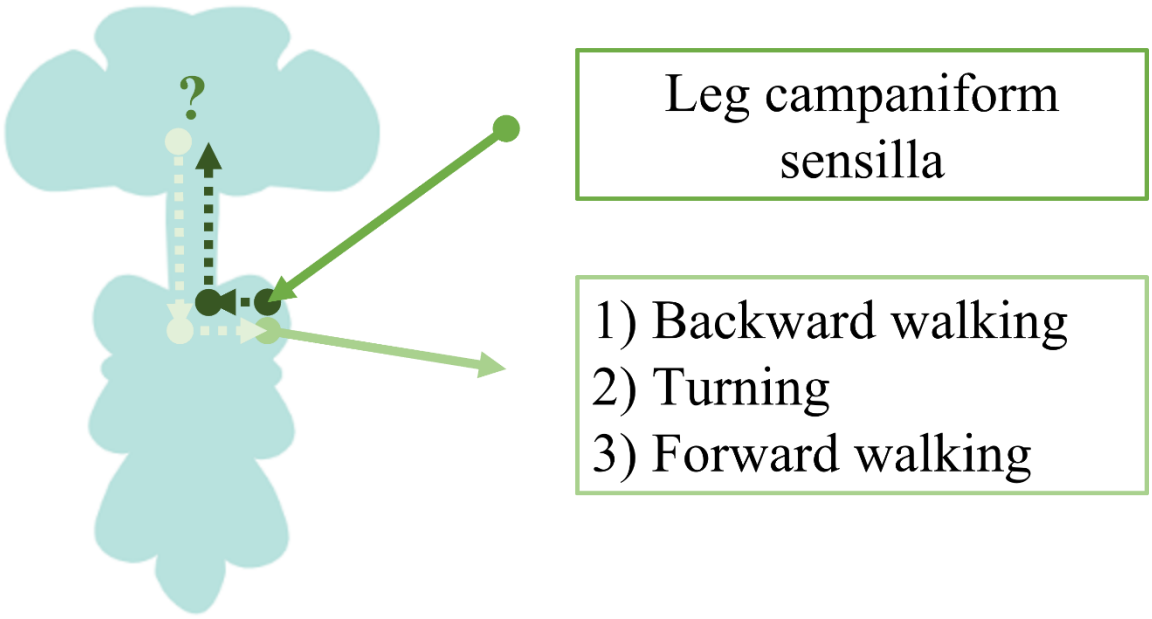

Figure 1.5 – The neural circuit between campaniform sensilla activation and motor output
Visual representation of the neural circuit known at the start of the present study. We can observe the input of the Leg campaniform sensilla coming from the leg and into the neuropil, where some neuron or sets of neurons will transport the information to some region in the central brain (dark green). This information is going to be processed. Afterwards, another neuron or sets of neurons will transport the information back to the VNC (light green), resulting in the aforementioned motor output described as a three-phased behaviour: backward walking, turning, and frontward walking in a different direction to the original.

1.5 Backward walking and turning behaviours

As previously described, the activation of leg campaniform sensilla leads to a three-component behaviour, composed by backward walking, turning and forward walking. Here we will further describe what is known about both backward walking and turning behaviours in *Drosophila melanogaster*.

Backward walking has recently been heavily described upon the identification of the Moonwalker Descending Neurons (MDN, Bidaye et al., 2014). This set of neurons has been shown not only to be sufficient to induce backward walking once activated, but also to be necessary for backward walking as the ablation of these neurons results in an inability to walk backwards. The MDN are shown to be important to control both the swing and the stance phases while moving backwards (Feng et al., 2020), as well as to also being associated with sensory inputs, both visual (Sen et al., 2017) and tactile (Sen et al., 2019). This increases the possibility of this set of neurons being in some way associated with the behaviour described when activating the leg campaniform sensilla.

Turning behaviour in *Drosophila* has been described in various levels, starting with the kinematics (Strauβ, R., Heisenberg, M., 1990) and how the turning occurs during motion, until which regions of the CNS might be associated with turning. The Central Complex (CX), a region of the central brain, has been associated with sensory cues integration, as well as producing motor outputs that can result in turning behaviours (Strauss, R., 2002; Pfeiffer, K., Homberg, U., 2014; Strauss, R., Heisenberg, M., 1993). Regions of the CX such as the Ellipsoid Body (EB) have also been associated with turning behaviour, and more specifically turning impairments upon inactivation of certain regions or sets of neurons, such as the Ring neuron circuits, and the E-PGs, a set of columnar neurons that connect the EB to the Protocerebral bridge and the Gall (Kottler et al., 2019). In fact, inactivation of the R2/R4m and R3/R4d regions of the EB showed different turning abilities in freely moving flies, as well as the inactivation of the E-PG neurons. Given the importance of the CX to the sensorimotor capabilities of the fly, it would also make sense that this region is associated with the behaviour that results upon activation of the leg campaniform sensilla.

1.6 Objectives

Taking into consideration the paradigm resultant of the activation of the leg campaniform sensilla, and the specific motor output it produces (characterized by moving backwards, turning, and moving in another direction), the present project has as the main objective to further describe and characterize this neural circuit. After chapter 2, where we detail the material and methods used throughout the project, we present in chapter 3 the results following specific objectives. In 3.1., we describe and quantify the walking behaviour that is produced upon leg CS activation in immobile flies; we also explore the role of the antennae and the projections to the antennal lobes in the motor output of the leg CS line. Subchapter 3.2 is dedicated to the study of the activation of the mechanosensory structures in moving flies, with the creation of a new paradigm based on making flies move across a laser beam. In 3.3., we test the function of the leg CS by inactivating this structure in a context dependant assay, by using a tunnel designed to place pressure around the flies. Subchapter 3.4 focus on the search for intermediates between the CS input and the motor output, proposing several candidates that might be responsible for the different components of the behaviour. In the fifth and final subchapter we perform a small screen where we search for Split-Gal4 lines that mark the leg campaniform sensilla, with the goal of providing new tools for the study of this structure. Finally in chapter 4 the results will be discussed, and future lines of research mentioned.

2 Materials and methods

2.1 Fly stocks and conditions

Table 2.1 – Fly stocks
All lines utilised in the different sections of the present work.

Line	Genotype	Origin
Canton S	Wild-type (WT)	Bloomington stock centre
ChAT-Gal4.DBD	; UAS-2xEGFP ; ChAT-Gal4.DBD (J8A1)	Bloomington stock centre: BL 23869
CO	$;\frac{\text{ato-FLP}}{\text{CyO}};\frac{\text{GMR79E02-Gal4 (attp2)}}{\text{Tm6b}}$	Bloomington stock centre: BL 48623
CS (DacRE-FLP)	$;\frac{\text{DacRE-FLP}}{\text{CyO}};\frac{\text{GMR22E04-Gal4 (attp2)}}{\text{Tm6b}}$	Bloomington stock centre: BL 49873
CS (Eyeless-FLP)	$;\frac{\text{Eyeless-FLP}}{\text{CyO}};\frac{\text{GMR22E04-Gal4 (attp2)}}{\text{Tm6b}}$	Bloomington stock centre: BL 49873
CS (Recombinant)	$;\frac{\text{DacRE-FLP}}{\text{CyO}};\frac{\text{GMR22E04-Gal4(attp2).UAS>>Chrimson.mVenus(VK5)}}{\text{Tm6b}}$	Bloomington stock centre: BL 49873
EB-R2/R4m-LexA	$;\frac{\text{GMR32H08-LexA (attp40)}}{\text{CyO}};\frac{Tm2}{\text{Tm6b}}$	Bloomington stock centre: BL 53566
EB-R3/R4d-LexA	$;\frac{\text{GMR70B04-LexA (attp40)}}{\text{CyO}};\frac{Tm2}{\text{Tm6b}}$	Bloomington stock centre: BL 61589
Empty-LexA	$;\frac{\text{(empty)-LexA (attp40)}}{\text{CyO}};\frac{Tm2}{\text{Tm6b}}$	Bloomington stock centre: BL 77691
E-PG-LexA	$;\frac{\text{GMR60D05-LexA (attp40)}}{\text{CyO}};\frac{Tm2}{\text{Tm6b}}$	Bloomington stock centre: BL 52867
LexO-Kir2.1	$W^{-};\frac{\text{Sp}}{\text{CyO}};\frac{\text{LexAop-Kir2.1}}{\text{Tm2,Ubx}}$	Gift from Barry Dickson
MDN-LexA	$;\frac{\text{VT044845-LexA (attp40)}}{\text{CyO}};\frac{Tm2}{\text{Tm6b}}$	Gift from Barry Dickson
nSyb-Gal4.DBD	;; R57C10-Gal4.DBD (attp2)	Bloomington stock centre: BL 69852
SG1 (Gal4.AD)	$;\frac{\text{R14F05-Gal4.AD (attp40)}}{\text{CyO}};\frac{\text{Tm2}}{\text{Tm6b}}$	Bloomington stock centre: BL 68295
SG2 (Gal4.AD)	$;\frac{\text{R39B11 -Gal4.AD (attp40)}}{\text{CyO}};\frac{\text{Tm2}}{\text{Tm6b}}$	Bloomington stock centre: BL 71040
SG3 (Gal4.AD)	$;\frac{\text{R72H06 -Gal4.AD (attp40)}}{\text{CyO}};\frac{\text{Tm2}}{\text{Tm6b}}$	Bloomington stock centre: BL 71129
SG4 (Gal4.AD)	$;\frac{\text{R70C12 -Gal4.AD (attp40)}}{\text{CyO}};\frac{\text{Tm2}}{\text{Tm6b}}$	Bloomington stock centre: BL 71123
SG5 (Gal4.AD)	$;\frac{\text{R22E04 -Gal4.AD (attp40)}}{\text{CyO}};\frac{\text{Tm2}}{\text{Tm6b}}$	Bloomington stock centre: BL 69487
SG6 (Gal4.DBD)	$;\frac{\text{Bl}}{\text{CyO}};\frac{\text{R43C10-Gal4.DBD (attp2)}}{\text{Tm2}}$	Bloomington stock centre: BL 69610
SG7 (Gal4.DBD)	$;\frac{\text{Bl}}{\text{CyO}};\frac{\text{R14F05-Gal4.DBD (attp2)}}{\text{Tm2}}$	Bloomington stock centre: BL 68941
SG8 (Gal4.DBD)	$;\frac{\text{Bl}}{\text{CyO}};\frac{\text{R22E04 -Gal4.DBD (attp2)}}{\text{Tm2}}$	Bloomington stock centre: BL 68303
SG9 (Gal4.DBD)	$;\frac{\text{Bl}}{\text{CyO}};\frac{\text{R70C12 -Gal4.DBD (attp2)}}{\text{Tm2}}$	Bloomington stock centre: BL 69821
UAS>>Chrimson	;; UAS>>Chrimson-mVenus	Shirangi et al., 2016
UAS>>Ricin	;; UAS>>Ricin (attp2)	Bloomington stock centre: BL 29001
UAS-GFP (II)	$;\frac{\text{20xUAS-6xGFP}}{\text{CyO}};\frac{\text{Tm2}}{\text{Tm6b}}$	Venkatasubramanian et al., 2019
UAS-GFP (III)	$;\frac{Sp}{\text{CyO}}$; 20xUAS-6xGFP	Venkatasubramanian et al., 2019

All tested flies were females, between 1 and 4-days-old, maintained at 25°C, 70 % humidity and a 12h light, 12h dark cycle, with agar-based food. To select the correct genotypes, flies were numbed using ice, placed after selection in a new vial with fresh food. Flies were tested between 24h-72h after selection, to ensure the behaviour was not affected by the numbing process. Some stocks were raised in different food compositions - presence/absence of All Trans-Retinal, to activate/inactivate the Chrimson protein (more information ahead).

2.2 Expression systems and neuronal activation/inactivation

2.2.1 Gal4-UAS and FRT-FLP

The GAL4-UAS system is a molecular mechanism discovered in yeast (Brand, A. H., Perrimon, N., 1993), that functions by promoting the expression of a specific gene of interest downstream of your Upstream Activation Sequence, or UAS region, in the DNA. This enhancer is the binding location for the transcription activator protein GAL4, that will trigger the transcription of said gene of interest. By controlling the presence of the UAS region and the expression of the GAL4 protein, one can pinpoint where exactly there will be the expression of the gene of interest, since there will only be transcription in cells where both components are present.

To further restrict the expression to the leg of the fly, we also used an FRT-FLP recombination filter. By having a Flippase Recognition Targets (FRT)-STOP cassette between the UAS and the transcript, the expression of this protein is limited to cells that also have the recombinase flippase (FLP) protein (Struhl, G., Basler, K., 1993) , which "flips-out" the STOP cassette. In an analogous manner to what happens with the GAL4-UAS system, only by driving the expression of the Flp gene you can make sure that the FRT-bound cassette will be removed. This will allow the gene downstream of the UAS region to be transcribed, in the presence of the GAL4 protein. Figure 2.1 represents how the system works.

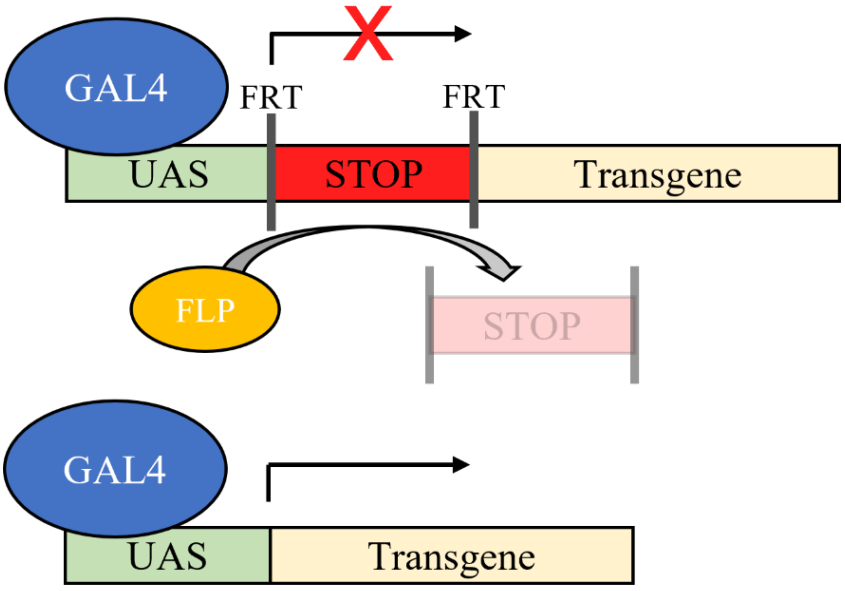

Figure 2.1 – The Gal4-UAS system, in combination with the Flp-FRT recombination filter
Visual representation of the functioning of the Gal4-UAS and the Flp-FRT systems combined. Above, the system in a functionally inactive form, where the FRT cassette possessing a STOP codon is present between the UAS region and the transgene. In the presence of a flippase protein, the FRT-bounded cassette will be removed, originating the active form of the system, as seen below. In this case, the transcription of the transgene is possible.

Like the previously described Gal4-UAS system, another binary expression system, the LexA-LexAop (for more information, see reference Lai, S., Lee, T., 2006), was also utilised.

2.2.2 Activating and inactivating neurons

In order to remotely activate the sensory structures, we used the Gal4-UAS system with a Flp-FRT recombination filter to express Chrimson (Klapoetke et al., 2014). This is a channelrhodopsin that, when shined upon with red light (590 nm), depolarizes the neuron it is being expressed in, meaning we could stimulate these mechanosensory structures on command. One aspect of this protein is the fact that it needs a cofactor to function, called All-Trans-Retinal (ATR). For these optogenetic experiments, flies were raised and maintained in food supplemented with 200 µM ATR. These vials were wrapped in aluminium foil to prevent light from stimulating the flies while developing. No ATR food was also utilised for the negative controls in optogenetics, and the remaining composition was the same as the agar-based food, but no ATR was added.

For neuron inactivation, and depending on the binary system used (Gal4-UAS or LexA-LexAop), two transgenes were expressed. For the Gal4-UAS system, we used Ricin (Moffat et al., 1992), a protein that leads to cell death where it is produced, providing a tool to do inactivation of the mechanosensory structures. In the case of the LexA-LexAop system, we used Kir 2.1. This is an ionic channel that hyperpolarises the neurons where it is expressed by letting potassium enter the cell (Baines et al., 2001), and thus inactivating the neurons as well.

2.2.3 Split-Gal4

During the duration of the current study, a new screen was also initiated, in the hopes of producing a new tool to genetically mark the different mechanosensory structures. This was done by taking advantage of previously described Split-Gal4 lines and testing possible combinations. The Split-GAL4 system is a derivative from the original GAL4-UAS, where the presence of the GAL4 protein transcribes the region that is downstream of the UAS region. However, in this case, the GAL4 protein is divided into two subunits – the Activation Domain unit (AD), and the DNA Binding Domain unit (DBD). The two units have been fused with leucine zipper dimerization motifs, allowing them to fuse together when expressed in the same cell. This produces a three-party system, where the expression of the transgene downstream of the UAS region is dependent on the presence of the GAL4-AD and GAL4-DBD subunits. This technique would allow us not to use a Flp-FRT recombination filter, and still have a restrict expression pattern.

2.3 Arenas, tracking and data analysis

Three sets of arenas were used during this project. For a first behavioural description, and dissection of the leg CS imposed behaviour, we used the open arena (sections 3.1 and 3.4). For in motion activation of mechanosensory structures, we used the laser arena (section 3.2). And for inactivation of the campaniform sensilla, we used a combination of two tunnels (slanted and linear tunnels – section 3.3). These are now going to be referred in more detail.

2.3.1 Open arena

The open arena was composed of a 54 mm translucid acrylic disc, surrounded with a slot where a ring of water ensures flies cannot climb up the walls. On top of the arena, a transparent acrylic disc was placed, with Sigmacote brushed on the inner faced side, to prevent flies from walking in the ceiling. On top, a black translucid ring was placed to black out the surroundings of the arena. The arena was then placed over a white acrylic sheet, that served as a diffuser for white light that backlit said arena. This ensured even lighting for tracking purposes.

The arena was surrounded by 6 far-red light-emitting diodes (LED) in series, controlled by a microcontroller board. This board was connected to a metal–oxide–semiconductor field-effect transistor (MOSFET), that transformed the 5 V signal coming from the microcontroller to the 12 V the LEDs needed to function properly, by opening a gate to let 12 V pass through. Between the MOSFET and the LEDs, a variable resistor was placed to calibrate the current that got to the LEDs for the stimulus to be bright enough to trigger the optogenetic system, but low enough not to trigger Canton S flies due to the brightness of the LEDs. This resistor was set to 52 Ω. This results on an average intensity of the LEDs of 0.016 mW/mm^2. Below is a schematic representation of the circuit used (Figure 2.2).

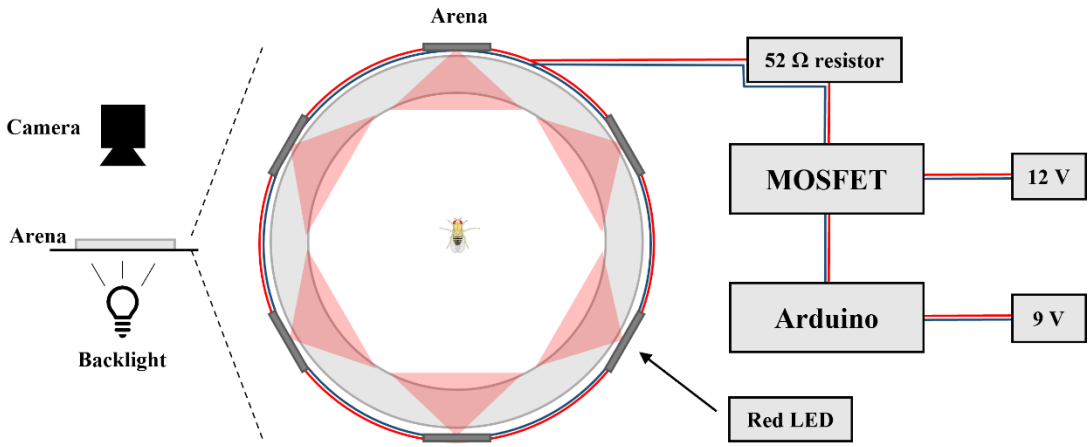

Figure 2.2 – Open arena setup and wiring
Visual representation of the open arena setup, as well as the wiring for the red LED used in optogenetic stimulation. The open arena is located between a backlight to illuminate the arena, and a camera that is used to film the flies. It composed by a 54 mm in diameter circular region where the fly is placed, surrounded by a ring and with a transparent glass on top. Surrounding the arena are 6 red LED that are used to activate the Chrimson protein. To control these LED there is an Arduino microcontroller, connected to a 9 V power supply, and to a MOSFET. The MOSFET is connected to a 12 V power supply that will power the LED, with a resistor between them to modulate the available current. Once the Arduino is activated, the MOSFET will let the power go through the resistor and into the LED, activating the Chrimson protein expressed in the fly.

To run experiments in the open arena, flies were placed inside the arena, and once the fly stopped moving (completely still – could not be grooming), the red light was activated, flashing one time with the duration of 100 ms. Afterwards, the resulting video of the stimulation was analysed to check if the fly was moving before the light came on. If it did, another video was recorded. Otherwise, the fly was taken out of the arena and another fly would be placed to repeat the procedure.

2.3.2 Tunnel arenas

Two sets of tunnels were designed for the current study. Both are composed of three sheets of acrylic (a 3 mm transparent sheet on top, a 1.5 mm transparent sheet in the middle, and a 3 mm translucid sheet on the bottom). Only the middle sheet is different between the two tunnels, and the three sheets of acrylic were kept together with M4 bolts and nuts.

For the Linear Tunnel, a 1.5 x 78 mm rectangular slot, with a 4 mm diameter hole on the beginning, was cut (Figure 2.3, top)

For the Slanted Tunnel, a 1.5 x 18 mm rectangular slot, followed by 1.5 x 60 mm triangular slot was cut. As with the linear tunnel, there was also a 4 mm diameter hole in the beginning of the tunnel (Figure 2.3, bottom).

The height of the tunnels was such that the fly was able to move freely, but not being able to turn around (1.5 mm high). This ensured that the fly could either move forwards in the tunnel, towards the ending, or backwards, towards the entrance.

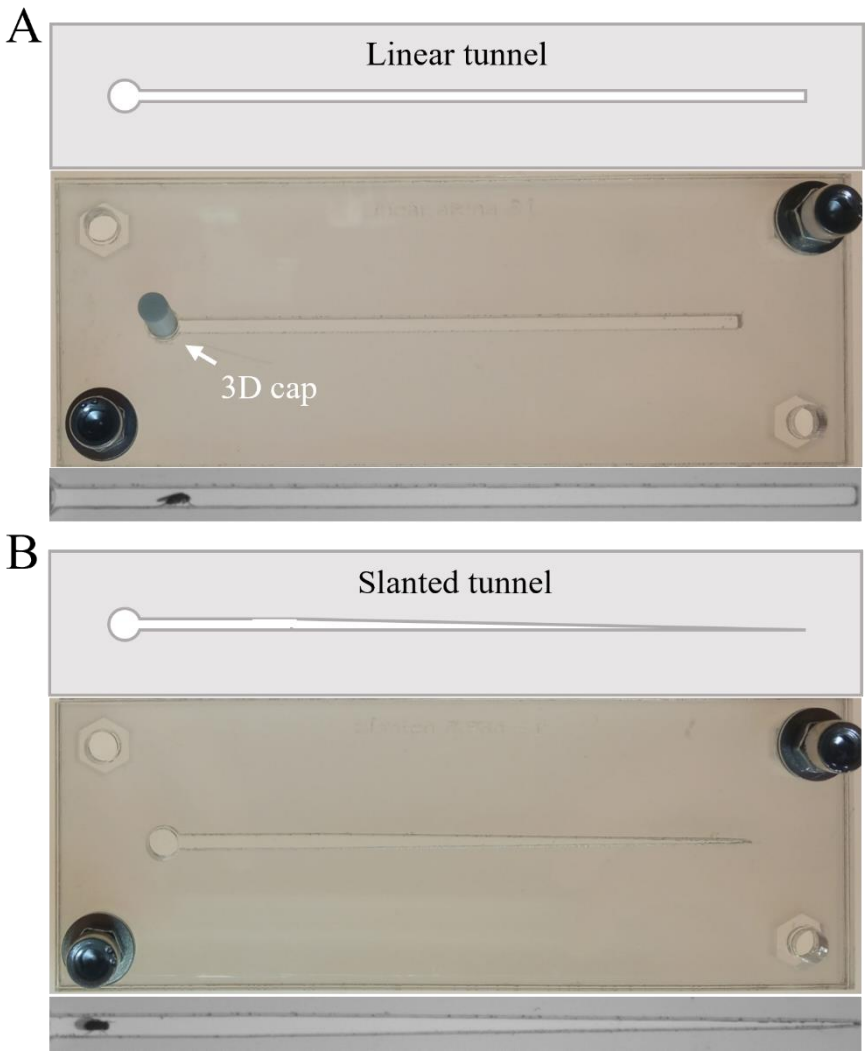

Figure 2.3 – Linear and slanted tunnels
The two tunnels used to test campaniform sensilla inactivation. A) Linear tunnel, characterized by a rectangular slot (1.5 x 1.5 x 78 mm) with a circular cut in the beginning to insert the fly inside the tunnel. Above is a visual representation, and below is a frame from a video with a fly inside the tunnel. B) Slanted tunnel, given its name due to the progressively smaller height of the tunnel as the fly moves forward (right triangle of 1.5 x 60 mm). The size of the tunnels is such that the fly cannot turn around (1.5 mm high), ensuring they are always moving forwards or backwards, facing the same direction. White arrow points to the small 3D printed cylinder that caps the tunnel so that the fly cannot get out after starting the experiment.

To run flies in the tunnels, a fly would be placed via the circular hole and the hole would be closed using a 3D printed insert. Flies would then be filmed for 10 minutes in the slanted tunnel, and 15 minutes in the linear tunnel. After the time had passed, these flies would be removed, and another one would be placed to repeat the experiment.

All acrylics were designed using Inkscape (version 0.92.4) and cut using a laser cutter.

2.3.3 Laser arena

Another setup that was created for the present project consists of a fully 3D printed arena and laser setup. This arena was composed of several 3D printer pieces that formed a 60 x 20 x 2 mm rectangle, as well as one glass slide and one coverslip (Figure 2.4). In each end of this arena, one optical fibre cable connected to an Ultraviolet (UV) light source (2 in total) would be used to attract the fly. Above this setup, a laser would cast a line of red light onto the middle of the arena, separating it into two regions. The fly would be upside down in the arena (to facilitate the light illuminating the legs) and then be attracted to each end of the arena consecutively, via the UV lights, making it go through the red-light line in the middle.

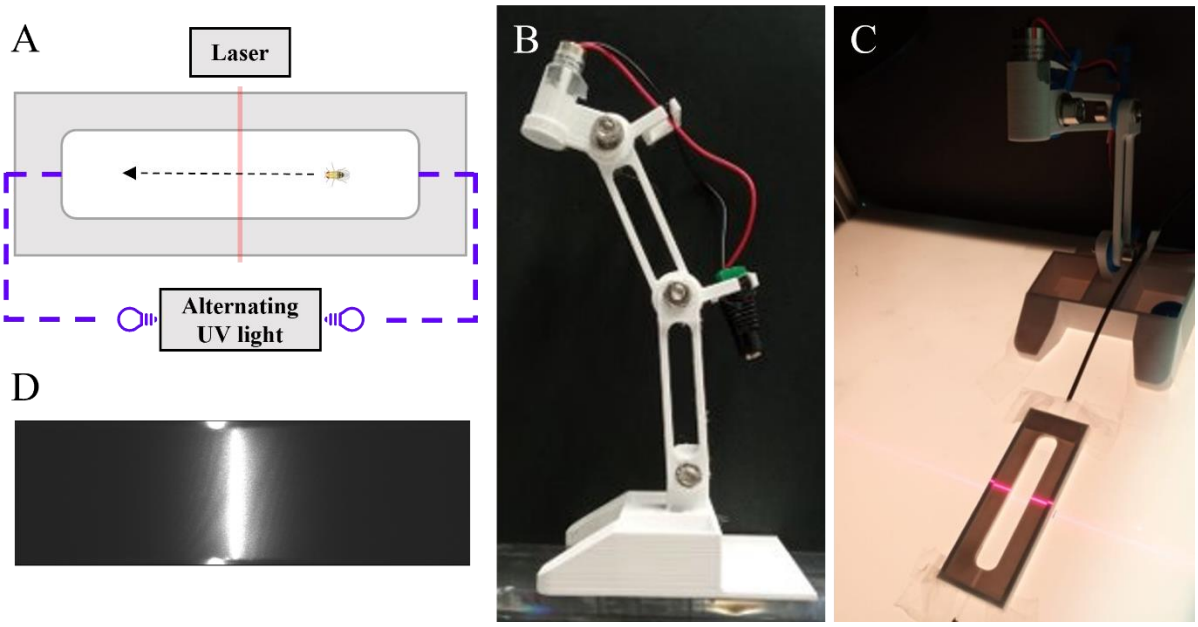

Figure 2.4 – Laser arena
Arena with a laser across the middle, to experiment with optogenetic stimulation during movement. A) Visual representation of the designed arena, composed of a 3D printed part that delimits the arena area, and has a slot on each end for an optical fibre cable to be placed. B) Picture of the 3D printed laser setup, composed by a base, arms connected with M6 bolts, and a head that holds a 5V laser. C) Picture of the arena in place, with the laser turned on and crossing the midline of the arena. D) Image of the intensity of the red-light beam crossing the middle of the arena.

2.3.4 Recording and video processing

Videos were recorded using a Point Grey Research Flea3 camera (model FL3-U3-32S2M), and the FlyCap2 program (version 2.13.3.61) to control its settings. All camera settings were maintained throughout testing. For optogenetic experiments, a red-light filter was used to remove the flashing of the LEDs. After recording, each video was cut using the Photron Fastcam Viewer 4 (PFV4), version 4.0.3.4.

For optogenetic experiments, the frame of stimulation (moment where the LEDs would turn on) was identified in the PFV4 software, and the videos were cut 60 frames before, and 300 frames after said stimulation frame. This ensured all videos were the same size, and the temporal positioning of the frame of stimulation was consistent to facilitate data analysis.

For the tunnel experiments, videos were cut to a total of 9000 and 11000 frames, for slanted and linear tunnels, respectively. This was also done in PFV4, and ensured all videos in each condition were the same size.

2.3.5 Tracking and data analysis

For open arena experiments, flies were tracked using FlyTracker (Eyjolfsdottir et al., 2014), a MATLAB based software that tracks the fly's position, and outputs a file with several parameters such as position in x and y axis, orientation, velocity, and angular velocity.

Files originated from the FlyTracker were then processed using a Python script written specifically for this work, and with which all analysis were performed, as well as all plots were created. The script was created using JupiterLab (version 2.2.6), and Python 3 (Figure 2.5, left).

For the tunnel experiments, a tracker was developed in Bonsai (*Bonsai*, n.d.), by a collaborator, due to some inconsistencies when using FlyTracker. This tracker detects the fly using a pixel intensity threshold, and then outputs the position of the fly to a Comma-separated values (CSV) file. Using another Python script written for this analysis, the positions are then used to calculate the velocity of the fly (Figure 2.5, right).

We have empirically established that, if the velocity is above 0.6 mm/s in absolute value (independent of direction of movement), the fly is considered to be moving. This threshold considers the slight errors that can occur when tracking a moving object, that could lead to a false reading of the movement.

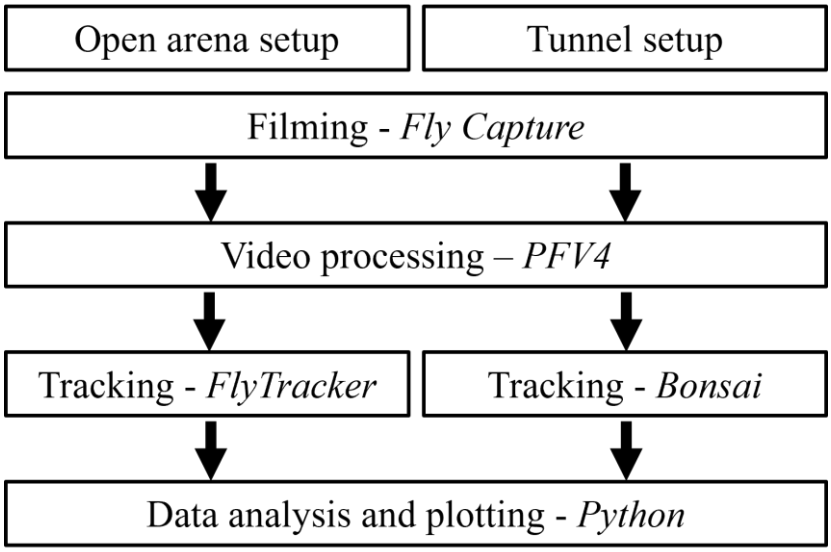

Figure 2.5 – Video analysis pipeline
Work pipeline for video filming, tracking and analysis for both the open arena and tunnel setups. The main difference between these two setups is the fact that videos were tracked in a different tracker (FlyTracker for open arena, and Bonsai for the tunnels).

Datasets were tested for normality using the Shapiro-Wilks normality test (Shapiro, S. S., Wilk, M. B., 1965). Followed by the Kruskal–Wallis one-way analysis of variance test (Kruskal, W. H., Wallis, W. A., 1952) for significant differences between different conditions, and Mann–Whitney U test (Mann, H. B., Whitney, D. R., 1947) for pairwise comparisons. All tests were performed in Python, using the *SciPy* module.

To increase the power of the statistical analysis for open arena experiments, the comparisons between different conditions were done in blocks. After the frame of stimulation, blocks of two frames would be created, resulting in a set of nine blocks per condition (18 frames in total). For each comparison between conditions, the Mann-Whitney U test would be applied to each block comparison, allowing for a more robust analysis. The sizing of the blocks (two frames) was empirically chosen as the one that most

accurately represented the observed behaviour. Significance of the comparisons can be found in the Annexes section.

2.4 3D designing and printing

All 3D printed designs were created using Fusion 360 (version 2.0.12392). Files were then sliced with PrusaSlicer (version 2.3.x) and printed in PLA filament (Polylactic acid) on an Ender-5 plus FFF (Fused filament fabrication) 3D printer.

2.5 Dissection and microscopy

2.5.1 CNS dissection

To confirm the expression pattern of the LexA line used, dissections and imaging of the CNS were performed. This was done following the Janelia FlyLight protocols for "Dissection and 2% PFA fixation for adult *Drosophila* CNS" and "Glycerol mounting" (FlyLight Protocols, n.d.).

Briefly, flies were dissected in Phosphate-buffered saline (PBS) solution, fixed with 2% Paraformaldehyde (PFA) for 1h, and then washed 4 times in 0.5% Triton solution diluted with PBS (PBST), for 10-20 minutes. Tissues were left overnight in 0.5% PBST, in a shaker, at 4°C. The second day of the protocol starts by a 30-minute wash in 0.5% Saponin solution diluted with 0.5% PBST. After removing the medium, tissues were left incubating in the Primary antibody (PAb), at a concentration of 1:10 (diluted in 0.5% PBST), for 3 overnights. The PAb used was NC82, a marker for Bruchpilot, that shows all presynaptic active zones (DSHB Cat# nc82, RRID: AB_2314866). On the fifth day, 3 washes of 30 minutes each were performed to remove the PAb. Afterwards, the Secondary antibody (SAb) was added to the tissues, at a concentration of 1:250 (also diluted in 0.5% PBST), and left at 4°C for 3 overnights. The SAb used was Alexa 647 Donkey Anti-mouse (Jackson ImmunoResearch Labs Cat# 715-605-150, RRID: AB_2340862). In the last day (day 8) the protocol starts with 3 washes with 0.5% PBST and a duration of 30 minutes, and then 1 wash with PBS for 20 minutes. Tissues were then mounted in 80% Glycerol (diluted in PBS) and kept at 4°C until imaging.

All dissected tissues (with exception to the EB-R2/R4m-LexA line) were imaged in a Confocal Zeiss LSM 710, using lighting in wavelengths of 647 nm and 488 nm, for both the SAb and the GFP expressed, respectively.

The EB-R2/R4m-LexA line was imaged with a Confocal Zeiss LSM 980, using lighting in the wavelengths of 639 nm and 488 nm, for both the SAb and the GFP expressed, respectively.

All images were then compiled using ImageJ, taking advantage of the Bio-formats plugin.

2.5.2 Leg dissection

To identify the mechanosensory structures that each Split-Gal4 line marked, we followed the (Guan et al., 2018) protocol for dissection and imaging of the front leg, using GFP expressing lines.

All samples were then imaged in a Widefield Axioimager Z2 microscope, using a combination of white light, as well as the wavelengths of 590 nm and 488 nm, to image the overall leg structure, cuticle autofluorescence and GFP expression signal, respectively.

All images were compiled using ImageJ.

3 Results

3.1 Optogenetic activation in immobile flies

3.1.1 Leg campaniform sensilla activation

The first set of experiments performed consisted in repeating the work that had previously been done (Medeiros and Mendes, unpublished), testing for its reproducibility and increasing the sample size. We started by using two lines, analysing a total of three conditions: 1. the line for the chordotonal organ (positive control for the optogenetic activation); 2. the leg campaniform sensilla line raised in food with ATR; and 3. the line for the leg campaniform sensilla raised in no-ATR food (negative control for the optogenetic activation). All lines were tested in the open arena assay, and optogenetic stimulation was given once the fly stopped moving. These videos were then analysed with a tracker, and the data produced was processed with a Python script written for this project.

In Figure 3.1 we have a visual representation of a single fly from each condition, showing the usual response post-activation of the sensory structures. For each line we show the position of the fly in each frame (*X* and *Y* axis), starting in the point marked with 'X,' and following the black line that connects each moment. It is important to notice that points have different colours. The colour corresponds to the velocity of the fly in that specific moment, the red points are for positive velocities, meaning that the fly is moving forwards, and blue points are for negative velocities, meaning that the fly is moving backwards. Moments where the fly is not moving or at a very low speed are represented in greyish tones. This figure shows that the campaniform sensilla line raised in no-ATR food (A) produced little to no movement at all, standing still and not reacting to the stimulus. The Chordotonal organ line (B) shows a different scenario; from the moment the stimulation started until the end of the presented data, the fly showed a positive velocity, as seen by the red markings – walked forward. In contrast, in the campaniform sensilla line raised in ATR food (C), the fly has a different response to the ones observed in the controls. Here, the fly first moved backwards, then turned and started moving forwards in another direction. These three components of movement are represented on diagram D, that shows the backward walking (i), the turning (ii) and the moving forward in another direction (iii).

All responses for the three conditions coincided with the ones that were described previously (Medeiros and Mendes, unpublished), and were common amongst tested flies.

The data from all the flies of each condition were compiled and sectioned into time windows of 2 frames (for a more in-depth description on this approach, see section 2.3.5.). The velocity and angular velocity data were tested for normality within these windows, and, since most of the data did not show a normal distribution (p-values lower than 0.05), all further analysis was done using the median values (the results can be found in Tables 6.1 and 6.2, in the Annexes section). In Figure 3.2 we have the distribution of the medians of the complete dataset for both the Velocity (A) and Angular Velocity (B), for the three conditions (CS with no-ATR food in orange, CO and CS with ATR food in blue and green, respectively). The shaded areas around each line represent the median absolute deviation (a measure of variability), and the large, red bar represents the time of the stimulus (100 ms, as reported in the section 2.3.1 of the Materials and Methods). Every two frames after stimulation (approximately 0.066 s) there is a vertical bar that marks the division of sets of values used for statistical analysis.

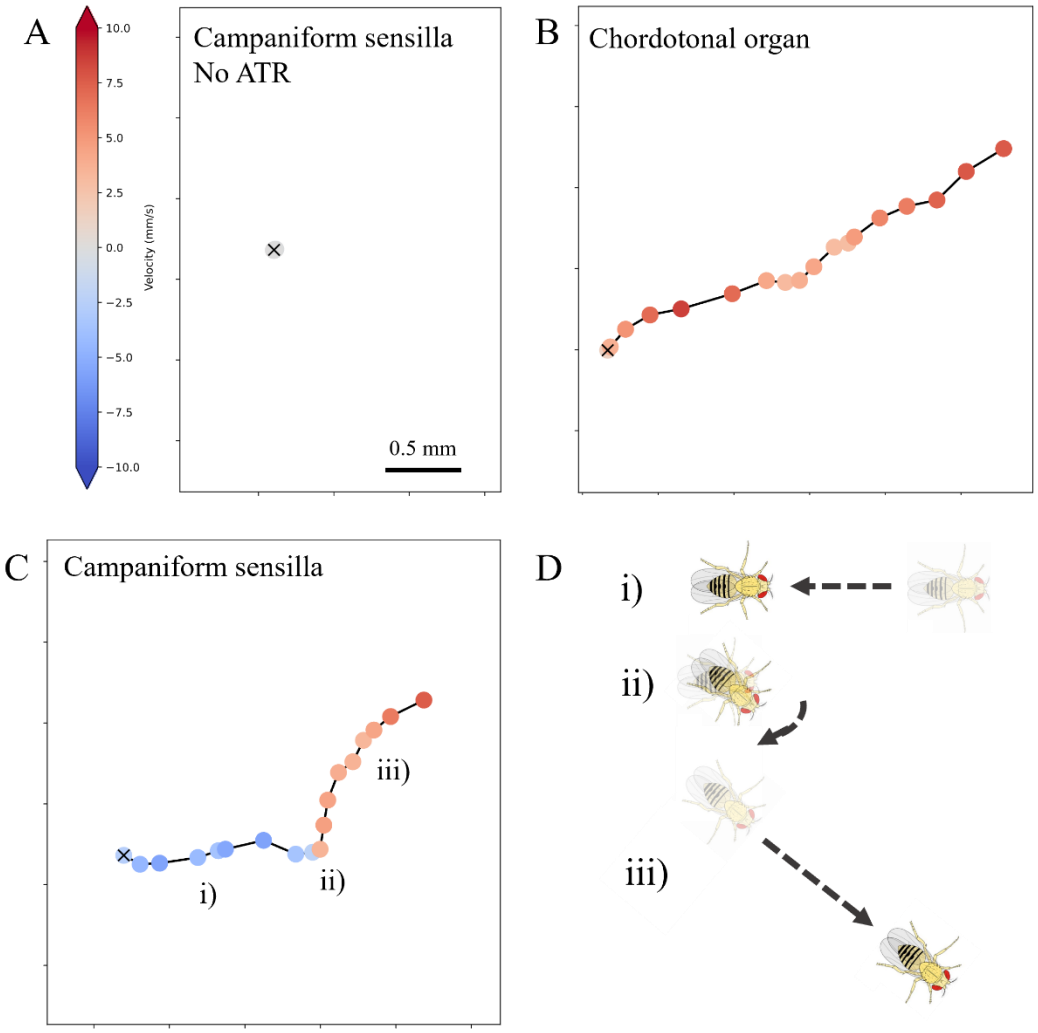

Figure 3.1- Visual representation of optogenetic activation of mechanosensory structures

Representation of the movement of singular flies after stimulation, in three different conditions. Each point represents a frame starting after stimulation (first frame marked with "X"), and has a colour that is consistent with the velocity of the fly at that moment. This colour can go from blue (negative velocity - backward walking) to red (positive velocity - frontward walking). A) Representation of the position of the fly from the campaniform sensilla line without ATR (negative control). These flies would not react to the stimulus (n = 19). B) Sample from the chordotonal organ line. Flies from this line would react to the stimulus by moving forwards (n = 15). C and D) Fly from the campaniform sensilla line raised in ATR (n = 17). These flies show a consistent behaviour of backward walking (correspondent to phase i) on panel D), followed by turning to a different direction (phase ii) in panel D) and then the fly would walk forwards, now in a new direction (phase iii) of panel D). Scalebar on panel A corresponds to 0.5 mm and is common for both axes.

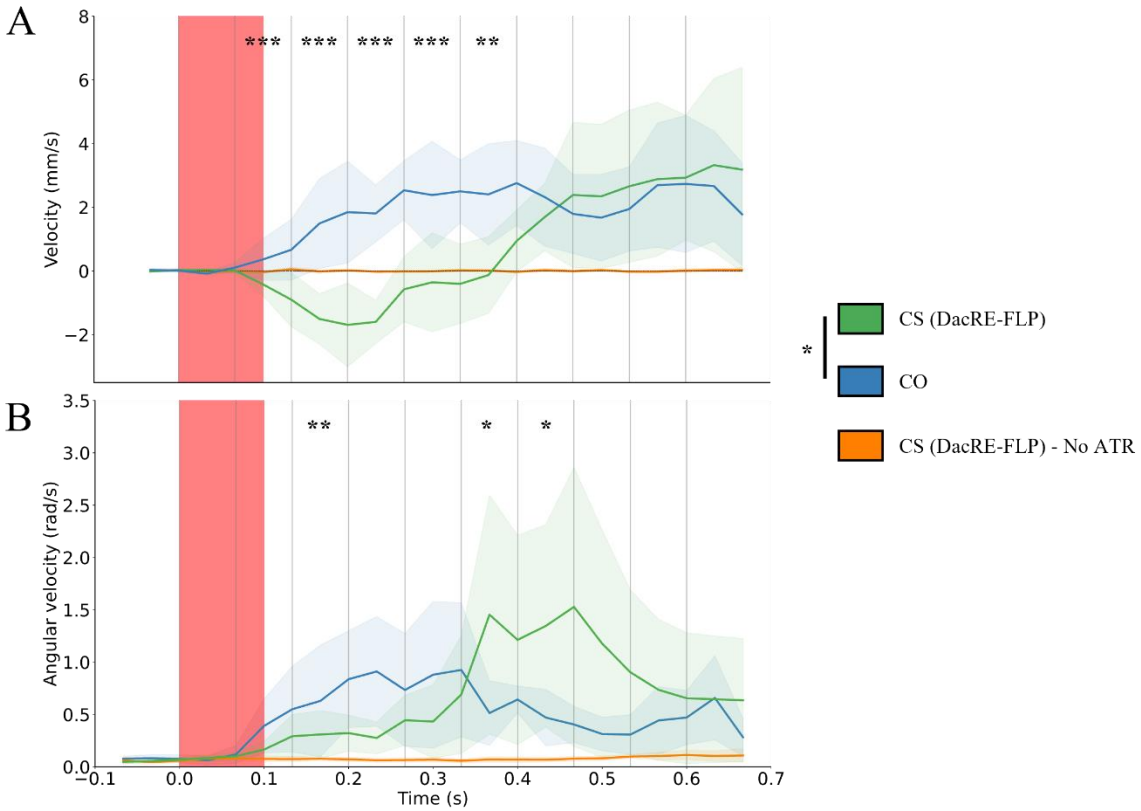

Figure 3.2- Quantification of velocity and angular velocity for optogenetic activation of mechanosensory structures
Plot for the median values of both the velocity and the angular velocity of the CS line raised in no-ATR food (n = 19), CO line (n = 15) and CS line raised in ATR food (n = 17). Shadowed regions with the same colour as the curves show the median absolute deviation. Vertical lines every 2 frames (approximately 0.066 seconds) demark the windows used for the statistical analysis between lines. Asterisks correspond to the significance of the comparison between the CS and the CO lines. Time of stimulation characterized by the red shaded bar. A) Velocity over time, with time starting at the moment of stimulation. The campaniform sensilla line without ATR (orange) shows no response to the optogenetic activation. The chordotonal organ line (blue) shows a clear forward movement, with positive values of velocity. The CS line raised in ATR (green) shows two moments, starting with a backward walking motion, and followed by a switch in movement direction. B) Angular velocity over time. The line without ATR shows again no response to the stimulus, while the CO and CS lines show a positive response. It is important to point out the large peak in angular velocity from the CS line, that corresponds to the changing of direction that is seen in the graph above. For more information on the significance of the comparisons between all conditions, for both velocity and angular velocity, see Table 6.3 in Annexes).

As seen in Figure 3.1, Figure 3.2.A shows that the three tested lines have different responses to the stimulation. The line without ATR shows no response at all (orange), while the other two lines show a motor output being initiated after stimulation. The CO line (blue) shows, as described previously and shown in Figure 3.1.B, a forward motion, characterized by the positive sign on the velocity after the beginning of the optogenetic activation. The line that marks the leg CS shows a similar response to the one presented in Figure 3.1.C with two components, a negative velocity section, and a positive velocity section. It is important to notice that these two lines (CO and CS (DacRE-FLP)) only present significant differences until the 0.4 s; after the inversion of sign of the CS line, these two lines start showing the same trend (significance values can be found in Table 6.3, in Annexes).

In Figure 3.2.B is represented the angular velocity after stimulation of the same conditions. We can see some similarities with the Figure 3.2.A graph but also differences. First, the line without ATR (in orange) shows no response to the stimulation, as had been seen in the velocity. The same way, the other two lines showed some response to the stimulus. The CO line shows a peak after stimulation, followed by an apparent plateau and consequent decrease, while the CS line shows a later response but with a higher peak, that seems to happen in the moment of the inversion of movement direction seen in 3.2.A

- around the 0.4 s. It is important to point out that in this moment, the CO line no longer is responding to the stimulation.

This set of responses is consistent to what had previously been seen by Medeiros and Mendes (unpublished), where the activation of the mechanosensory structures induces a motor output. These motor outputs are specific to each structure activated.

3.1.2 Antennal role in motor output

As it had been shown in Figure 1.3.B, the line for leg campaniform sensilla showed some projections coming from the antennal lobes. These neurons are expressing Chrimson as well, and are being activated by the optogenetic stimulation. This meant we needed to test if they have any role in the behaviour demonstrated in the previous section. We did this using two approaches: by analysing the data that had been previously produced with flies that had their antennae amputated (Medeiros and Mendes, unpublished); and using the same Gal4-driver, but with a different Flp-driver. By using the Eyeless driver (instead of the DacRE-FLP), that should restrict the expression of Flp to the head capsule, we hoped to activate solely the cells on the antennae that project to the antennal lobes.

In a first analysis of the videos of both lines, the CS (Eyeless-FLP) line presented a different motor output than the original CS (DacRE-FLP). While these flies reacted to the stimulus, this response was a small startle, that started earlier than the response of the CS (DacRE-FLP) line (more instantaneous). In fact, the reaction time looked much more like the one the CO line had (Figure 3.2.A). There was also no clear backward walking component of the movement, nor was there a strong turning behaviour as we saw after the fly had stopped backing away. In contrast, the flies without antennae seemed to produce the same motor output than the corresponding line without antennal amputation.

We then analysed the videos using the same tracker as in the other open arena analysis and ran the data in the same Python script. The results for the normality test showed again a non-normal distribution for the Eyeless-FLP line and the line without antennae (results in Tables 6.1 and 6.2, in Annexes). Given these results, we proceed with the same non-parametric analysis. We also analysed the moment where the velocity of the flies would change from negative to positive. Since the normality test of this data resulted in a P-value of 0.023 to the CS (Eyeless-FLP) line, we proceeded with a non-parametric analysis.

In Figure 3.3 we can see the results for this set of experiments, where we compare the already described CS (DacRE-FLP) line (in green) with CS (Eyeless-FLP) line in purple, and the CS (DacRE-FLP) line with amputated antennae (in black). On the top (Figure 3.3.A) we have the median velocity of all flies over time, and on the bottom (Figure 3.3.C) we have the median angular velocity of all flies over time, for each of the conditions. Each curve is surrounded by a shaded area, that as before, corresponds to the median absolute deviation. Figure 3.2.B shows the quantification of the moment of inversion of sign (moment that negative velocity changes to positive velocity) for both the CS (Eyeless-FLP) and CS (DacRE-FLP) lines. Asterisks show significance of comparisons between CS (DacRE-FLP) and CS (Eyeless-FLP) in purple, and CS with (DacRE-FLP) and without antennae (DacRE-FLP – no Antennae) in black.

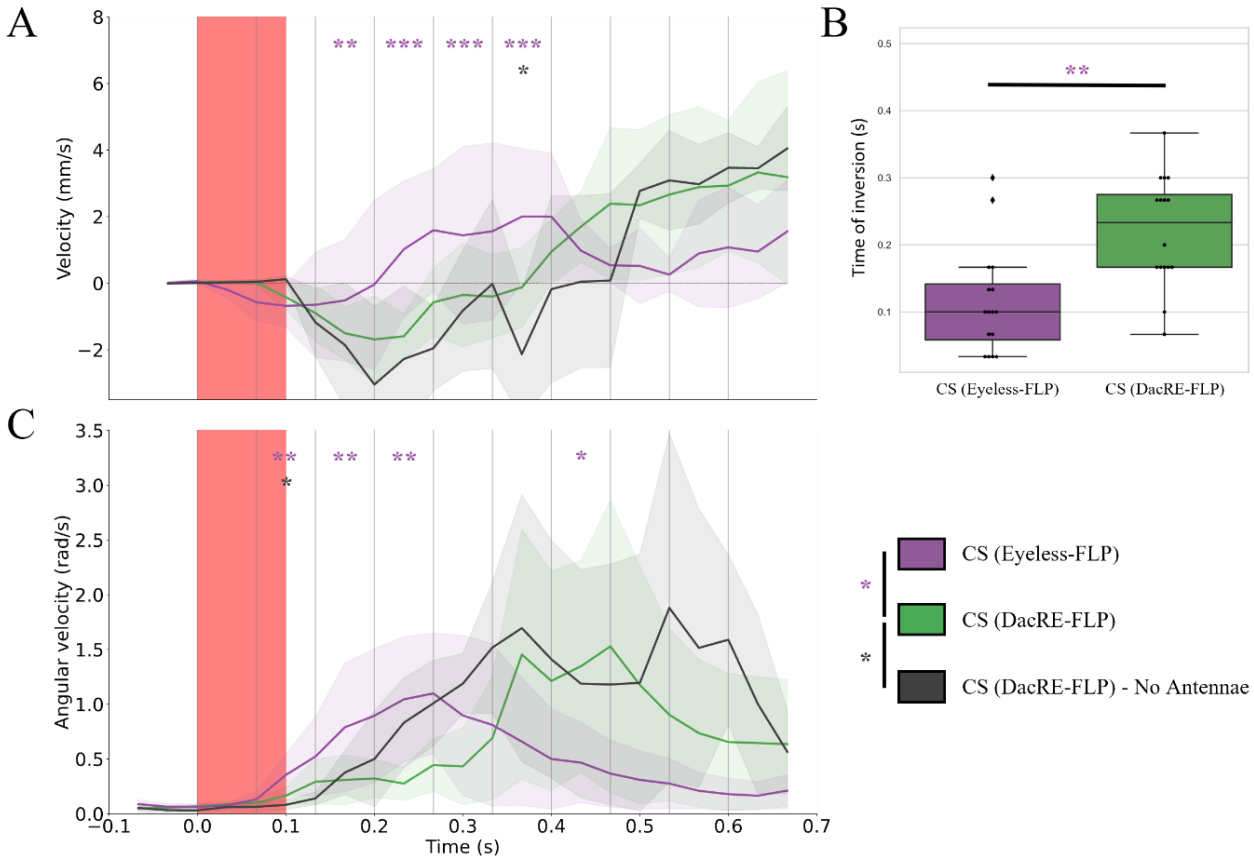

Figure 3.3 - Role of antennal expression in campaniform sensilla induced behaviour
Median values of velocity and angular velocity of the CS (DacRE-FLP) line raised in ATR food (n = 17), as well as CS (DacRE-FLP) line with the antennae amputated (n = 9), and the CS (Eyeless-FLP) line (n = 18). Around each coloured line, a shadowed region with the same colour shows the median absolute deviation. Vertical lines every 2 frames (approximately 0.066 seconds) show time-windows used for the statistical analysis between lines. Asterisks above correspond to the significance of the comparison between the CS (DacRE-FLP) and the CS (Eyeless-FLP) lines (in purple), and the comparison between CS (DacRE-FLP) and CS (DacRE-FLP) - Amputated antennae lines (in black). Red-shaded region corresponds to the stimulation. A) Velocity over time, with time starting at the moment of stimulation. The green dataset shows the same data that was observed in Figure 3.2 for the CS (DacRE-FLP) line, characterized by the negative velocity after stimulation, followed by a switch of sign and consequent forward motion. The campaniform sensilla line with the Eyeless-FLP (purple) shows a faster response to the one presented by the CS (DacRE-FLP). The response has a smaller duration of negative velocity component, resulting in a faster change of sign. The CS (DacRE-FLP) line with amputated antennae (black), from Medeiros and Mendes (unpublished), shows a similar response to the flies with antennae, with little to no significant differences. B) Quantification of the moment where the velocity sign changed from negative to positive for the CS (Eyeless-FLP) and CS (DacRE-FLP) lines. C) Angular velocity over time for the three lines. The CS (DacRE-FLP) line without antennae (in black) shows again little to no difference when compared to the CS (DacRE-FLP) line with antennae (green). There is, again, a clear difference between the line with the Eyeless-FLP when compared to the original CS (DacRE-FLP) line, presenting a faster response and a smaller peak of angular velocity.

In Figure 3.3.A it seems clear that the velocity of the response was, indeed, very distinct between the different Flp-drivers. The CS (Eyeless-FLP) line (in purple) has an almost immediate backwards motion response that lasts half the time of the CS (DacRE-FLP) backward motion (in green). In fact, there are significant differences from the third block onwards (asterisks on the top, in purple), and up until after the changing in direction of the CS (DacRE-FLP) flies (significance values can be found in Annexes Table 6.4). After the change in direction of the DacRE-FLP line, there is no longer a significant difference between the two Flp-drivers. For the flies without antennae, there is a singular moment where the differences are significant between these and the CS (DacRE-FLP) flies with antennae. Otherwise, the velocity of these two conditions is consistent along the activation of the leg campaniform sensilla.

Figure 3.3.B shows the quantification of the moment where the sign of velocity for the CS (Eyeless-FLP) and CS (DacRE-FLP) lines changes from negative to positive. It is clear there is a difference between these two, with a P-value of $5.70x10^{-3}$, showing how smaller the overall duration of the backward walking response is in the CS (Eyeless-FLP).

In Figure 3.3.C, where we can see the angular velocity of all flies from the same three conditions, the results are similar to the ones we were observing in panel A. The CS (Eyeless-FLP) line, again, shows a fast response with a smaller peak of angular velocity, similar to the one seen by the CO line in Figure 3.2.B. There are significant differences between this line and the original CS (DacRE-FLP) line, that correspond to the different moments the two peaks take place (from 0.06 s up until the 0.26 s, and in the interval 0.40-0.46 s, for the Eyeless and the DacRE flippases). As previously observed, the CS lines with and without antennae show near to no differences in response, having a single moment where there is a significant difference between the two curves. Significances for these comparisons can be found in Table 6.4, in the Annexes section.

These results go along with what had previously been seen in the first visual observation, where the flies without antennae seemed to show little to no difference to the reaction of the flies with antennae. On the other hand, the two Flp-drivers do in fact show different responses to the activation of the chrimson protein.

3.2 Optogenetic activation during motion

In order to further describe the motor behaviour resultant of leg campaniform sensilla activation, we tried to develop a paradigm that would allow us to test flies by using optogenetics to activate the mechanosensory structures, while the fly is in motion. However, due to the difficulty in timing the activation of the light with the movement of the fly and maintaining a consistent activation between different flies and conditions, we decided to follow a different direction and create a new assay.

Given the knowledge that flies are attracted to UV-light, we designed a rectangular arena that had a UV-light on each end (for more information, see section 2.3.3.). By alternating the activation of these UV-lights, we were able to make the fly move from one end of the arena to the other, pursuing the UV-lights. In the middle of the arena, perpendicular to the movement of the fly, was a line of red-light, cast with the aid of a laser. By turning the laser beam on or off, we would create two conditions that each fly would be tested in (with and without activation) and compare the resulting motor output upon optogenetic activation.

We ran this assay for the CS line without ATR as a negative control, and the CO and mechanosensory bristles line (MB) with ATR as positive controls. We also ran the CS line with ATR as the testing line. However, from the three lines that should react to the laser (CS with ATR, CO and MB), only the MB line showed a response. Taking into consideration these results, we decided not to proceed with the assay.

3.3 Leg campaniform sensilla inactivation

3.3.1 Context dependent assay

In order to further dissect the function of the leg campaniform sensilla, we opted to perform an assay that would be based on inactivation of this structure. Our objective was to create a scenario where the campaniform sensilla, a load-sensor, would be activated. With this purpose we designed a tunnel similar to the ones used in other previous works (Bidaye et al., 2014), but with a difference. Instead of having

a constant height, this tunnel gets narrower as the fly moves forwards (more information can be found in section 2.3.2.).

For this experiment we placed flies inside the tunnel and record their movement for a total of five minutes (9000 frames at 30 fps). Two genotypes were used in this assay: one line that expressed Ricin, driven by the same system utilised with Chrimson in the previous experiments, and a fly that had no UAS region nor transgene to be driven (negative control). These flies were be filmed, and the videos were then tracked (more information in section 2.3.5.).

Upon visualisation of the videos, it appeared that the line with ricin had a bigger tendency to move further into the tunnel, and most flies would actually get stuck and not be able to move backwards. The negative control did not present this behaviour so often, as only one fly had this issue.

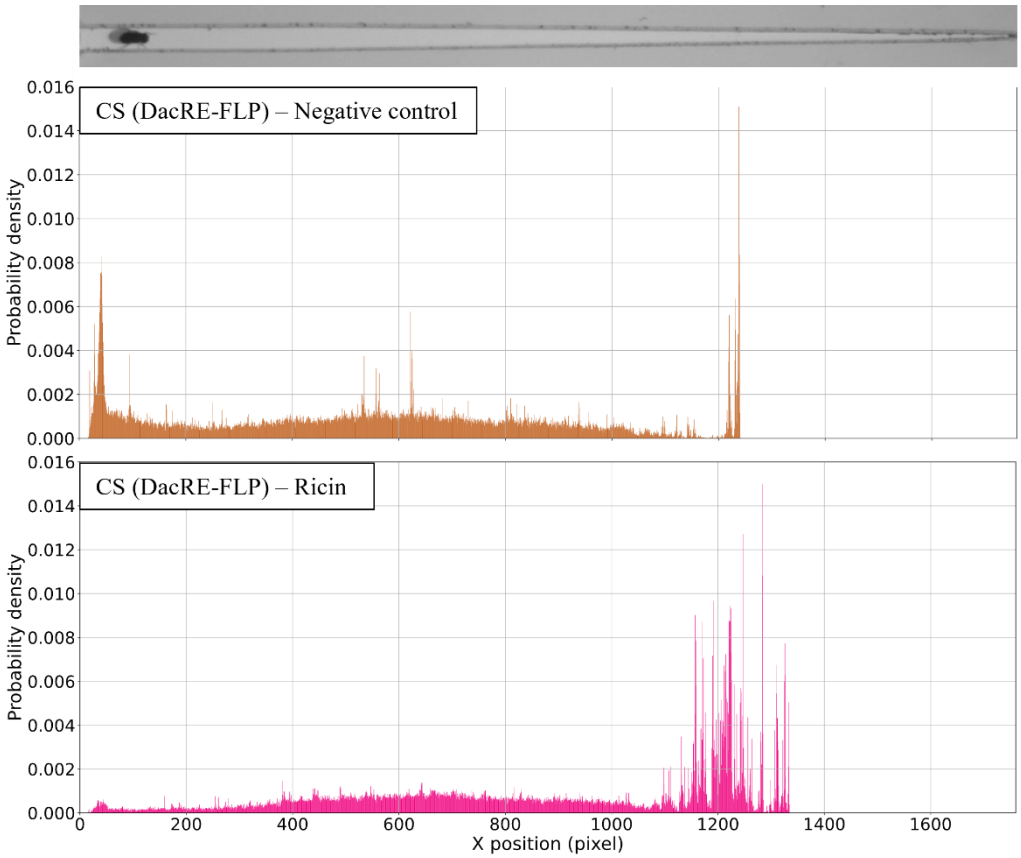

Figure 3.4- Probability density of position inside the slanted tunnel
Representation of the position of the flies from the negative control, and the flies expressing ricin in the leg campaniform sensilla. Above is a frame of a video from the negative control line, and shows how the position in the X axis is correspondent to the position inside the tunnel. Below are the probability densities of the negative control (in brown) and the line expressing ricin (in pink). Negative control has an n = 13, and ricin expressing line has an n = 16.

In figure 3.4 we have a first approach to see the data produced by the tracker. On top, we have a visual representation of the tunnel with one fly inside, and below we have two plots that show the probability density of the position of all flies along the x axis for each condition (negative control in brown, and line with ricin in pink). The position in the x axis is correspondent to the position inside the tunnel (0 is the beginning of the tunnel, and the end of the axis is the end of the tunnel). The negative control flies seem to present a preference for the beginning and the end of the tunnel, with higher probabilities at around positions 50 and 1250. In between these two values, the distribution of the data seems to be quite uniform. The flies that expressed ricin in their leg campaniform sensilla, however, show a different

response. In fact, these flies seem to prefer the end of the tunnel, and seem to move further into the tunnel, getting to places where the tunnel is narrower.

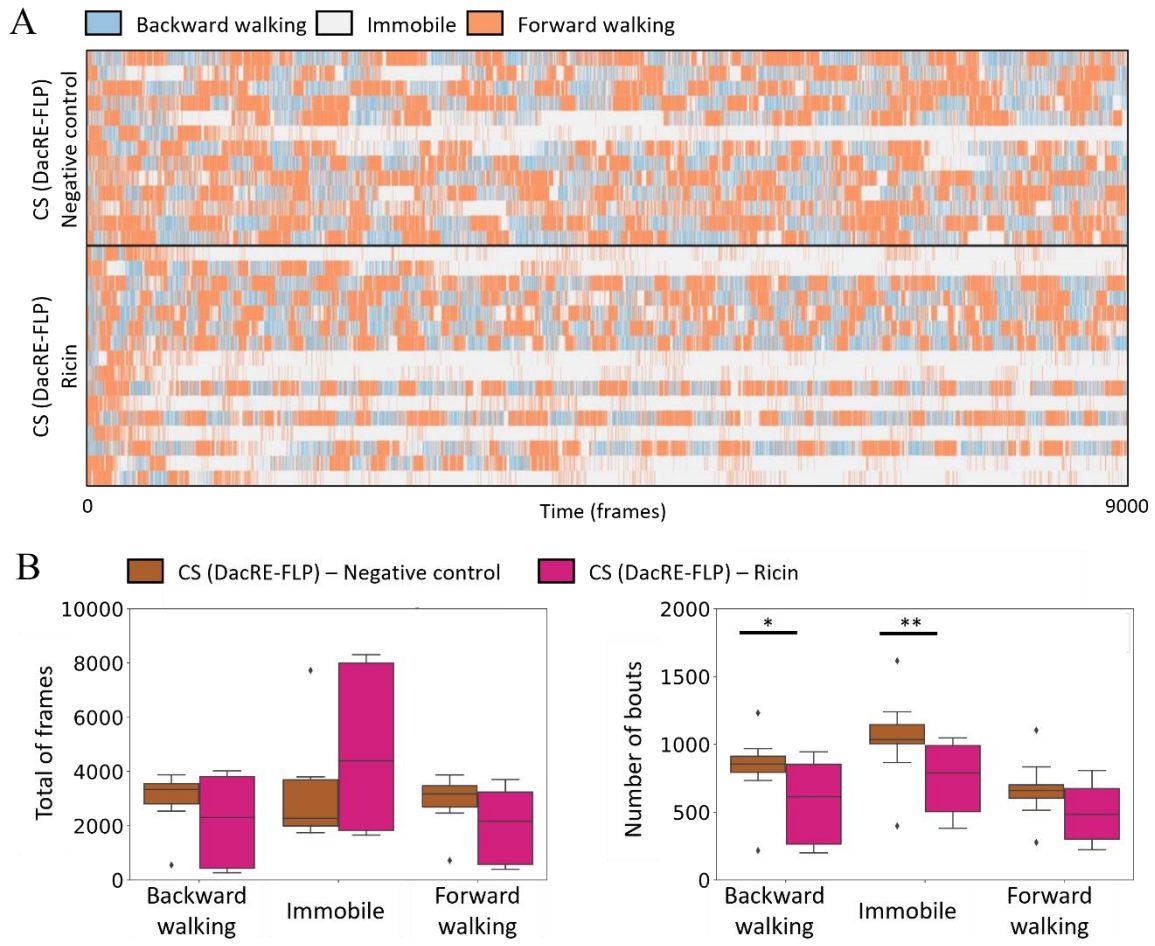

Figure 3.5- Behavioural analysis of flies in slanted tunnel
Negative control has an n = 13, and ricin expressing line has an n = 16. A) Raster plot composed of two conditions separated by a black line: Negative control and ricin expressed in the campaniform sensilla. Each line of data corresponds to one fly, and each vertical line corresponds to a frame. Every frame is marked with a colour correspondent to the motor behaviour (backward walking in blue, forward walking in orange, and no movement in grey). B) Quantification of forward walking, backward walking, and immobile behaviour in the slanted tunnel assay. Left - Quantification of the total amount of frames spent moving forward, backward, or not moving for each fly, in each condition – Negative control in brown, and leg CS inactivation in pink; Right - total number of bouts (more than 1 consecutive frame spent performing the same motor behaviour) for each fly, in each condition.

Figure 3.5 shows an analysis on the behaviour of the fly as time progresses. In Figure 3.5.A we have a raster plot of the movement of the fly as time moves forward, divided into two sections: above the black line, the negative control, and below, the line expressing ricin. Each horizontal section represents a single fly, and is composed by several vertical lines that represent backward walking (moving towards the beginning of the tunnel – in blue), not moving (in grey) and forward walking (moving towards the narrower side of the tunnel – in orange). In a first glance, it seems clear that flies move forwards and backwards several times throughout the assay, and also stop for some periods of time. It seems also clear that the flies on the ricin section (below) seem to have more moments where there is no movement, and that usually is maintained until the end of the video.

In Figure 3.5.B we have the quantification for two different measurements, the distribution of the total number of frames spent moving backwards, forwards, or not at all for each fly; and the number of bouts (continuous sections of the same behaviour; > 1 frame) moving backwards, forwards, or not moving. For the total number of frames, we see there is a trend (even though it is not significant), where flies

with ricin (in pink) tend to have increased number of frames not moving, and decreased number of frames moving forwards or backwards. This is consistent with what has been seen in Figure 3.5.A, and can also be seen in annex Figure 6.2. When looking at the total number of bouts, we now see significant decreases in the number of bouts moving backwards (P-value of 0.034) and not moving (P-value of 0.033) for flies with ricin, and a clear (yet not significant) decrease in the number of bouts moving forward.

3.3.2 Backward walking assay

By observing that flies from the CS line expressing ricin would get stuck inside the tunnels, and taking into consideration that when activated, the leg campaniform sensilla produced a backward walking motion, we hypothesized that maybe these flies where the structure had been inactivated had difficulty in moving backwards. We then considered a new assay, similar to the slanted tunnel, but simpler. Here, the tunnel would have a consistent height along the length and would end in a perpendicular wall (dead-end). This would force flies to walk backwards. For more detail, see section 2.3.2.

In these experiments, we once again tested two conditions: the CS line driving the expression of ricin, and the CS line without a UAS component (negative control). Flies would be placed inside the linear tunnel arena and filmed for 11000 frames at 30 fps (6.1 minutes), and the resulting videos would then be passed through a tracker to identify and output the position of the fly along the tunnel (more information in section 2.3.5.).

A first visual analysis of the videos seemed to show no clear differences between the negative control, and the line expressing ricin, as both lines seemed to show a preference for staying at the end of the tunnel.

Just like the analysis to the data of the slanted tunnels, we first analysed the data of the position of the fly along the x axis, and plotted the probability density of these values (Figure 3.6). Above the plots, we have a frame from one of the flies in the linear arena, that can be used as reference for the x axis. In this first set of results, we see that both the negative control (in brown) and the line expressing ricin in the leg CS (in pink) seem to show a preference for the end of the tunnel, represented by the peak in probability density at around pixel 1700. However, the flies with ricin do seem to have a higher peak of probability than the one shown by the negative control.

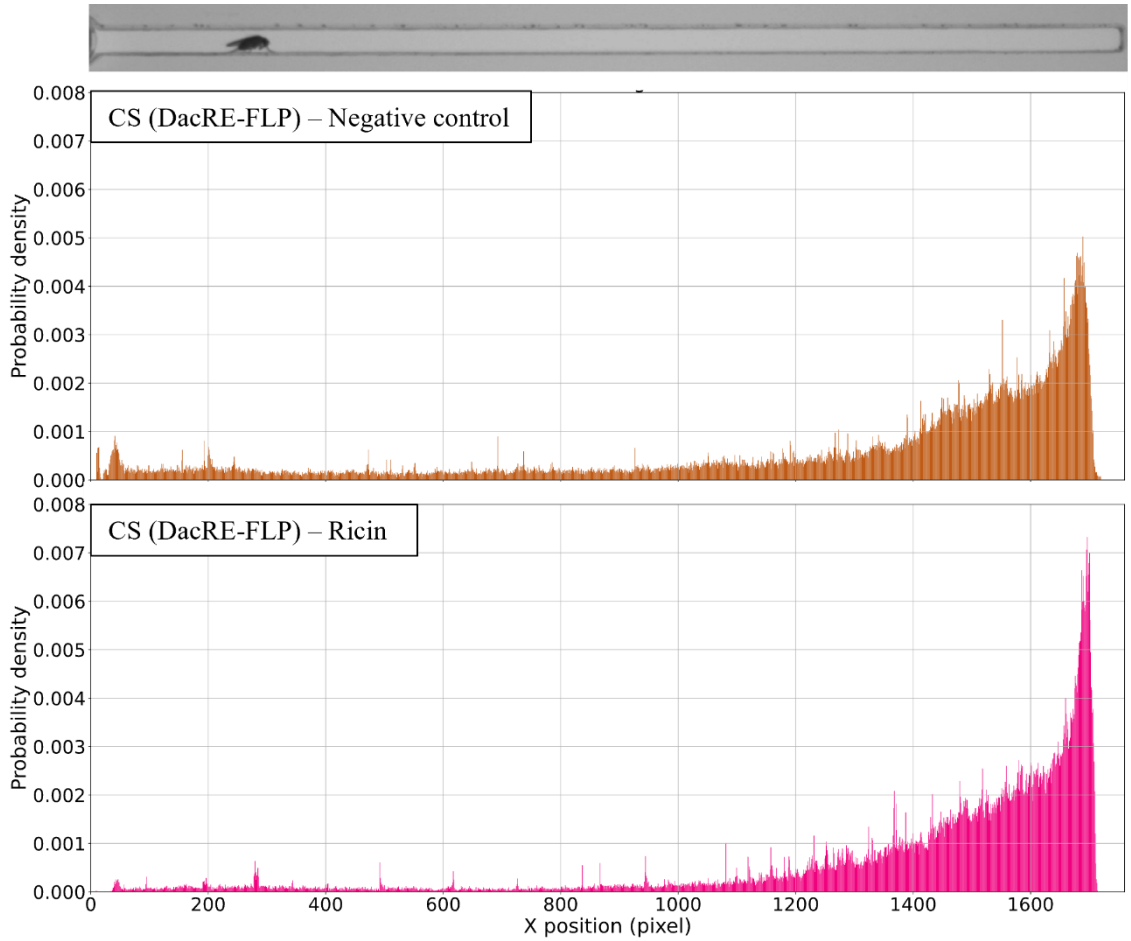

Figure 3.6- Probability density of position inside the linear tunnel
Distribution of the position of the flies from the negative control, and the flies expressing ricin in the leg campaniform sensilla in a linear tunnel. Above is a frame of a video from the negative control line, that shows how the position in the X axis is correspondent to the position inside the tunnel. Below are the probability densities of the negative control (in brown) and the line expressing ricin (in pink). Both conditions show an n = 15.

In Figure 3.7 we again show a different set of plots that take into consideration the movement of the flies, more specifically if the fly is moving backwards (blue), forwards (orange) or not moving at all (grey). In the raster plot above we have the movement of the flies as time moves forward, showing the direction of movement of the fly in each moment. Above the black line, we have the negative control flies, and below the flies expressing ricin in the leg CS. Each horizontal line is a single fly, and each vertical bar is correspondent to a single frame. Contrary to what we saw in the slanted tunnels, these two plots seem to show little to no difference, where all flies seem to move backwards and forwards, with occasional moments where they stop moving.

Below the raster plot we have again the comparison between the two conditions, now analysing the number of frames that present a specific behaviour (backward walking, forward walking or not moving), and the number of bouts for each behaviour. We can see that the number of frames spent in each behaviour is much more similar in this assay when comparing the two conditions, even in the line with ricin shows a significant increase in the number of frames spent immobile. In the number of bouts, we see no significant nor apparent differences between each condition, reinforcing the information obtained up until this point, and the observations done when analysing the videos.

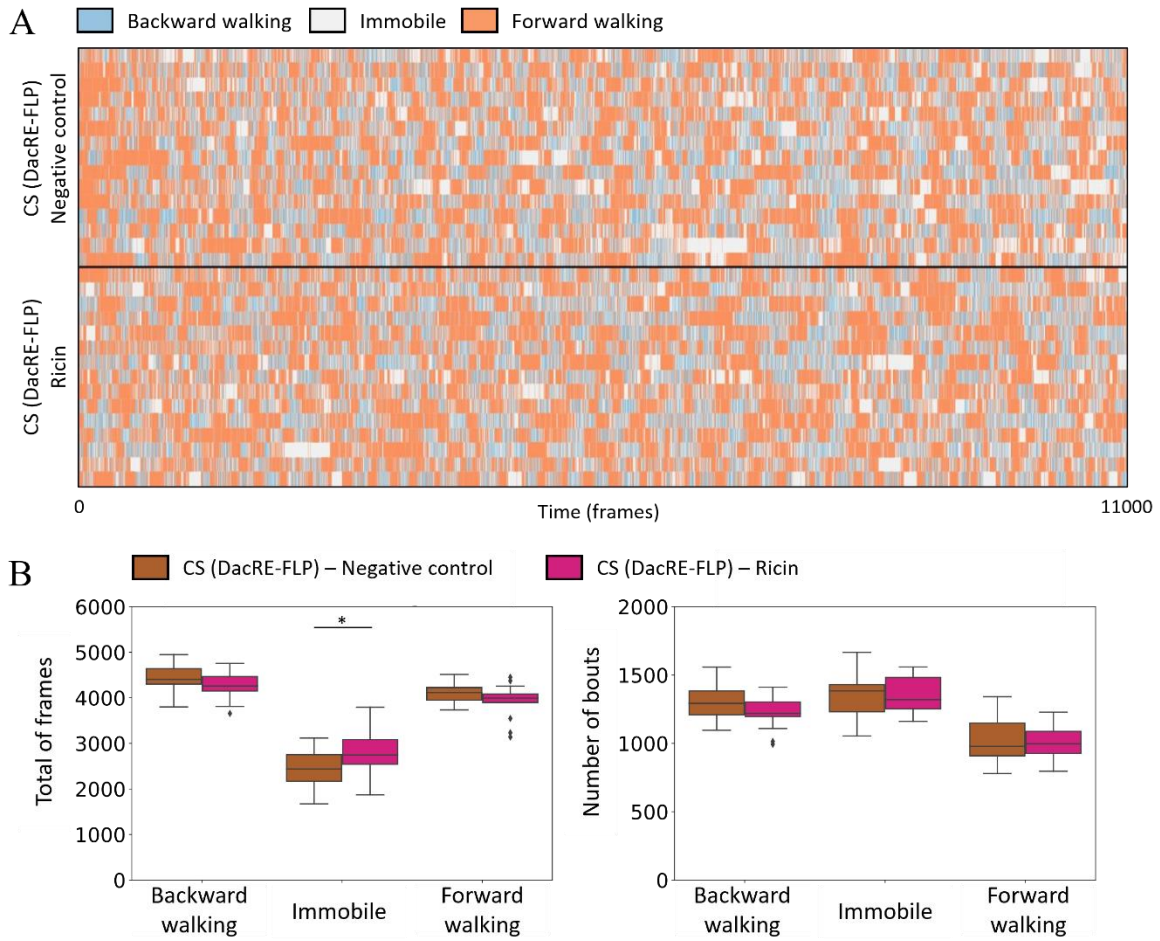

Figure 3.7- Behavioural analysis of flies in linear tunnel
A) Raster plot composed of two conditions separated by a black line: Negative control and ricin expressed in the campaniform sensilla. Each line of data corresponds to one fly, and each vertical line corresponds to a frame. Every frame is marked with a colour correspondent to the motor behaviour (backward walking in blue, forward walking in orange, and no movement in grey). B) Quantification of forward walking, backward walking, and immobile behaviour in the linear tunnel assay. Left - Quantification of the total amount of frames spent moving forward, backward, or not moving for each fly, in each condition – Negative control in brown, and leg CS inactivation in pink; Right - total number of bouts (more than 1 consecutive frame spent performing the same motor behaviour) for each fly, in each condition. Both conditions show an n = 15.

3.4 Uncovering the neural circuit: an approach

3.4.1 Recombinant

Previous work from the lab had shown that the activation of the leg campaniform sensilla led to the described motor output of backward walking, followed by a turning behaviour and forward walking in another direction. It had also been shown that decapitated flies did not produce this motion, leading to the conclusion that the Central Brain has some role in the motor output, as well as ascending and descending neurons that transport information between the brain and the VNC. In order to further explore the composition of this neural circuit that has as an input the leg campaniform sensilla, and results in the observed behaviour, we decided on a two expression-system approach, to activate the CS and inactivate other sections of the neural circuit.

By using a second expression system - the LexA-LexAop system - to drive the expression of a protein that hyperpolarizes neurons, the Kir 2.1, we could have this simultaneous activation and inactivation. However, to use these two expression systems simultaneously, we needed to create a recombinant line

due to genetic constraints: we needed a place on the second chromosome and one on the third to place the LexA driver and the LexAop-Kir2.1, and the third pair of chromosomes already had a copy with CS-Gal4 and another with UAS>>Chrimson.mVenus. Given that these two insertions on the third chromosome were in different locations (attp2 and VK5, respectively), we decided to recombine these two transgenes, thus creating the space for us to be able to express the LexAop-Kir 2.1 in the third chromosome with no further issues. This resulted in the CS (Recombinant) line shown in section 2.1.

3.4.2 LexA drivers

As previously mentioned, we intended on using the LexA-LexAop system, in unison with the Gal4-UAS, to drive the expression of Kir 2.1 and hyperpolarize neurons or regions that might be a part of the neural circuit under study. This meant we had to decide on a set of LexA-drivers that would be relevant for driving the inactivation of neurons and regions associated with backward walking or turning behaviour. We ended with a set of four LexA-lines, plus the Empty-LexA as a negative control for the Kir 2.1 (Table 3.1).

Table 3.1– LexA drivers

Set of LexA drivers to drive the expression of LexAop-Kir 2.1

Line	**Description**	**Origin**
Empty-LexA	Has no enhancer to drive expression of LexA. Serves as a negative control for the LexAop-Kir2.1, and a positive control for the Recombinant line.	Bloomington stock centre BL 77691
EB-R2/R4m-LexA	Drives the expression in rings R2 and R4m (median layer) of the ellipsoid body. Has been associated with impairments in turning behaviour upon inactivation (Kottler et al., 2019).	Bloomington stock centre: BL 53566
EB-R3/R4d-LexA	Drives the expression in rings R3 and R4d (distal layer) of the ellipsoid body. Has been associated with impairments in turning behaviour when inactivated (Kottler et al., 2019).	Bloomington stock centre: BL 61589
E-PG-LexA	Marks a set of neurons on the Central Complex that connect the Ellipsoid body to the Protocerebral-bridge and the Gall (hence the name E-PG). These have been shown to modulate patterns of turning behaviour (Kottler et al., 2019).	Bloomington stock centre: BL 52867
MDN-LexA	Drives the expression in a set of neurons, including the Moonwalker Descending Neurons (MDN). These specifically have been demonstrated to be sufficient and necessary for backward walking (Bidaye et al., 2014).	Gift from Barry Dickson

In Figure 3.8 we can see the expression pattern of the LexA-drivers for the brain (VNCs showed no expression, and images can be found in annex Figure 6.1). In the first column, in magenta, we have the antibody NC-82, that marks the overall neural structures. In green, we have the LexA-LexAop system driving the expression of GFP, and in the third column we have the overlay of these two channels.

The Empty-LexA line shows, as expected, no expression of GFP in any section of the brain. Both lines for the ellipsoid body (EB-R2/R4m-LexA and EB-R3-R4d-LexA) show expression of GFP, in the rings 2 and 4 medial, and the rings 3 and 4 distal, respectively. The remaining two lines (E-PG-LexA and MDN-LexA) show no expression of GFP.

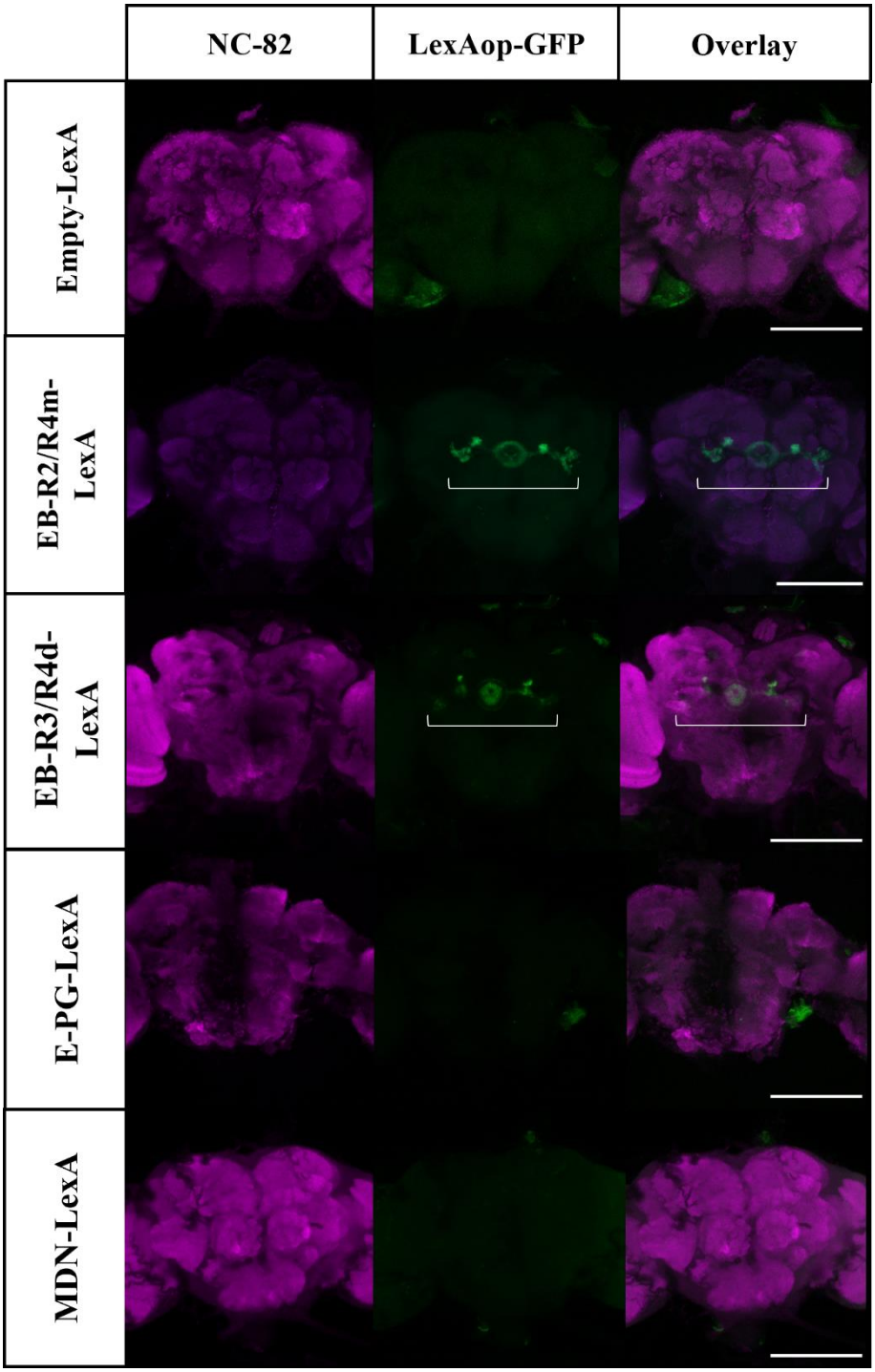

Figure 3.8 - Expression pattern of LexA drivers
GFP expression driven by the LexA-LexAop system. The first column, in magenta, shows the expression pattern of NC-82, an antibody for neurons, and the second column shows the expression of GFP in green. The third column represents the overlay of the two channels. White brackets show the GFP marked cells in the lines where there was expression (EB-R2/R4m-LexA and EB-R3/R4d-LexA). Scale bars represent 100 µm.

3.4.3 Empty-LexA

Even though several LexA-drivers were proposed in the beginning of the project, and a total of five lines were imaged, for the sake of time we were only able to explore the Empty-LexA driver. This line serves as both a positive control for the functioning of the recombinant line, and a negative control for the expression of Kir 2.1. Flies from this condition were tested under the same circumstances as all other lines tested in the open arena setup, using optogenetics to stimulate for 100 ms the leg campaniform sensilla when the fly was immobile.

Upon first analysis of the videos, these flies seemed to show no difference in response when compared to the original leg CS line. These videos were then analysed with a tracker, and the data was processed with the same python script used for the other open arena assays.

The data from the line Recombinant + Empty-LexA was tested for normality, and the result showed a non-normal distribution. This means all analysis from this point forward were done using non-parametric tests. For the results on this test, see Table 6.1, in the Annexes section.

Figure 3.9 shows the response of the flies from the Recombinant + Empty-LexA driver for Kir 2.1 (in yellow) to the stimulus (vertical red bar), in comparison with the CS (DacRE-FLP) line raised with and without ATR food (green and orange, respectively). Each condition is represented by the median of the values for all flies, and shaded areas are correspondent to the median absolute deviation. The vertical grey bars represent the 2-frame block separation that was used in the statistical analysis, and all asterisks are referring to the comparison between the Recombinant + Empty-LexA and CS (DacRE-FLP) lines.

In the first plot, showing the velocity of the flies as time progresses, we can see that in fact the flies from the Empty-LexA line react to the stimulus and in a very similar manner to the one seen in the original CS (DacRE-FLP) line, with only one section (0.33-0.4 s) where there is a significant difference between the two, with a significance of ($1.15x10^{-3}$). This response is characterized by a first backward walking component, followed by a change in direction of movement, with a forward walking component. In the second plot, where we see the angular velocity of the flies, there are some more significant differences, with emphasis on sections 0.06-0.13 s and 0.13-0.20 s, with significances of (P-value: $3.59x10^{-3}$) and (P-value: 0.016). However, when comparing the two curves, we can see how similar they look, with a slow response that increases as the flies approach the moment where there is a switch in walking direction, that we have previously associated with the moment where there is the turning response. After this peak, the Empty-LexA line seems to show yet another, higher peak, that seems to continue beyond the time frame of the analysis performed, with significant differences of ($8.66x10^{-3}$) and ($1.55x10^{-3}$).

The data suggests what has been observed in the first visual analysis of the videos, where the Recombinant + Empty-LexA line shows a similar response to the one seen in the original CS (DacRE-FLP).

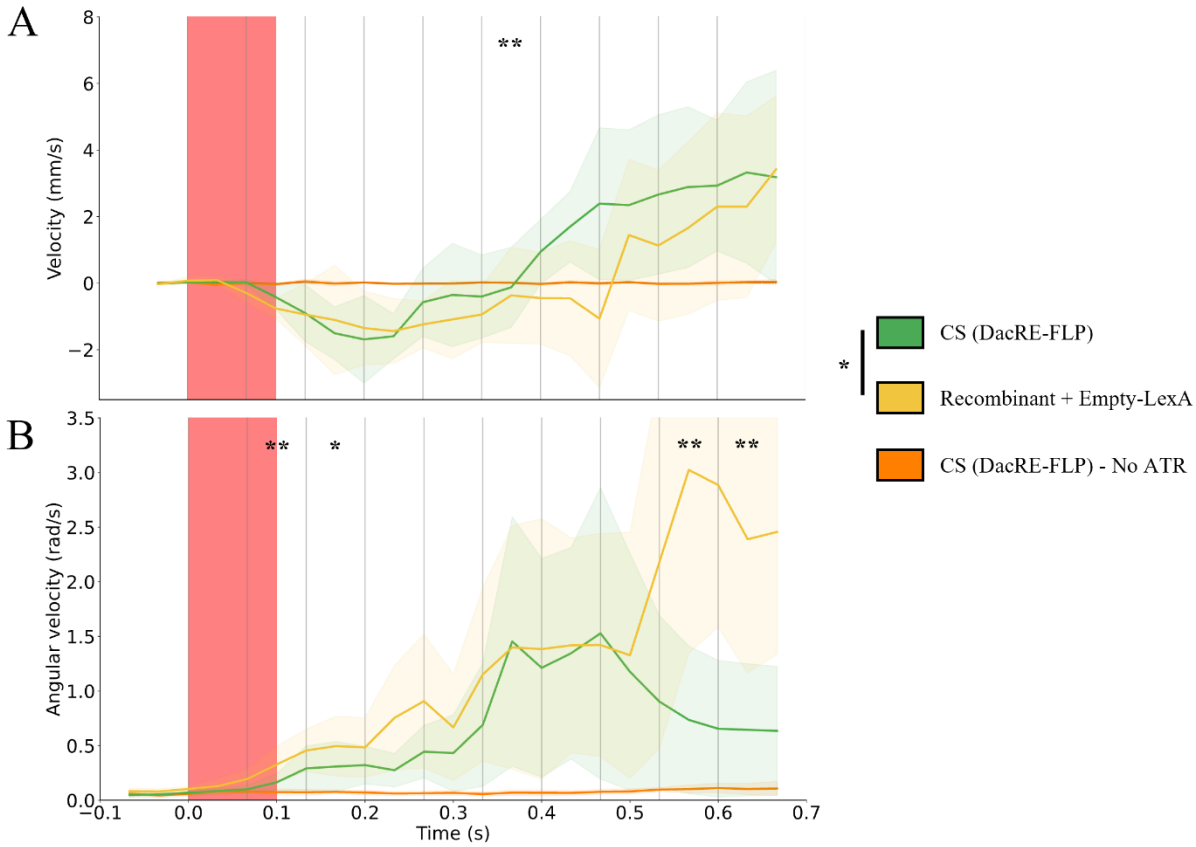

Figure 3.9- Velocity and angular velocity analysis of the Recombinant + Empty-LexA line
Plot for the median values of both the velocity and the angular velocity of the CS line raised in food with and without ATR (n = 17 and n = 19, respectively), and the Recombinant line with the Empty-LexA driver raised in ATR food (n = 16). This last line serves as a positive control for the CS-Gal4 system, and a negative control for the LexA-LexAop system. Shadowed regions with the same colour as the curves show the median absolute deviation. Vertical lines every 2 frames (approximately 0.066 seconds) demark the windows used for the statistical analysis between lines. Asterisks correspond to the significance of the comparison between the CS and the Recombinant lines. Time of stimulation characterized by the red shaded bar. A) Velocity over time, with time starting at the moment of stimulation. The campaniform sensilla line without ATR (orange) shows no response to the optogenetic activation. Both the CS line raised in ATR and Recombinant line show two moments, starting with a backward walking motion, and followed by a switch in movement direction. B) Angular velocity over time. The line without ATR shows again no response to the stimulus. The Recombinant +Empty-LexA line shows a similar response to the one presented by the CS (DacRE-FLP) line, even though there are several instances where it shows significant differences. For more information on the significance of the comparisons between all conditions, for both velocity and angular velocity, see annex Table 6.5.

3.5 Split-Gal4 screen

When trying to mark specific cell types, there are several approaches that can be used. In the lab, one of the most common ones is the use of a Gal4 driver in combination with an FRT-Flp recombination filter to further localize the expression to a certain set of cells. In this section, we took advantage of a previous unpublished screen that had been compiled in the lab, of lines that marked mechanosensory structures in the *Drosophila*'s leg, and searched Split-Gal4 lines for those specific drivers. The Split-Gal4 system is also a three-party system, as the one used, but here we take advantage of the Gal4 protein being separated into two subunits (the GAL4-AD and the GAL4-DBD – more information on this technique in section 2.2.3.). This allows us not to use the recombination filter and maintain the restrictive expression pattern.

We started with a set of five GAL4-AD lines (SG[1-5]) that were combined with ChAD-GAL4-DBD (marker for cholinergic neurons) and nSyb-GAL4-DBD (marker for the nervous system) lines to show a first expression pattern of these lines alone, by driving the expression of UAS-GFP. This resulted in a total of 10 genotypes that were dissected, imaged, and analysed. These GAL4-AD lines were then combined with the four selected GAL4-DBD lines (SG[6-9]), driving again the expression of GFP. This resulted in an extra 20 combinations of genotypes that were also dissected, imaged, and analysed.

From the resulting images, we observed that six lines showed non-specific or no expression of GFP in the legs, 13 lines showed expression in leg campaniform sensilla from the sets FeFF and TrFF (for reference, see Figure 1.3), and one line showed expression of leg CS and chordotonal organ. The results are summarized in Table 3.2, and all images can be found in Figures 6.5-6.9 in the Annexes section.

Table 3.2- Expression pattern description for Split-Gal4 combinations

Several lines showed expression of GFP in the femoral and trochanteral fields (FeFF and TrFF, respectively).

	SG6 (DBD)	SG7 (DBD)	SG8 (DBD)	SG9 (DBD)
SG1 (AD)	No cells were marked.	Non-specific expression.	Set of CS in the FeFF.	Set of CS in the FeFF.
SG2 (AD)	Set of CS in the FeFF, and cells from the CO.	Set of CS in the FeFF.	Set of CS in the FeFF.	Set of CS in the FeFF.
SG3 (AD)	No cells were marked.	Set of CS in the FeFF.	Set of CS in the FeFF.	Set of CS in the TrFF.
SG4 (AD)	Set of CS in the FeFF.	Set of CS in the FeFF.	Set of CS in the FeFF.	No cells were marked.
SG5 (AD)	No cells were marked.	No cells were marked.	Set of CS in the FeFF.	Set of CS in the FeFF.

In Figure 3.10 we show one of the combinations that drove the expression of GFP in leg campaniform sensilla (SG2 driver combined with SG8 driver). Figures 3.10.A and 3.10.B show the overall structure of the leg captured with the autofluorescence of the cuticle, and the squared region in A is enlarged for the remaining panels. The white arrows on panels C and D point to a set of leg campaniform sensilla that, considering previous descriptions such as the one shown in figure 1.3, seem to correspond to a subset of the femoral field (FeFF).

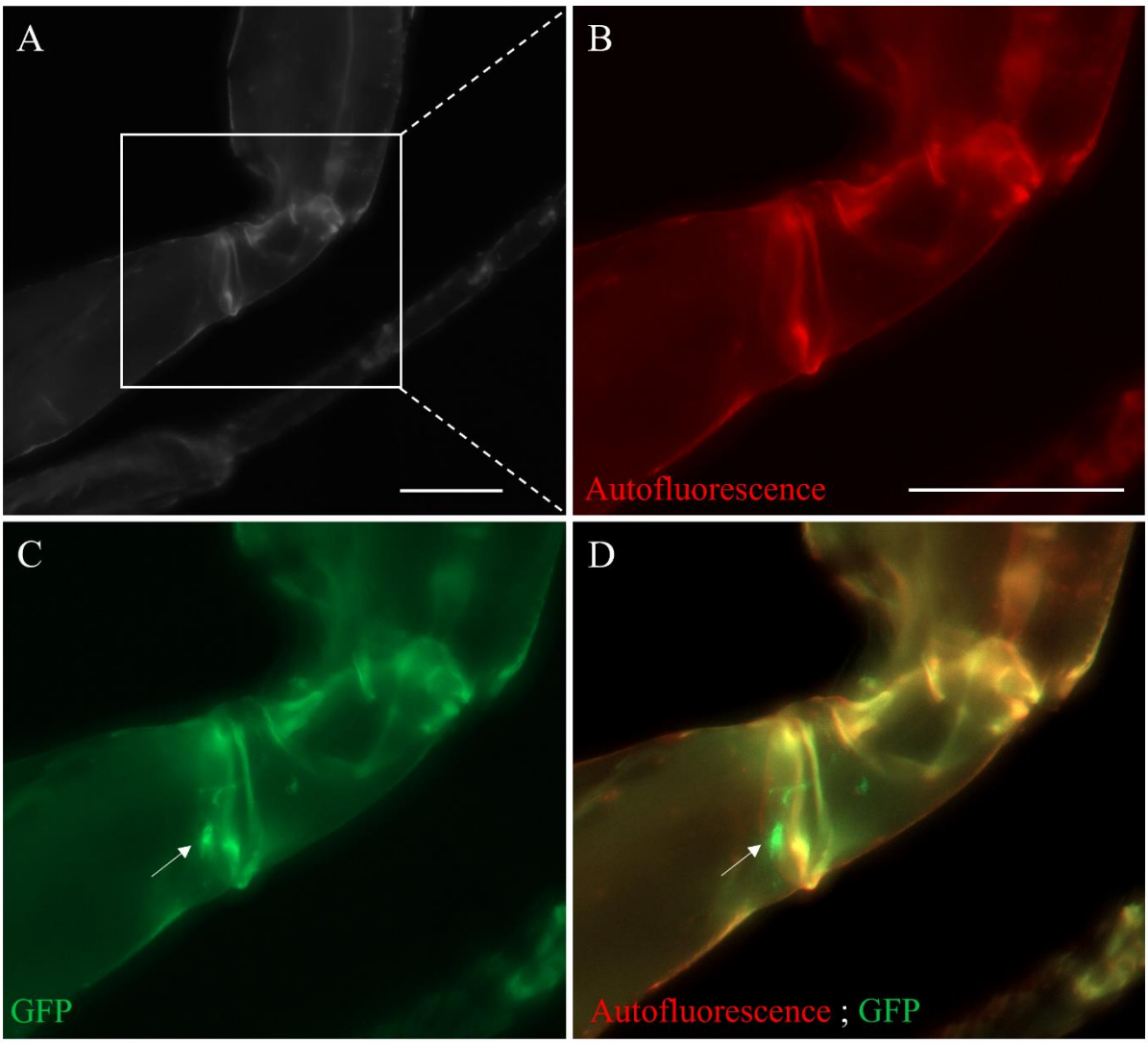

Figure 3.10 - Split-Gal4 driven expression of GFP
Expression pattern of the combination between lines SG2 and SG8, driving the expression of UAS-GFP, in fixed leg of *Drosophila melanogaster*. A) and B) Autofluorescence of cuticle from the dissected leg. C) GFP expression driven by the Split-Gal4 system. Arrow points to CS cells, seeming to be a part of the FeFF subset (Figure 1.3 for reference on the denomination). D) Overlay of cuticle autofluorescence and GFP expression. White arrow shows CS cells seen in C). Scale bar corresponds to 100 µm.

4 Discussion

4.1 Leg campaniform sensilla activation produces motor output

4.1.1 There is specificity in motor output when activating different mechanosensory structures

Previous work from the lab had shown that optogenetic activation of the leg campaniform sensilla produced a very characteristic behaviour, described by three phases: Backward walking, turning, and frontward walking in a different direction. Our first approach (section 3.1) was to repeat this experiment in the same open arena, with the same mode of activation (red-light pulse for 100 ms), using three lines: CS (DacRE-FLP) raised in no-ATR food, and CS (DacRE-FLP) and CO raised in ATR food (Figures 3.1 and 3.2).

When compared to the negative control (CS (DacRE-FLP) without ATR), the CS (DacRE-FLP) line showed a clear response to the stimulus that could be seen in visual representations of the movement

(Figures 3.1.C and 3.1.D). As expected, and seen in Figure 3.2, the fly first moves with a negative velocity (backward walking), followed by a change in direction (seen as a peak of angular velocity), and then starts moving with a positive velocity (forward walking). Contrasting, the CO line presented a simple forward walking response, with no turning component.

As proposed by Medeiros and Mendes (unpublished), the activation of CS and CO result in different motor outputs, demonstrating how there is specificity in these responses (Figure 4.1, left).

The motor output that we observe upon the activation of the leg campaniform sensilla is similar to previously described evasive behaviours observed in *Drosophila melanogaster* when encountering a predator (Parigi et al., 2019). In fact, it has been shown that flies present a retreat behaviour composed of backward walking, followed by turning, when they encounter a predator (juvenile praying mantids). Moreover, it has also been described by Wu and colleagues (2016) that artificial stimulation of neurons (in this case, the LC16, a set of neurons associated with visual stimuli) can induce a retreat response such as the one described by Parigi et al. (2019). Such behaviours have also been observed in other insects such as the cockroach, upon physical stimulation of the antennae (Burdohan, J. A., Comer, C. M., 1990). This reinforces the idea that the activation of different sensory inputs can induce a retreat response.

Taking into consideration the function of the leg campaniform sensilla as load-sensors, sensory inputs responsible for encoding information such as the load that is being applied to the body of the fly, it would make sense that the activation of these structures would induce some motor output. Given that there are several CS being activated at once, this signal could be originated by a crushing force that is being applied to the fly. It is likely that some sort of retreat behaviour such as the one presented is activated to protect the body from further damage.

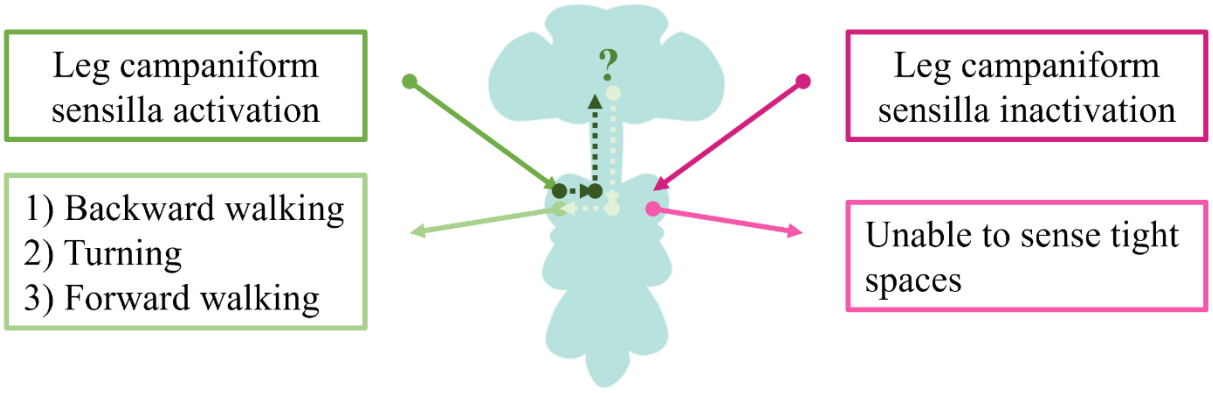

Figure 4.1 - Activation and inactivation of leg CS produces different results
A visual representation of the resulting response for activation and inactivation of the leg campaniform sensilla circuit. The activation of this circuit, composed of the CS as an input, ascending neurons, neurons in the higher order centre and descending neurons leads to the motor behaviour of backward walking, turning and forward walking. The inactivation of this neural circuit leads to a decreased ability to sense if there is pressure being applied to the body of the fly.

4.1.2 Antennae seem to have no role in leg campaniform sensilla mediated behaviour

As described in section 1.4, the line utilised to activate the leg campaniform sensilla showed some neurons projecting from the antennae to the ventral lobes. The reason why there was expression in the antennae is probably due to the fact that both the legs and the antennae share the same developmental origin (Schneuwly et al., 1987). Taking also into consideration the importance of the *dachshung* (dac) gene (which enhancer drives the expression of Flp in the DacRE-Flp driver) in leg and antennal development (Giorgianni, M. W., Mann, R. S., 2011; Mardon et al., 1994; Dong et al., 2002), it seems clear why there is expression of the transgene in the antennae. However, this expression in the antennae could still be the responsible for the behaviour seen when activating the leg campaniform sensilla. In

fact, there have been descriptions where the activation of olfactory neurons would induce backward walking behaviours such as the one Medeiros and Mendes (unpublished) observed (Israel et al., 2022).

To answer this question, we utilised two approaches: amputation of the antennae, and utilisation of a different Flp-driver to restrict the expression of chrimson to the head capsule (Eyeless-FLP). Our results showed that flies with amputated antennae present little to no significant differences in behaviour, when compared to the original CS (DacRE-FLP) line. Contrasting, flies from the CS (Eyeless-FLP) line presented significantly different responses to the original line, producing a different motor behaviour (Figure 3.3). These experiments seem to suggest the leg campaniform sensilla are the responsible for the motor output characterized by backward walking, followed by turning and frontward walking.

These two first sets of experiments allowed us not only to further characterize the behaviour that is resulting of the activation of the leg campaniform sensilla, while comparing it to the behaviour resultant from another proprioceptor (chordotonal organ), but also to further investigate the role of the antennal projections and if they are in any way responsible for it. Together with the information that had been described by Medeiros and Mendes (unpublished) on the necessity of the head for this behaviour to take place, we can conclude that the neural circuit is composed by the leg campaniform sensilla, that serve as sensory input, a set of interneurons that will transport the information to the central brain (where this information is processed by other higher order centres), from which information will come back to the ventral nerve cord via descending neurons, to produce the motor output described: backward walking, turning, and forward walking.

4.2 Laser beam activation of the leg campaniform sensilla produced no motor output

The laser arena was created with the intuit of activating the leg campaniform sensilla while the fly is in motion, as all activation assays up until this point had been performed in immobile flies. The rationale behind this assay was that, by alternating the activation of a UV light to attract the fly to one end of the arena, the fly would be obligated to cross the laser beam that was projected in the middle of the arena, thus activating the mechanosensory structures. However, this assay did not function as two of the lines supposed to react to the stimulus (campaniform sensilla and chordotonal organ) did not react to crossing the beam (data not shown). Furthermore, we observed that the line that drives the expression of chrimson in the mechanosensory bristles did react to the stimulus but did not cross the laser beam. This was an interesting result, but not informative for the current study, hence we decided not to further apply the protocol of this assay.

Probably the laser was not strong enough to penetrate the tissue and get to the cells marked in the campaniform sensilla and chordotonal organ lines, but was strong enough to get to the mechanosensory bristles, as these structures (and respective sensory neurons) are more superficial, and in greater number. It is also important to point out that the light used to stimulate the mechanosensory structures in this assay was a gradient, and the intensity increased as the fly would approach the centre of the arena, and then decrease as the fly would step away from the beam (Figure 2.4.D). Another reason that could explain this behaviour (or rather lack of it) is the fact that the optogenetic activation was being produced not by a small burst of light with a short span, but a laser that was constantly on and, even with some structures to block light from illuminating other regions of the arena, there could be some leaking.

The importance of understanding if the activation of the leg CS during motion has any behavioural response increases as we uncover more information about this circuit. Taking what has been described in other insects on the role of this structure as a load-sensor, that informs the body if the leg is pressing the floor during motion or if there is any load applied to the body, and that we know that *Drosophila* changes its kinematics under load (Mendes et al., 2014), we expect that the activation of the leg campaniform sensilla during motion should alter the behaviour of the fly.

4.3 Inactivation of leg campaniform sensilla leads to apparent decrease in load sensing capability

The activation of leg campaniform sensilla has shown to produce a very particular motor output that starts with a backward walking component, followed by turning and forward walking. We then sought out to find what is the result of inactivating these mechanosensory structures. However, the inactivation of these structures could not be tested in an open arena setup, so we had to create a new assay. Following the rationale that the leg campaniform sensilla are responsible for sensing load, whether it is from the leg being pressed to the ground or load being applied to the body, we developed a protocol to create pressure over the body of the fly, resulting in the possible activation of these structures. So, we designed a tunnel that would get narrower as the fly moved forwards, and where it was unable to turn around (restricting the movement to backward and forward walking).

Our results showed that flies with functional CS move forwards and backwards with ease, but have a preference to stay in the beginning of the tunnel (Figures 3.5.A and 3.4). However, when the CS are inactivated by expressing ricin, these flies show a different response, spending a lot of time in the narrower region of the tunnel, and consistently getting stuck in that area (Figure 3.4). These flies also present a decreased number of bouts (Figure 3.5.B), possibly caused by the fact that they get stuck and spend most of their time immobile.

These results indicate that flies with inactive leg CS have difficulty in sensing if the space they are in is too narrow for them, resulting in the inability to retreat from this space. This would make sense as the leg campaniform sensilla are load-sensors that are responsible for informing the body of load that is being applied to it.

This hypothesis is also aided by the fact that flies with inactive campaniform sensilla seem to have no difficulty in moving backwards, as we can see in the experiments done in the linear tunnel, where the height of the space was constant. In fact, these flies seemed to show no differences to the negative control in both the distribution of their positions along the tunnel (Figure 3.6) and their behaviour as time progresses (Figure 3.7).

These results further reinforce the idea that the inactivation of the leg campaniform sensilla in some way disrupts the ability of a fly to sense load that is being applied to its body (Figure 4.1, right), as they show no difficulty in backing up, but rather in not sensing how far into the slanted tunnel they should move and when to stop.

4.4 UAS-Gal4 recombinant for CS activation shows a similar behaviour to the original CS line

From previous experiments in the lab, we knew the head of the fly was important for the motor output resulting from the optogenetic activation of the leg campaniform sensilla, as headless flies no longer produced this behaviour (Medeiros and Mendes, unpublished). This meant that, in order to produce the backward walking, the turning and the forward walking, there is a need for circuitry that processes the information coming from the CS and that triggers this behaviour (Figure 4.1).

We proposed to dissect the neural circuit behind the leg campaniform sensilla activation by inactivating sets of neurons that have been associated with behaviours such as backward walking and turning at the same time, taking advantage of the LexA-LexAop expression system to express Kir 2.1, a protein that hyperpolarizes the neurons.

We first showed the expression patterns of the lines selected (Figure 3.8), where three of the five lines showed no GFP expression. The first line, the Empty-LexA, was intended to show no expression as it has no enhancer to drive the expression of the LexA protein. However, the other two lines (MDN-LexA and E-PG-LexA) were supposed to show some expression in the brain (and VNC, for the MDN line). The inexistence of GFP expression might be a result of weak signal coming from this protein, and thus

the sensor of the microscope is not able to capture this signal. The remaining two lines (EB-R2/R4m-LexA and EB-R3/R4d-LexA) showed the expression pattern expected by the literature.

In the current study we were only able to test the function of this double expression system by driving the expression of LexAop-Kir 2.1 with an Empty-LexA driver, due to time constraints. Flies from this line showed a similar result to the one that had been previously seen in the original CS (DacRE-FLP) line, confirming the well-functioning of the recombinant created (Figure 3.9). These flies showed some increased variability that might be responsible for the significant differences that were observed in the analysis of velocity and angular velocity, as an empirical analysis on the videos showed no difference in behaviour.

This result showed us that the recombinant line produces a behaviour similar to the one presented by the original CS (DacRE-FLP), and provided us a control for future comparisons by using the Empty-LexA. However, the fact that this line produced some differences in behaviour can be concerning, possibly explained by the number of insertions these flies have (two in the second chromosome, and three in the third). In fact, it has been previously described that P-element insertions in *Drosophila* can induce phenotypic differences besides the expected ones, such as in wing dimensions (Webber et al., 2005). Nonetheless, the creation of this recombinant line is a step into studying the other necessary circuits in this complex neural circuit with input in the leg campaniform sensilla, and a motor output of backward walking, turning, and forward walking.

4.5 Several Split-Gal4 combinations mark cells contained in the CS (DacRE-FLP) line

The Split-Gal4 system is an approach widely used when searching for restricting expression patterns of lines, due to its combinational basis. For the current work, we searched for lines that, in combination with one another, could provide new tools to further dissect which sets of leg CS might be responsible for the motor output seen when we activated these structures. After selecting the lines, balancing them, and testing all possible combinations for their expression patterns in the legs of the fly (Table 3.2 and Figures 6.5-6.9), we finished with 13 lines that mark mainly the femoral field of CS (FeFF), with the exception of one of the lines that marked the trochanteral field (TrFF - combination SG3 x SG9).

Taking into consideration that the original CS (DacRE-FLP) marked sets of cells from both the FeFF and the TrFF groups, this means we now have tools to drive expression in each of these subsets, and with a range of possibilities to do so.

4.6 Future work

There is still a lot of work that can be done regarding the study of the leg campaniform sensilla. In the first section of the work, where we describe the motor behaviour, there could be more metrics such as the distribution of the turning behaviour (is there any bias towards the side of the turn, for example), the correlation between the peak of angular velocity and the moment of change of sign in velocity, as well as the delay until the reaction started. All these metrics can be important to further characterize the behaviour.

As we have previously said, another important aspect that should be done is to design a new assay to study the stimulation of mechanosensory structures during motion. One change might be, to increase consistency of signal, to utilize the 100 ms pulse instead of the laser beam. Perhaps utilising an arena similar to the one set for the laser beam, with the alternating UV light to attract the fly, but activating the red-light pulse as the fly is moving could be a solution.

Regarding the tunnel arenas, there are also some experiments that could be done, such as optogenetic activation of the leg CS in the slanted tunnel, but activating before the flies get to a point where they

would naturally stop moving forward. This might show us that we could impose a limit on how far towards inside the tunnel a fly could move, as the artificial activation of the CS would inform the fly that the height of the tunnel is smaller than it actually is.

Regarding the study of the interaction between circuits and which neurons/populations of neurons are a part of the neural circuit, it would be important to test all the other proposed LexA drivers: moonwalker descending neurons (MDN) for the backward walking phase, and the two ellipsoid-body (EB) lines plus the E-PG line for the turning component. We expect that flies with inactive MDN should have a smaller backward walking phase, and flies with inactive EB or E-PG neurons should have some changes in peak angular velocity.

It would also be important to do some expression pattern analysis, such as checking the expression pattern of the CS (Eyeless-FLP) to see if there are cells marked in the leg, and if the cells in the antennae are being targeted, as well as to repeat the expression patterns of the LexA lines, this time utilising the anti-GFP antibody to ensure there are cells marked in the MDN-LexA and E-PG-LexA lines. For the Split-Gal4 lines, it would also be necessary to check for expression of transgene in the central nervous system (brain and VNC), to check if the line is capable of targeting just the CS without any other cells being marked. If there are "clean" lines, checking their behaviour with optogenetic activation would also be advised to try and recreate the behaviour that we see with the CS (DacRE-FLP) line.

To finalize, there could also be improvements on the way flies are tested. At the moment, the researcher waits for the fly to fully stop and has to have the reaction time to press a button on the Arduino in order to activate the light stimulus. This means we fail to collect a lot of data due to human constraints. That could be resolved using Bonsai to detect that the fly is not moving, and activate the optogenetic stimulus (closed-loop). It could also be beneficial to try using a different tracker to track the fly in the videos, as the FlyTracker produces an apparently random error that incapacitates it from running a rather large number of videos (~30%). Just these two changes alone would increase the efficiency of data collection and provide more robust tools to do behavioural analysis.

4.7 Final remarks

The present work has shown that the activation of the leg campaniform sensilla leads to the production of a motor output described by a backward walking motion, followed by a turn, and then forward walking in a different direction. This behaviour is not produced by the activation of the antennae, as flies without antennae show the same behaviour. It is also specific to this mechanosensory structure, as the activation of another proprioceptor such as the chordotonal organ induces a completely different motor output.

We have also shown how the inactivation of the leg campaniform sensilla can induce another phenotype. These flies seem to show a difficulty in sensing how narrow a space is, perhaps due to the fact that some of their load-sensors are inactive. This meant that flies with non-functional CS tended to get stuck in the narrowing tunnels, even though they showed no difficulty in backing up when placed in tunnels with a constant height.

To finalize, we have produced two new tools that allow the study of the leg campaniform sensilla, by having a dual expression system to test simultaneous activation of the CS, and inactivation of candidate regions/populations of neurons, as well as a set of split-Gal4 combinations that drive the expression of a transgene in the leg campaniform sensilla.

However, this work scratches just the surface of the function of the CS in *Drosophila melanogaster* and their influence in locomotive behaviours. As proprioception is one of the facilitators into fine motor

control, animals rely on it for all tasks, no matter how simple they might be. Given the similarities between proprioceptive structures when comparing insects and mammals, a greater understanding of the neural circuits behind these structures and how they manipulate locomotion in invertebrates can provide with new insights on how the corresponding structures in mammals are integrated into motor control, and how they can be useful in treating lesions or other sensorimotor malfunctions.

5 Bibliography

Agrawal, S., Dickinson, E. S., Sustar, A., Gurung, P., Shepherd, D., Truman, J. W., & Tuthill, J. C. (2020). Central processing of leg proprioception in drosophila. *ELife*, *9*, 1–32. https://doi.org/10.7554/ELIFE.60299

Baines, R. A., Uhler, J. P., Thompson, A., Sweeney, S. T., & Bate, M. (2001). Altered electrical properties in Drosophila neurons developing without synaptic transmission. *Journal of Neuroscience*, *21*(5), 1523–1531. https://doi.org/10.1523/jneurosci.21-05-01523.2001

Bidaye, S. S., Machacek, C., Wu, Y., & Dickson, B. J. (2014). Neuronal control of Drosophila walking direction. *Science*, *344*(6179), 97–101. https://doi.org/10.1126/science.1249964

Bonsai. (n.d.). Bonsai. Retrieved May 13, 2022, from https://bonsai-rx.org/

Booker, R., & Quinn, W. G. (1981). Conditioning of leg position in normal and mutant Drosophila. *Proceedings of the National Academy of Sciences of the United States of America*, *78*(6 I), 3940–3944. https://doi.org/10.1073/pnas.78.6.3940

Brand, A. H., & Perrimon, N. (1993). Targeted gene expression as a means of altering cell fates and generating dominant phenotypes. *Development*, *118*(2), 401–415. https://doi.org/10.1242/dev.118.2.401

Bueschges, A., & Manira, A. El. (1998). Sensory pathways and their modulation in the control of locomotion. *Current Opinion in Neurobiology*, *8*, 733–739. https://doi.org/https://www.sciencedirect.com/science/article/pii/S0959438898801153

Burdohan, J. A., & Comer, C. M. (1990). An antennal-derived mechanosensory pathway in the cockroach: descending interneurons as a substrate for evasive behavior. *Brain Research*, *535*(2), 347–352. https://doi.org/10.1016/0006-8993(90)91623-O

Court, R., Namiki, S., Armstrong, J. D., Börner, J., Card, G., Costa, M., Dickinson, M., Duch, C., Korff, W., Mann, R., Merritt, D., Murphey, R. K., Seeds, A. M., Shirangi, T., Simpson, J. H., Truman, J. W., Tuthill, J. C., Williams, D. W., & Shepherd, D. (2020). A Systematic Nomenclature for the Drosophila Ventral Nerve Cord. *Neuron*, *107*(6), 1071-1079.e2. https://doi.org/10.1016/j.neuron.2020.08.005

DEAN, J. (1991). Effect of Load on Leg Movement and Step Coordination of the Stick Insect Carausius Morosus . *Journal of Experimental Biology*, *159*(1), 449–471. https://doi.org/10.1242/jeb.159.1.449

DEAN, J., & WENDLER, G. (1983). Stick Insect Locomotion on a Walking Wheel: Interleg Coordination of Leg Position. *Journal of Experimental Biology*, *103*(1), 75–94. https://doi.org/10.1242/jeb.103.1.75

Dickinson, M. H., Farley, C. T., Full, R. J., Koehl, M. A. R., Kram, R., & Lehman, S. (2000). How animals move: An integrative view. *Science*, *288*(5463), 100–106. https://doi.org/10.1126/science.288.5463.100

Dinges, G. F., Chockley, A. S., Bockemühl, T., Ito, K., Blanke, A., & Büschges, A. (2021). Location and arrangement of campaniform sensilla in Drosophila melanogaster. *Journal of Comparative Neurology*, *529*(4), 905–925. https://doi.org/10.1002/cne.24987

Eyjolfsdottir, E., Branson, S., Burgos-Artizzu, X. P., Hoopfer, E. D., Schor, J., Anderson, D. J., & Perona, P. (2014). Detecting social actions of fruit flies. *Lecture Notes in Computer Science (Including Subseries Lecture Notes in Artificial Intelligence and Lecture Notes in Bioinformatics)*, *8690 LNCS*(PART 2), 772–787. https://doi.org/10.1007/978-3-319-10605-2_50

Feng, K., Sen, R., Minegishi, R., Dübbert, M., Bockemühl, T., Büschges, A., & Dickson, B. J. (2020). Distributed control of motor circuits for backward walking in Drosophila. *Nature Communications*, *11*(1). https://doi.org/10.1038/s41467-020-19936-x

Fiala, A., Suska, A., & Schlüter, O. M. (2010). Optogenetic approaches in neuroscience. *Current Biology*, *20*(20). https://doi.org/10.1016/j.cub.2010.08.053

FlyLight protocols. (n.d.). FlyLight Protocols. Retrieved May 13, 2022, from https://www.janelia.org/project-team/flylight/protocols

Giorgianni, M. W., & Mann, R. S. (2011). Establishment of Medial Fates along the Proximodistal Axis of the Drosophila Leg through Direct Activation of dachshund by Distalless. *Developmental Cell*, *20*(4), 455–468. https://doi.org/10.1016/j.devcel.2011.03.017

Guan, W., Venkatasubramanian, L., Baek, M., Mann, R. S., & Enriquez, J. (2018). Visualize Drosophila Leg Motor Neuron Axons Through the Adult Cuticle. *Journal of Visualized Experiments : JoVE*, *140*. https://doi.org/10.3791/58365

Hampel, S., Eichler, K., Yamada, D., Bock, D. D., Kamikouchi, A., & Seeds, A. M. (2020). Distinct subpopulations of mechanosensory chordotonal organ neurons elicit grooming of the fruit fly antennae. *ELife*, *9*, 1–55. https://doi.org/10.7554/eLife.59976

Israel, S., Rozenfeld, E., Weber, D., Huetteroth, W., & Parnas, M. (2022). Olfactory stimuli and moonwalker SEZ neurons can drive backward locomotion in Drosophila. *Current Biology*, *32*(5), 1131-1149.e7. https://doi.org/10.1016/j.cub.2022.01.035

Keil, T. A. (1997). Functional morphology of insect mechanoreceptors. *Microscopy Research and Technique*, *39*(6), 506–531. https://doi.org/10.1002/(SICI)1097-0029(19971215)39:6<506::AID-JEMT5>3.0.CO;2-B

Kernan, M. J. (2007). Mechanotransduction and auditory transduction in Drosophila. *Pflugers Archiv European Journal of Physiology*, *454*(5), 703–720. https://doi.org/10.1007/s00424-007-0263-x

Klapoetke, N. C., Murata, Y., Kim, S. S., Pulver, S. R., Birdsey-Benson, A., Cho, Y. K., Morimoto, T. K., Chuong, A. S., Carpenter, E. J., Tian, Z., Wang, J., Xie, Y., Yan, Z., Zhang, Y., Chow, B. Y., Surek, B., Melkonian, M., Jayaraman, V., Constantine-Paton, M., … Boyden, E. S. (2014). Independent optical excitation of distinct neural populations. *Nature Methods*, *11*(3), 338–346. https://doi.org/10.1038/nmeth.2836

Kottler, B., Faville, R., Bridi, J. C., & Hirth, F. (2019). Inverse Control of Turning Behavior by Dopamine D1 Receptor Signaling in Columnar and Ring Neurons of the Central Complex in Drosophila. *Current Biology*, *29*(4), 567-577.e6. https://doi.org/10.1016/j.cub.2019.01.017

Kremers, G. J., Goedhart, J., Van Munster, E. B., & Gadella, T. W. J. (2006). Cyan and yellow super fluorescent proteins with improved brightness, protein folding, and FRET förster radius. *Biochemistry*, *45*(21), 6570–6580. https://doi.org/10.1021/bi0516273

Lai, S. L., & Lee, T. (2006). Genetic mosaic with dual binary transcriptional systems in Drosophila. *Nature Neuroscience*, *9*(5), 703–709. https://doi.org/10.1038/nn1681

Mann, H. B., & Whitney, D. R. (1947). On a Test of Whether one of Two Random Variables is Stochastically Larger than the Other. *The Annals of Mathematical Statistics*, *18*(1), 50–60. https://doi.org/10.1214/aoms/1177730491

Marder, E., & Bucher, D. (2001). Central pattern generators and the control of rhythmic movements. *Current Biology*, *11*(23). https://doi.org/10.1016/S0960-9822(01)00581-4

Mardon, G., Solomon, N. M., & Rubin, G. M. (1994). dachshund encodes a nuclear protein required for normal eye and leg development in Drosophila. *Development*, *120*(12), 3473–3486. https://doi.org/10.1242/dev.120.12.3473

Mendes, C. S., Bartos, I., Márka, Z., Akay, T., Márka, S., & Mann, R. S. (2015). Quantification of gait parameters in freely walking rodents. *BMC Biology*, *13*(1). https://doi.org/10.1186/s12915-015-0154-0

Mendes, C. S., Rajendren, S. V., Bartos, I., Márka, S., & Mann, R. S. (2014). Kinematic responses to changes in walking orientation and gravitational load in drosophila melanogaster. *PLoS ONE*, *9*(10). https://doi.org/10.1371/journal.pone.0109204

Merritt, D. J., & Murphey, R. K. (1992). Projections of leg proprioceptors within the CNS of the fly Phormia in relation to the generalized insect ganglion. *Journal of Comparative Neurology*, *322*(1), 16–34. https://doi.org/10.1002/cne.903220103

Moffat, K. G., Gould, J. H., Smith, H. K., & O'Kane, C. J. (1992). Inducible cell ablation in Drosophila by cold-sensitive ricin A chain. *Development*, *114*(3), 681–687. https://doi.org/10.1242/dev.114.3.681

Movement @ dictionary.cambridge.org. (n.d.). https://dictionary.cambridge.org/dictionary/english/movement

Namiki, S., Dickinson, M. H., Wong, A. M., Korff, W., & Card, G. M. (2018). The functional organization of descending sensory-motor pathways in drosophila. *ELife*, *7*. https://doi.org/10.7554/eLife.34272

Noah, A. J., Quimby, L., Frazier, F. S., & Zill, S. N. (2001). Force detection in cockroach walking reconsidered: Discharges of proximal tibial campaniform sensilla when body load is altered. *Journal of Comparative Physiology - A Sensory, Neural, and Behavioral Physiology*, *187*(10), 769–784. https://doi.org/10.1007/s00359-001-0247-9

Noah, J. A., Quimby, L., Frazier, S. F., & Zill, S. N. (2004). Sensing the effect of body load in legs: Responses of tibial campaniform sensilla to forces applied to the thorax in freely standing cockroaches. *Journal of Comparative Physiology A: Neuroethology, Sensory, Neural, and Behavioral Physiology*, *190*(3), 201–215. https://doi.org/10.1007/s00359-003-0487-y

Orlovsky, G. N., Deliagina, T. G., & Grillner, S. (2012). Walking in the stick insect and locust. *Neuronal Control of LocomotionFrom Mollusc to Man*, 84–97. https://doi.org/10.1093/acprof:oso/9780198524052.003.0006

Parigi, A., Porter, C., Cermak, M., Pitchers, W. R., & Dworkin, I. (2019). The behavioral repertoire of Drosophila melanogaster in the presence of two predator species that differ in hunting mode. *PLoS ONE*, *14*(5). https://doi.org/10.1371/journal.pone.0216860

Pfeiffer, K., & Homberg, U. (2014). Organization and functional roles of the central complex in the insect brain. *Annual Review of Entomology*, *59*, 165–184. https://doi.org/10.1146/annurev-ento-011613-162031

PRINGLE, J. W. S. (1938). Proprioception In Insects. *Journal of Experimental Biology*, *15*(1), 114–131. https://doi.org/10.1242/jeb.15.1.114

Ridgel, A. L., Frazier, S. F., DiCaprio, R. A., & Zill, S. N. (2000). Encoding of forces by cockroach tibial campaniform sensilla: Implications in dynamic control of posture and locomotion. *Journal of Comparative Physiology - A Sensory, Neural, and Behavioral Physiology*, *186*(4), 359–374. https://doi.org/10.1007/s003590050436

Schneuwly, S., Klemenz, R., & Gehring, W. J. (1987). Redesigning the body plan of Drosophila by ectopic expression of the homoeotic gene Antennapedia. *Nature*, *325*(6107), 816–818. https://doi.org/10.1038/325816a0

Schnorbus, H. (1971). Die subgenualen Sinnesorgane von Periplaneta americana: Histologie und Vibrationsschwellen. *Zeitschrift Für Vergleichende Physiologie*, *71*(1), 14–48. https://doi.org/10.1007/bf03395969

Sen, R., Wang, K., & Dickson, B. J. (2019). TwoLumps Ascending Neurons Mediate Touch-Evoked Reversal of Walking Direction in Drosophila. *Current Biology*, *29*(24), 4337-4344.e5. https://doi.org/10.1016/j.cub.2019.11.004

Sen, R., Wu, M., Branson, K., Robie, A., Rubin, G. M., & Dickson, B. J. (2017). Moonwalker Descending Neurons Mediate Visually Evoked Retreat in Drosophila. *Current Biology*, *27*(5), 766–771. https://doi.org/10.1016/j.cub.2017.02.008

Shirangi, T. R., Wong, A. M., Truman, J. W., & Stern, D. L. (2016). Doublesex Regulates the Connectivity of a Neural Circuit Controlling Drosophila Male Courtship Song. *Developmental Cell*, *37*(6), 533–544. https://doi.org/10.1016/j.devcel.2016.05.012

Si Dong, P. D., Dicks, J. S., & Panganiban, G. (2002). Distal-less and homothorax regulate multiple targets to pattern the Drosophila antenna. *Development*, *129*(8), 1967–1974. https://doi.org/10.1242/dev.129.8.1967

Sperelakis, N. (1979). Propagation mechanisms in heart. *Annual Review of Physiology*, *41*, 441–457. https://doi.org/10.1146/annurev.ph.41.030179.002301

Spinola, S. M., & Chapman, K. M. (1975). Proprioceptive indentation of the campaniform sensilla of cockroach legs. *Journal of Comparative Physiology ■ A*, *96*(3), 257–272. https://doi.org/10.1007/BF00612698

Strausfeld, N. J. (2009). Brain organization and the origin of insects: An assessment. *Proceedings of the Royal Society B: Biological Sciences*, *276*(1664), 1929–1937. https://doi.org/10.1098/rspb.2008.1471

Strauss, R., & Heisenberg, M. (1993). A higher control center of locomotor behavior in the Drosophila brain. *Journal of Neuroscience*, *13*(5), 1852–1861. https://doi.org/10.1523/jneurosci.13-05-01852.1993

Strauß, R., & Heisenberg, M. (1990). Coordination of legs during straight walking and turning in Drosophila melanogaster. *Journal of Comparative Physiology A*, *167*(3), 403–412. https://doi.org/10.1007/BF00192575

Strauss, Roland. (2002). The central complex and the genetic dissection of locomotor behaviour. *Current Opinion in Neurobiology*, *12*(6), 633–638. https://doi.org/10.1016/S0959-4388(02)00385-9

Struhl, G., & Basler, K. (1993). Organizing activity of wingless protein in Drosophila. *Cell*, *72*(4), 527–540. https://doi.org/10.1016/0092-8674(93)90072-X

Tresch, M. C., Saltiel, P., & Bizzi, E. (1999). The construction of movement by the spinal cord. *Nature Neuroscience*, *2*(2), 162–167. https://doi.org/10.1038/5721

Tsubouchi, A., Yano, T., Yokoyama, T. K., Murtin, C., Otsuna, H., & Ito, K. (2017). Topological and modality-specific representation of somatosensory information in the fly brain. *Science*, *358*(6363), 615–623. https://doi.org/10.1126/science.aan4428

Tuthill, J. C., & Azim, E. (2018). Proprioception. *Current Biology*, *28*(5), R194–R203. https://doi.org/10.1016/j.cub.2018.01.064

Tuthill, J. C., & Wilson, R. I. (2016). Parallel Transformation of Tactile Signals in Central Circuits of Drosophila. *Cell*, *164*(5), 1046–1059. https://doi.org/10.1016/j.cell.2016.01.014

Venkatasubramanian, L., Guo, Z., Xu, S., Tan, L., Xiao, Q., Nagarkar-Jaiswal, S., & Mann, R. S. (2019). Stereotyped terminal axon branching of leg motor neurons mediated by igsf proteins dip-α and dpr10. *ELife*, *8*. https://doi.org/10.7554/eLife.42692

Weber, K., Johnson, N., Champlin, D., & Patty, A. (2005). Many P-element insertions affect wing shape in Drosophila melanogaster. *Genetics*, *169*(3), 1461–1475. https://doi.org/10.1534/genetics.104.027748

WH, K., & WA., W. (1952). Use of ranks in one-criterion variance analysis. *Journal of the American Statistical Association*, *47*(260), 583–621.

Wilk, M. B., & Shapiro, S. S. (1965). An analysis of variance test for normality (complete samples). *Biometrika*, *52*(3–4), 591–611.

Wu, M., Nern, A., Ryan Williamson, W., Morimoto, M. M., Reiser, M. B., Card, G. M., & Rubin, G. M. (2016). Visual projection neurons in the Drosophila lobula link feature detection to distinct behavioral programs. *ELife*, *5*(DECEMBER2016). https://doi.org/10.7554/eLife.21022

Ye, S., Leung, V., Khan, A., Baba, Y., & Comer, C. M. (2003). The antennal system and cockroach evasive behavior. I. Roles for visual and mechanosensory cues in the response. *Journal of Comparative Physiology A: Neuroethology, Sensory, Neural, and Behavioral Physiology*, *189*(2), 89–96. https://doi.org/10.1007/s00359-002-0383-x

Zill, S. N., Keller, B. R., Chaudhry, S., Duke, E. R., Neff, D., Quinn, R., & Flannigan, C. (2010). Detecting substrate engagement: Responses of tarsal campaniform sensilla in cockroaches. *Journal of Comparative Physiology A: Neuroethology, Sensory, Neural, and Behavioral Physiology*, *196*(6), 407–420. https://doi.org/10.1007/s00359-010-0526-4

Zill, S. N., Ridgel, A. L., DiCaprio, R. A., & Frazier, S. F. (1999). Load signalling by cockroach trochanteral campaniform sensilla. *Brain Research*, *822*(1–2), 271–275. https://doi.org/10.1016/S0006-8993(99)01156-7

Zill, S., Schmitz, J., & Büschges, A. (2004). Load sensing and control of posture and locomotion. *Arthropod Structure and Development*, *33*(3), 273–286. https://doi.org/10.1016/j.asd.2004.05.005

6 Annexes

6.1 Block analysis

Table 6.1 - Significances of normality tests for each block – Velocity

	CS (DacRE-FLP) No ATR	CO	CS (DacRE-FLP)	CS (Eyeless-FLP)	CS (DacRE-FLP) No antennae	Recombinant Empty-LexA
Block 1 0.06-0.13 s	P-value: 0.070	P-value: $2.99x10^{-3}$	P-value: $1.96x10^{-5}$	P-value: $1.65x10^{-3}$	P-value: $1.47x10^{-3}$	P-value: $3.09x10^{-8}$
Block 2 0.13-0.20 s	P-value: 0.168	P-value: 0.708	P-value: $4.19x10^{-3}$	P-value: $1.61x10^{-3}$	P-value: 0.886	P-value: $1.46x10^{-5}$
Block 3 0.20-0.26 s	P-value: 0.394	P-value: $6.76x10^{-3}$	P-value: 0.783	P-value: $1.48x10^{-6}$	P-value: 0.562	P-value: $1.56x10^{-3}$
Block 4 0.26-0.33 s	P-value: 0.389	P-value: $2.01x10^{-3}$	P-value: 0.450	P-value: $1.66x10^{-7}$	P-value: 0.636	P-value: $2.51x10^{-4}$
Block 5 0.33-0.40 s	P-value: 0.433	P-value: $3.90x10^{-3}$	P-value: 0.596	P-value: $9.15x10^{-8}$	P-value: 0.514	P-value: $2.60x10^{-3}$
Block 6 0.40-0.46 s	P-value: 0.364	P-value: $8.78x10^{-5}$	P-value: 0.753	P-value: $5.89x10^{-9}$	P-value: 0.122	P-value: $2.96x10^{-3}$
Block 7 0.46-0.53 s	P-value: $1.20x10^{-3}$	P-value: $2.97x10^{-5}$	P-value: 0.129	P-value: $2.22x10^{-8}$	P-value: 0.079	P-value: 0.611
Block 8 0.53-0.60 s	P-value: $9.88x10^{-11}$	P-value: $4.71x10^{-5}$	P-value: $3.33x10^{-4}$	P-value: $5.48x10^{-8}$	P-value: $4.34x10^{-3}$	P-value: 0.203
Block 9 0.60-0.66 s	P-value: $1.78x10^{-12}$	P-value: $1.42x10^{-4}$	P-value: $3.12x10^{-5}$	P-value: $6.54x10^{-9}$	P-value: $2.86x10^{-3}$	P-value: 0.102

Table 6.2 - Significances of normality tests for each block – Angular velocity.

	CS (DacRE-FLP) No ATR	CO	CS (DacRE-FLP)	CS (Eyeless-FLP)	CS (DacRE-FLP) No antennae	Recombinant Empty-LexA
Block 1 0.06-0.13 s	P-value: 0.036	P-value: 6.56×10^{-6}	P-value: 3.27×10^{-7}	P-value: 5.50×10^{-6}	P-value: 5.65×10^{-4}	P-value: 6.53×10^{-9}
Block 2 0.13-0.20 s	P-value: 6.81×10^{-3}	P-value: 6.38×10^{-7}	P-value: 1.90×10^{-11}	P-value: 9.67×10^{-8}	P-value: 8.38×10^{-4}	P-value: 3.17×10^{-8}
Block 3 0.20-0.26 s	P-value: 1.74×10^{-4}	P-value: 1.60×10^{-6}	P-value: 3.28×10^{-10}	P-value: 2.58×10^{-7}	P-value: 0.046	P-value: 6.36×10^{-7}
Block 4 0.26-0.33 s	P-value: 7.30×10^{-8}	P-value: 2.04×10^{-4}	P-value: 5.22×10^{-8}	P-value: 1.09×10^{-7}	P-value: 0.360	P-value: 6.55×10^{-7}
Block 5 0.33-0.40 s	P-value: 1.02×10^{-5}	P-value: 9.33×10^{-5}	P-value: 6.49×10^{-6}	P-value: 2.45×10^{-8}	P-value: 0.042	P-value: 6.28×10^{-4}
Block 6 0.40-0.46 s	P-value: 6.16×10^{-4}	P-value: 1.08×10^{-8}	P-value: 8.40×10^{-6}	P-value: 5.08×10^{-9}	P-value: 0.035	P-value: 2.67×10^{-5}
Block 7 0.46-0.53 s	P-value: 0.074	P-value: 8.58×10^{-9}	P-value: 6.92×10^{-7}	P-value: 5.65×10^{-11}	P-value: 0.065	P-value: 1.50×10^{-4}
Block 8 0.53-0.60 s	P-value: 2.63×10^{-12}	P-value: 4.72×10^{-7}	P-value: 4.66×10^{-7}	P-value: 3.67×10^{-12}	P-value: 7.01×10^{-3}	P-value: 4.01×10^{-3}
Block 9 0.60-0.66 s	P-value: 3.37×10^{-11}	P-value: 3.51×10^{-7}	P-value: 1.50×10^{-6}	P-value: 3.07×10^{-12}	P-value: 5.94×10^{-3}	P-value: 5.96×10^{-4}

Table 6.3 - P-values of intra-block comparisons between CS (DacRE-FLP) with and without ATR, and CO.

	Velocity			Angular Velocity		
	CS (DacRE-FLP) x CS (DacRE-FLP) – No ATR	CS (DacRE-FLP) x CO	CO x CS (DacRE-FLP) – No ATR	CS (DacRE-FLP) x CS (DacRE-FLP) – No ATR	CS (DacRE-FLP) x CO	CO x CS (DacRE-FLP) – No ATR
Block 1	P-value: 5.92×10^{-8}	P-value: 2.47×10^{-6}	P-value: 0.012	P-value: 5.05×10^{-7}	P-value: 0.109	P-value: 4.00×10^{-6}
Block 2	P-value: 1.91×10^{-8}	P-value: 3.84×10^{-8}	P-value: 6.94×10^{-5}	P-value: 6.71×10^{-7}	P-value: 0.038	P-value: 1.69×10^{-10}
Block 3	P-value: 8.42×10^{-6}	P-value: 6.08×10^{-9}	P-value: 1.23×10^{-5}	P-value: 1.85×10^{-10}	P-value: 0.069	P-value: 2.21×10^{-11}
Block 4	P-value: 3.82×10^{-3}	P-value: 1.21×10^{-6}	P-value: 9.22×10^{-9}	P-value: 3.54×10^{-10}	P-value: 0.439	P-value: 2.61×10^{-10}
Block 5	P-value: 0.312	P-value: 1.79×10^{-3}	P-value: 1.17×10^{-5}	P-value: 3.66×10^{-11}	P-value: 0.021	P-value: 3.70×10^{-10}
Block 6	P-value: 4.04×10^{-5}	P-value: 0.341	P-value: 1.99×10^{-7}	P-value: 5.41×10^{-10}	P-value: 0.019	P-value: 3.70×10^{-10}
Block 7	P-value: 1.31×10^{-6}	P-value: 0.240	P-value: 1.31×10^{-12}	P-value: 1.31×10^{-7}	P-value: 0.107	P-value: 8.02×10^{-10}
Block 8	P-value: 1.54×10^{-9}	P-value: 0.423	P-value: 1.34×10^{-11}	P-value: 1.32×10^{-5}	P-value: 0.253	P-value: 2.67×10^{-9}
Block 9	P-value: 6.19×10^{-6}	P-value: 0.497	P-value: 1.14×10^{-8}	P-value: 3.67×10^{-5}	P-value: 0.341	P-value: 2.74×10^{-7}

Table 6.4 - P-values of intra-block comparisons between CS (DacRE-FLP) with and without antennae, and CS (Eyeless-FLP).

	Velocity			Angular Velocity		
	CS (DacRE-FLP) x CS (Eyeless-FLP)	CS (DacRE-FLP) x CS (DacRE-FLP) – No antennae	CS (Eyeless-FLP) x CS (DacRE-FLP) – No antennae	CS (DacRE-FLP) x CS (Eyeless-FLP)	CS (DacRE-FLP) x CS (DacRE-FLP) – No antennae	CS (Eyeless-FLP) x CS (DacRE-FLP) – No antennae
Block 1	P-value: 0.242	P-value: 0.061	P-value: 0.275	P-value: $9.53x10^{-3}$	P-value: 0.016	P-value: $8.14x10^{-5}$
Block 2	P-value: $3.38x10^{-3}$	P-value: 0.180	P-value: $4.97x10^{-3}$	P-value: $8.13x10^{-3}$	P-value: 0.473	P-value: $6.79x10^{-3}$
Block 3	P-value: $2.71x10^{-5}$	P-value: 0.166	P-value: $1.06x10^{-3}$	P-value: $5.30x10^{-3}$	P-value: 0.235	P-value: 0.058
Block 4	P-value: $2.07x10^{-4}$	P-value: 0.488	P-value: $3.79x10^{-3}$	P-value: 0.414	P-value: 0.224	P-value: 0.360
Block 5	P-value: $3.07x10^{-4}$	P-value: 0.036	P-value: $3.04x10^{-5}$	P-value: 0.078	P-value: 0.420	P-value: 0.150
Block 6	P-value: 0.382	P-value: 0.056	P-value: 0.020	P-value: 0.013	P-value: 0.305	P-value: 0.067
Block 7	P-value: 0.396	P-value: 0.390	P-value: 0.307	P-value: 0.070	P-value: 0.428	P-value: 0.035
Block 8	P-value: 0.343	P-value: 0.466	P-value: 0.402	P-value: 0.060	P-value: 0.247	P-value: $4.23x10^{-3}$
Block 9	P-value: 0.210	P-value: 0.412	P-value: 0.104	P-value: 0.087	P-value: 0.266	P-value: $4.01x10^{-3}$

Table 6.5 - P-values of intra-block comparisons between CS (DacRE-FLP) with and without ATR, and the Recombinant line + Empty-LexA.

	Velocity			Angular Velocity		
	CS (DacRE-FLP) x CS (DacRE-FLP) – No ATR	CS (DacRE-FLP) x Recombinant + Empty-LexA	Recombinant + Empty-LexA x CS (DacRE-FLP) – No ATR	CS (DacRE-FLP) x CS (DacRE-FLP) – No ATR	CS (DacRE-FLP) x Recombinant + Empty-LexA	Recombinant + Empty-LexA x CS (DacRE-FLP) – No ATR
Block 1	P-value: 5.92×10^{-8}	P-value: 0.462	P-value: 2.46×10^{-6}	P-value: 5.05×10^{-7}	P-value: 3.59×10^{-3}	P-value: 2.77×10^{-12}
Block 2	P-value: 1.91×10^{-8}	P-value: 0.280	P-value: 3.84×10^{-6}	P-value: 6.71×10^{-7}	P-value: 0.016	P-value: 5.60×10^{-13}
Block 3	P-value: 8.42×10^{-6}	P-value: 0.382	P-value: 2.32×10^{-8}	P-value: 1.85×10^{-10}	P-value: 0.154	P-value: 2.16×10^{-12}
Block 4	P-value: 3.82×10^{-3}	P-value: 0.338	P-value: 2.26×10^{-4}	P-value: 3.54×10^{-10}	P-value: 0.391	P-value: 4.54×10^{-10}
Block 5	P-value: 0.312	P-value: 0.293	P-value: 0.304	P-value: 3.66×10^{-11}	P-value: 0.421	P-value: 2.32×10^{-8}
Block 6	P-value: 4.04×10^{-5}	P-value: 1.15×10^{-3}	P-value: 0.138	P-value: 5.41×10^{-10}	P-value: 0.353	P-value: 6.87×10^{-9}
Block 7	P-value: 1.31×10^{-6}	P-value: 0.088	P-value: 3.92×10^{-3}	P-value: 1.31×10^{-7}	P-value: 0.139	P-value: 1.68×10^{-12}
Block 8	P-value: 1.54×10^{-9}	P-value: 0.057	P-value: 6.32×10^{-3}	P-value: 1.32×10^{-5}	P-value: 8.66×10^{-3}	P-value: 1.83×10^{-12}
Block 9	P-value: 6.19×10^{-6}	P-value: 0.151	P-value: 2.05×10^{-3}	P-value: 3.67×10^{-5}	P-value: 1.55×10^{-3}	P-value: 8.80×10^{-10}

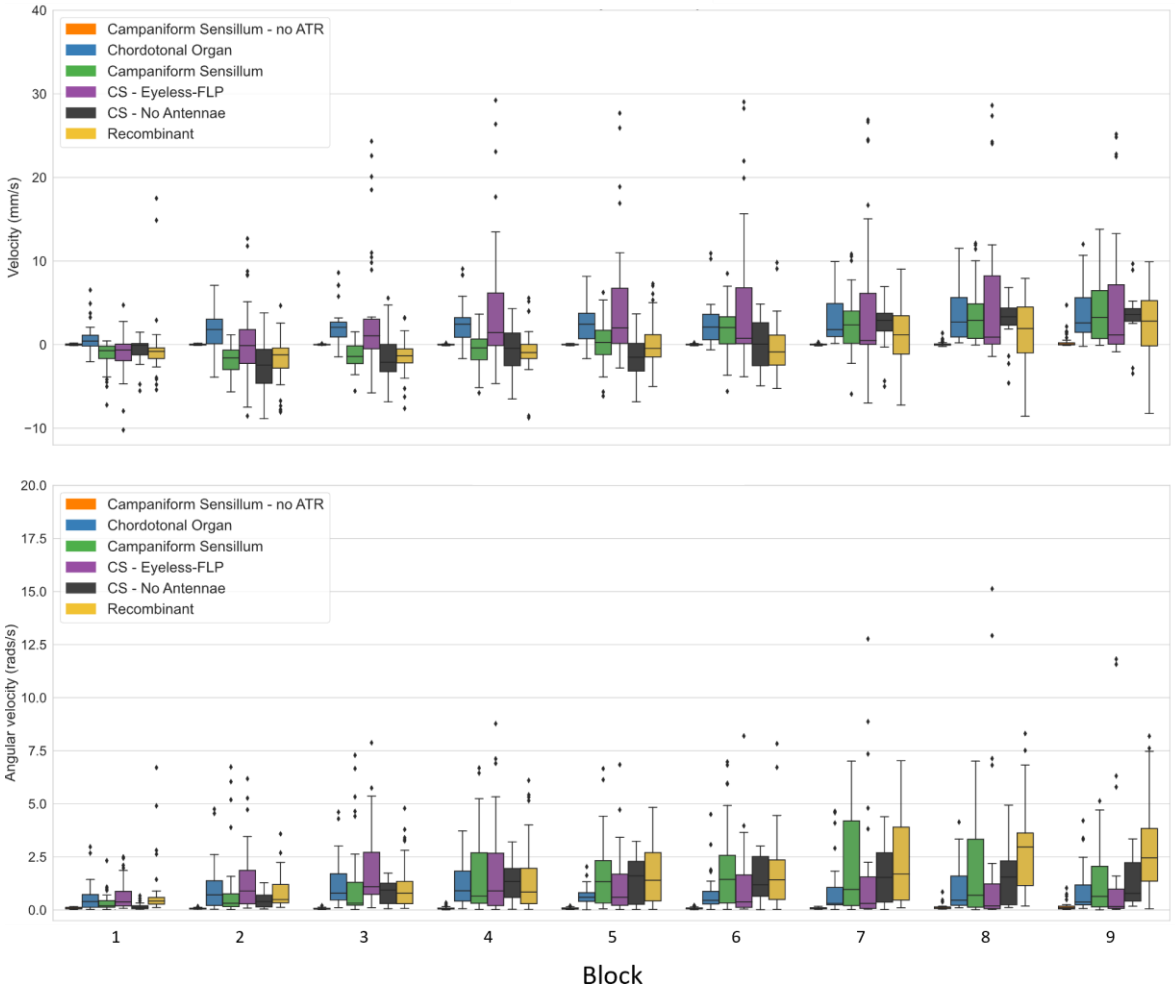

Figure 6.1 - Distribution of velocity and angular velocity data for each block, for all conditions
Each block is composed of two frames (~0.066 s). For each block, the significance of each comparison (relevant to the study) can be found in Tables 6.3-6.5.

6.2 Behavioural analysis for inactivation assays

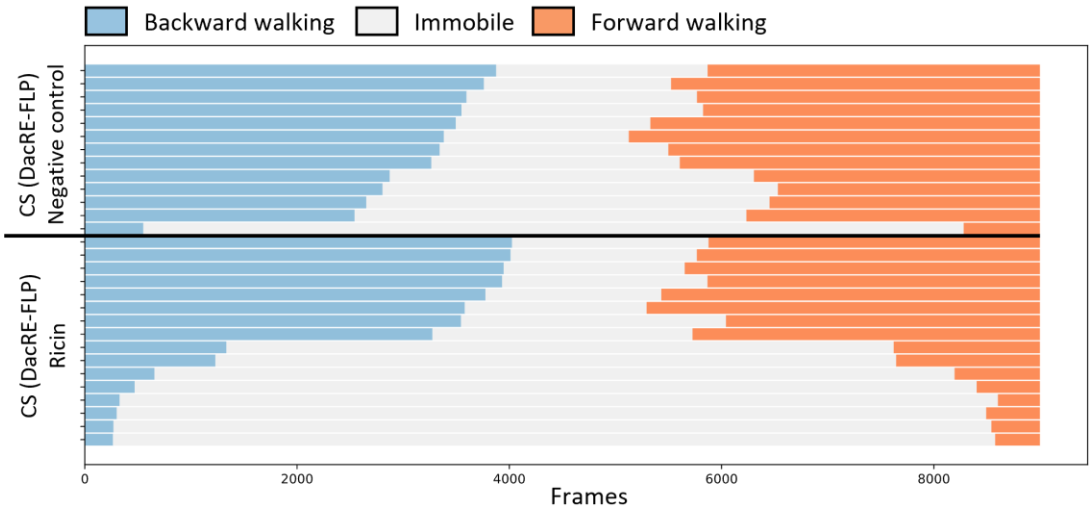

Figure 6.2 - Sum of behaviours for the slanted tunnels, per fly
For each condition, each line corresponds to a singular fly. The coloured bars show the sum of all of the moments where the fly presented any of the three behaviours: backward walking, immobility, or forward walking. Negative control has an n = 13, and ricin expressing line has an n = 16.

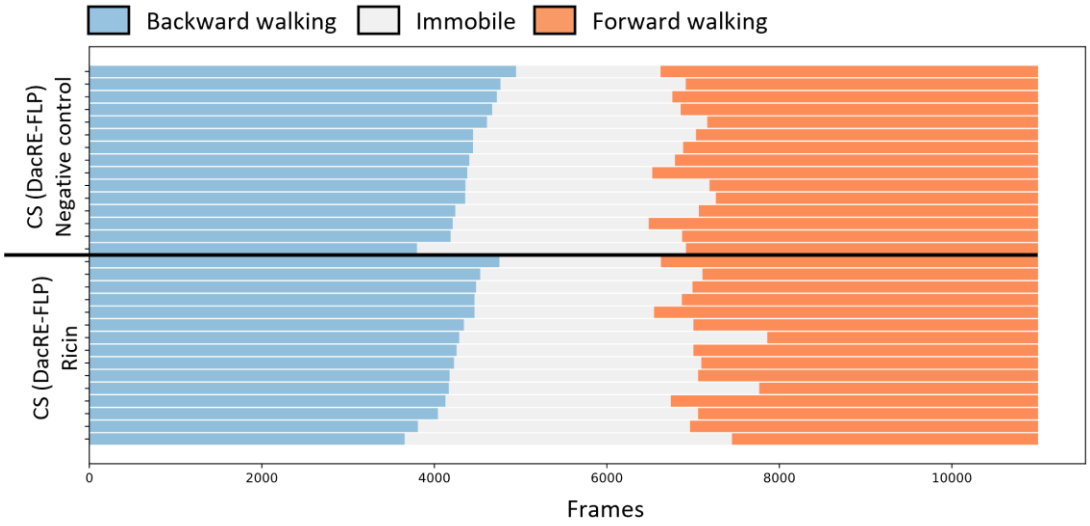

Figure 6.3 - Sum of behaviours for the linear tunnels, per fly
For each condition, each line corresponds to a singular fly. The coloured bars show the sum of all of the moments where the fly presented any of the three behaviours: backward walking, immobility, or forward walking. Both conditions show an n = 15.

6.3 LexA-drivers

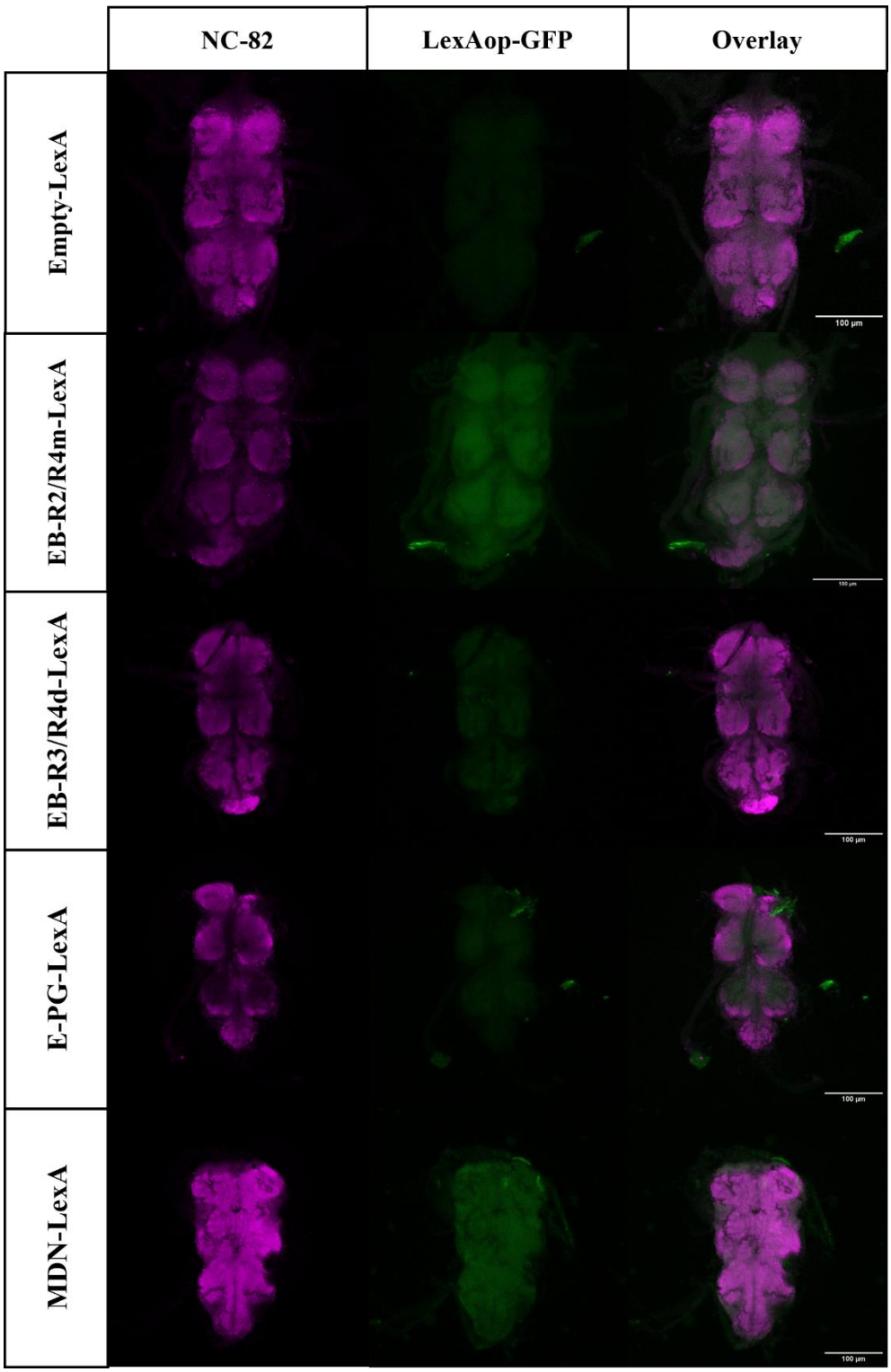

Figure 6.4 - Expression pattern of ventral nerve cords for the LexA-drivers
First column shows expression pattern of NC82, an all-neuron marker, in magenta. Second column shows GFP expression in green. Third column presents the overlay of the two channels. Scale bar corresponds to 100 µm.

6.4 Split-Gal4 expression patterns

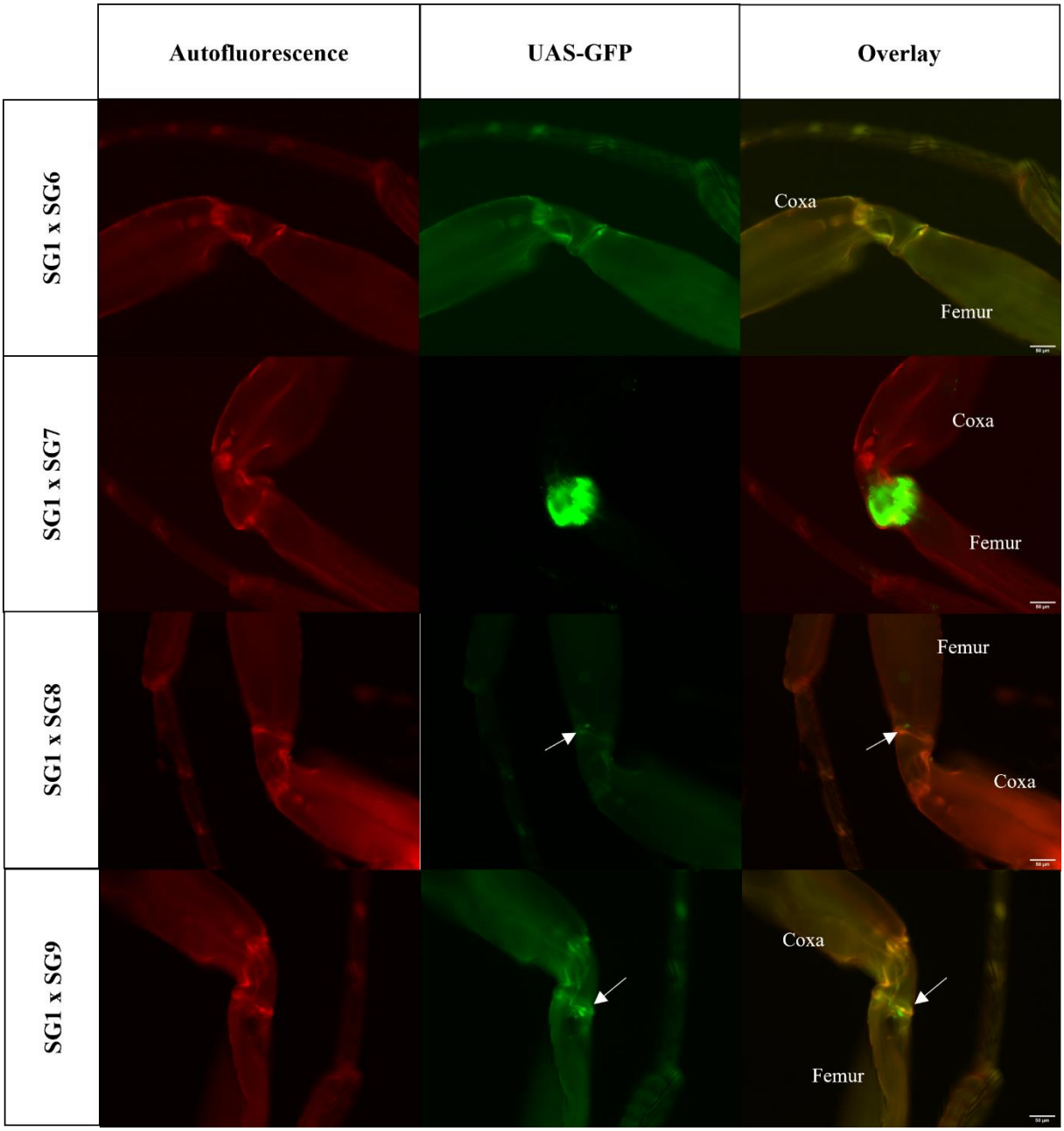

Figure 6.5 - Expression pattern of Split-Gal4 combinations – SG1 (AD) with SG[6-9] (DBD)
First column shows the cuticle autofluorescence in red, second column shows the GFP expression. Third column shows the overlay of the two signals. Combination SG1 x SG8 and SG1 x SG9 marked cells from the femoral fields (FeFF), marked with white arrows. Scale bar corresponds to 50 µm.

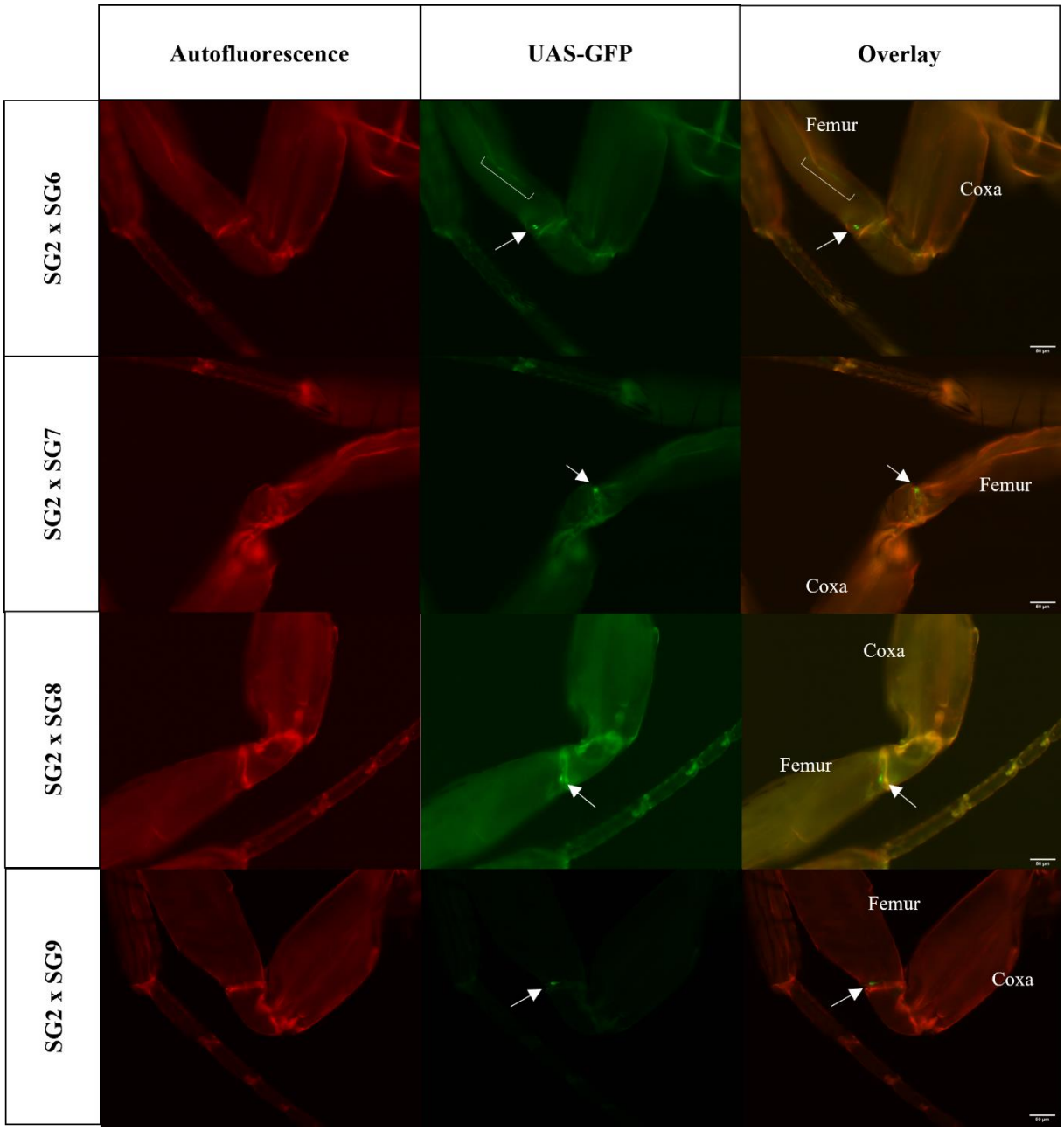

Figure 6.6 - Expression pattern of Split-Gal4 combinations – SG2 (AD) with SG[6-9] (DBD)
First column shows the cuticle autofluorescence in red, second column shows the GFP expression. Third column shows the overlay of the two signals. All four combination marked cells from the femoral fields (FeFF), shown with white arrows. Combination SG2 x SG6 also marked chordotonal organ. Scale bar corresponds to 50 µm.

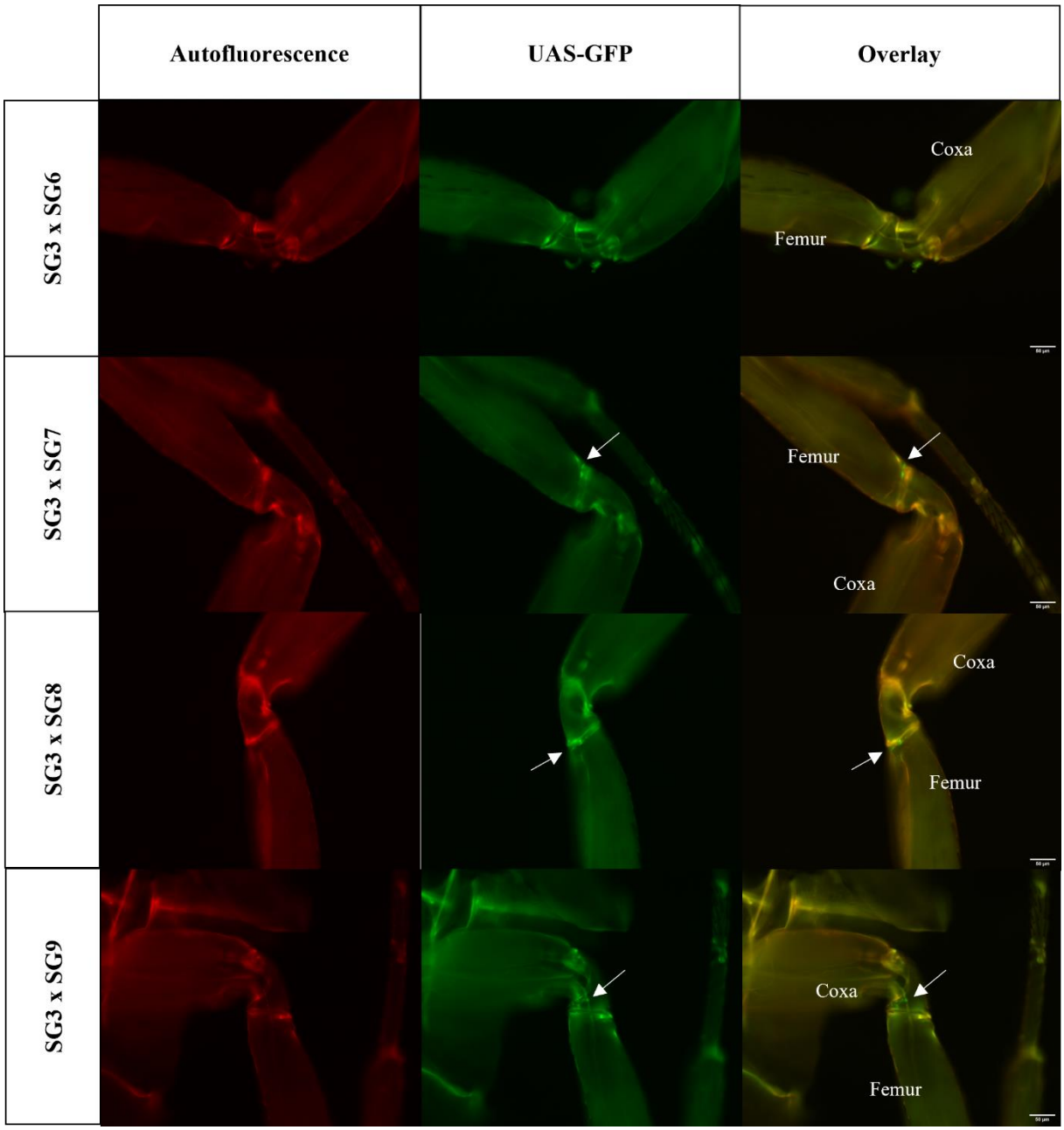

Figure 6.7 - Expression pattern of Split-Gal4 combinations – SG3 (AD) with SG[6-9] (DBD)
First column shows the cuticle autofluorescence in red, second column shows the GFP expression. Third column shows the overlay of the two signals. Combination SG3 x SG7 and SG3 x SG8 marked cells from the femoral fields (FeFF), and the combination SG3 x SG9 marked cells in the trochanteral field (TrFF). White arrows show location of CS cells. Scale bar corresponds to 50 µm.

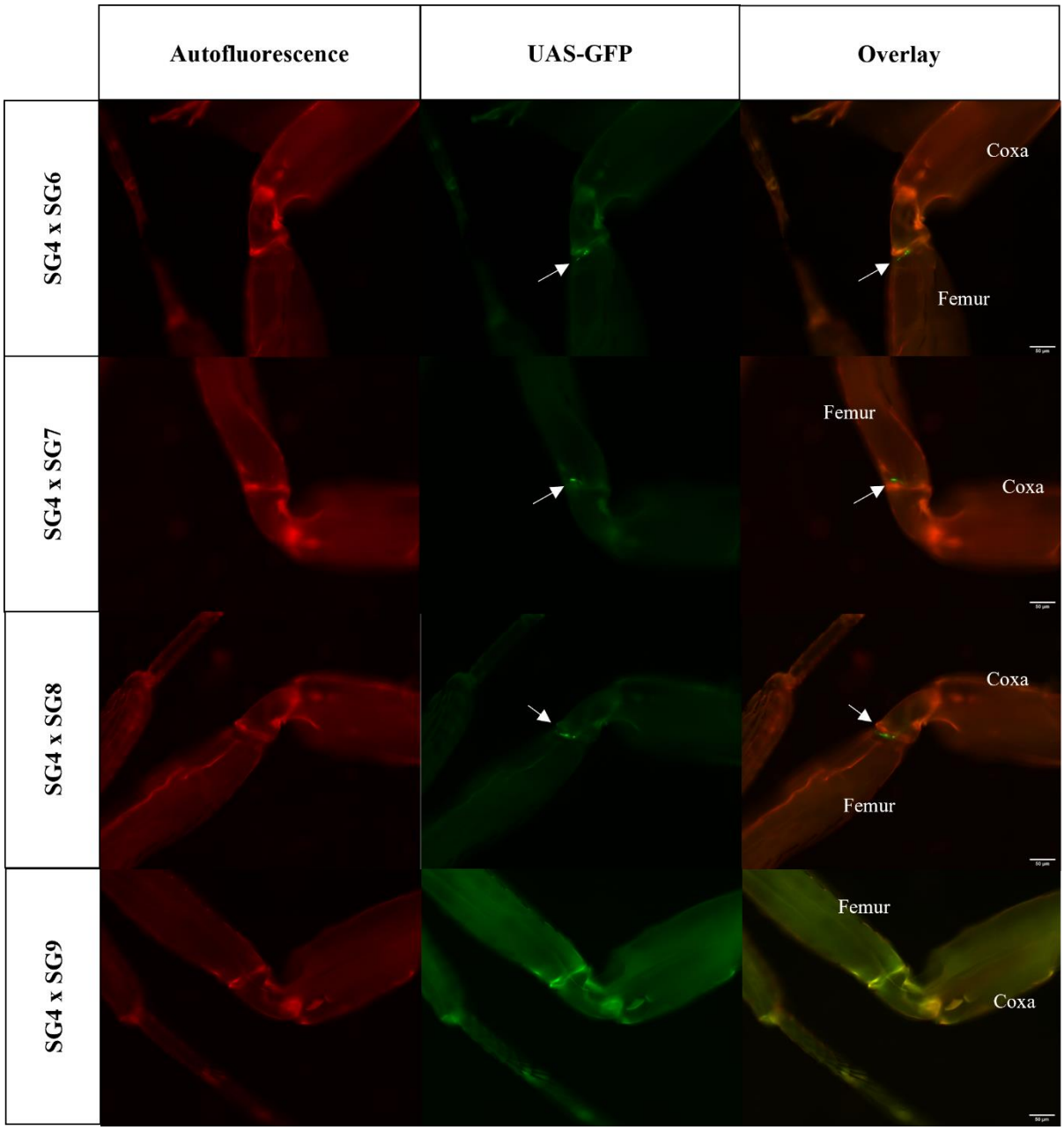

Figure 6.8 - Expression pattern of Split-Gal4 combinations – SG4 (AD) with SG[6-9] (DBD)
First column shows the cuticle autofluorescence in red, second column shows the GFP expression. Third column shows the overlay of the two signals. Combination SG4 x SG7, SG4 x SG8 and SG4 x SG9 marked cells from the femoral fields (FeFF), marked with white arrows. Scale bar corresponds to 50 µm.

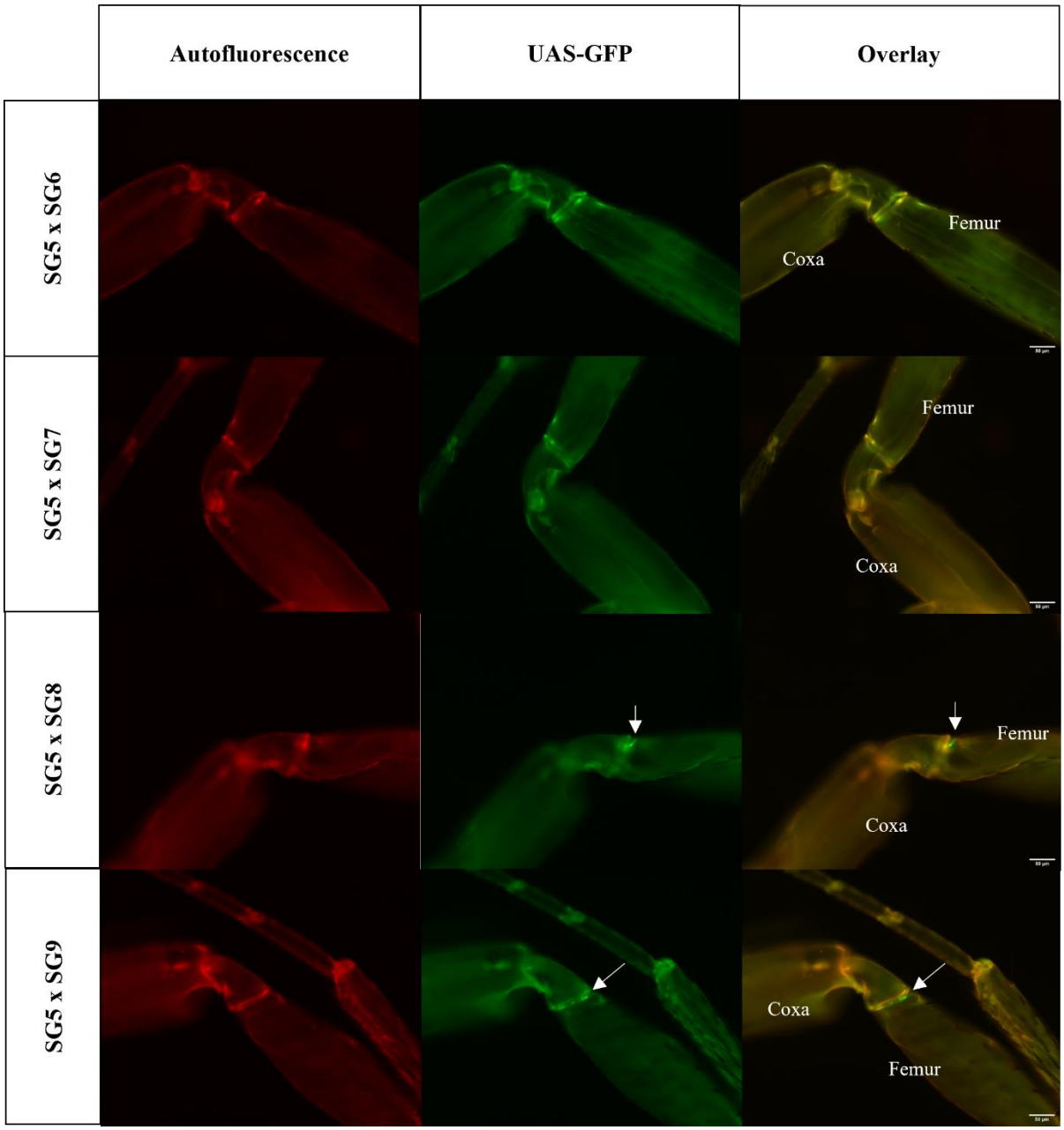

Figure 6.9 - Expression pattern of Split-Gal4 combinations – SG5 (AD) with SG[6-9] (DBD)
First column shows the cuticle autofluorescence in red, second column shows the GFP expression. Third column shows the overlay of the two signals. Combination SG5 x SG8 and SG5 x SG9 marked cells from the femoral fields (FeFF), marked with white arrows. Scale bar corresponds to 50 µm.